Title
ANALYSIS OF AN INTERESTING COSMIC RAY EVENT

Author
Hagstrom, Ray.

Publication Date
1978-09-01

Lawrence Berkeley Laboratory
UNIVERSITY OF CALIFORNIA, BERKELEY, CA

Physics, Computer Science & Mathematics Division

ANALYSIS OF AN INTERESTING COSMIC RAY EVENT

Ray Hagstrom
(Ph. D. thesis)

September 1978

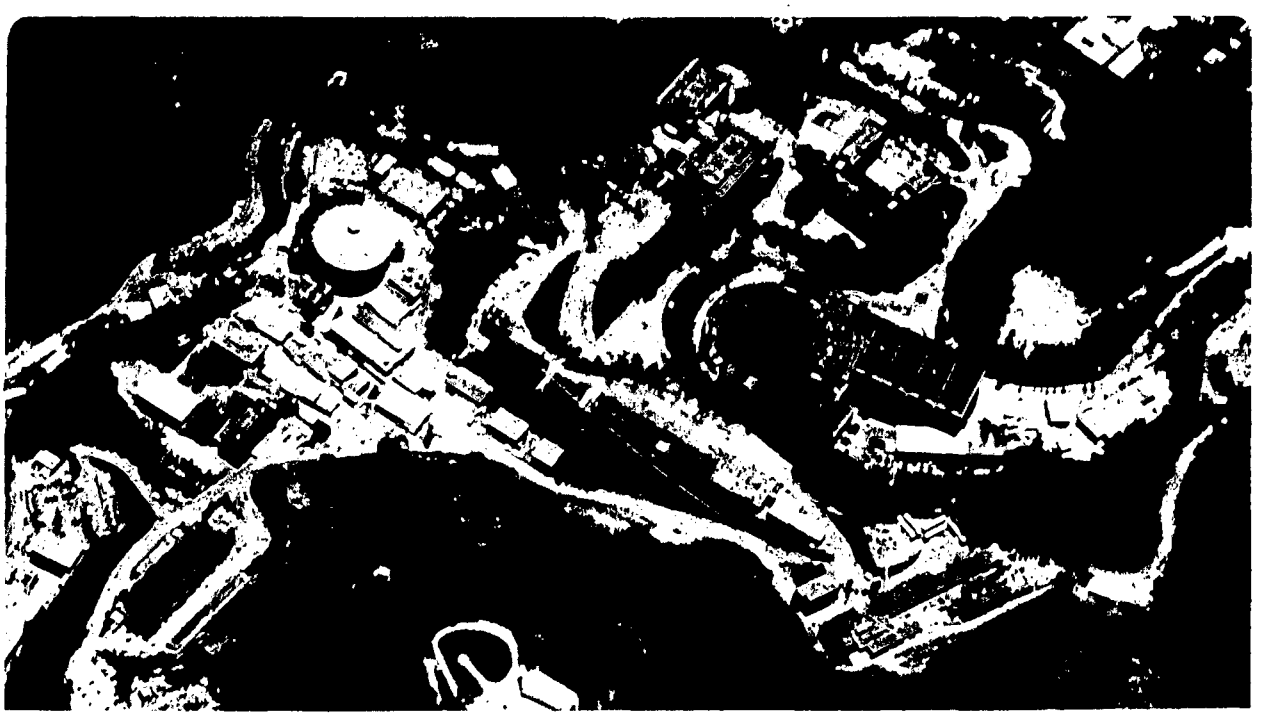

Prepared for the U.S. Department of Energy under Contract W-7405-ENG-48

DISCLAIMER

Lawrence Berkeley Laboratory
University of California
Berkeley, California 94720
Telephone 415/486-4000
FTS: 451-4000

October 29, 1979

Technical Information Center
U. S. Department of Energy
P.O. Box 62
Oak Ridge, TN 37830

Gentlemen:

We are enclosing two copies of LBL-9917 for your information and retention. This report is of a sensitive nature and some of the data contained in it may be unverified or speculative.

It is requested that no further distribution be given to this document without permission from LBL, and that it not be listed in Energy Research Abstracts. All requests for this report should be referred to us.

Sincerely,

Candace L. Voelker

Candace L. Voelker
Publications Coordinator
Technical Information Department

Enclosure (LBL-9917)

Analysis of an Interesting Cosmic Ray Event

Ray Hagstrom

Department of Physics
University of California
Berkeley, California

ABSTRACT

We independently consider the possible interpretations of an unusual cosmic ray event which was reported by Price *et al.* among the primary cosmic radiation.[1] This particle was observed in three separate track recording instruments, a photographic Cerenkov detector, nuclear emulsions, and a track etchable dielectric stack. In this work, we will not be considering data from the nuclear emulsions. From the data we shall consider, we will reach several conclusions: Although this particle was identified by its discoverers as a Dirac monopole, we find that it may readily be explained in terms of a wide class of normal nuclei, all necessarily having speeds in excess of $\beta = v/c \geqslant 0.55$ and having $|Z/\beta| \approx 114$. Some of these hypothetical normal nuclei need to have undergone nuclear fragmentation reactions to be consistent with the data as reported by Price, *et al.* , but the lower bound, $\beta \geqslant 0.55$ obtains *regardless* of any assumed sequence of interactions. We also propose a few less conventional explanations of the data. These unconventional explanations may prove to be the most difficult to refute even when the nuclear emulsion data may be brought fully to bear.

September 19, 1978

Analysis of an Interesting Cosmic Ray Event

Ray Hagstrom

September 19, 1978

1. Introduction

In this work we will consider interpretations of an unusual particle track recorded on September 18, 1973 as part of a collaborative experiment that measured cosmic radiation with a balloon-borne detector package.[1] The package contained three types of detectors: polycarbonate (Lexan) track-etchable sheets, nuclear emulsions, and a photographic Cerenkov detector. The polycarbonate detectors were prepared by P. B. Price and E. K. Shirk; the nuclear emulsions were prepared by W. Z. Osborne; and the photographic Cerenkov detectors were prepared by L. S. Pinsky.

In 1975 these workers reported an unusual track, which they interpreted as having been made by a magnetic monopole. This interpretation was immediately criticized and has been the subject of controversy ever since.[2-7] Briefly, Price *et al.* based their interpretation on the constant ionization rate inferred from the polycarbonate detectors and on the particle velocity indicated by the Cerenkov detectors and nuclear emulsion. The critics, on the other hand, maintained that the track could have been made by certain normal nuclei undergoing nuclear reactions. In this work, we will consider carefully a number of possible interpretations of the experimental data of Price *et al.*

We shall limit ourselves to commenting upon the data from the Cerenkov detector and the polycarbonate detectors. We cannot consider the nuclear emulsion data because they have not as yet been published. We will develop an understanding of the intrinsic limitations of the photographic Cerenkov detector and show why this detector cannot provide good enough data for our desired level of rigor. We shall also discuss how data from polycarbonate detectors are customarily treated. Applying the customary treatment of the etch rate data we shall find a large number of conceivable normal nucleus interpretations that could explain the tracks observed in the polycarbonate detectors. We shall criticize the customary treatment of etch rate data and shall find that this customary treatment is not sufficient to provide arguments of the strength we desire. We shall develop a new method of treating the etch rate data. This new method will provide much more straightforward and uncontroversial conclusions than the customary method of treating the data; we shall be able to set certain lower bounds upon the initial speed of the particle in question, if it were a normal nucleus, without needing to invoke arguments of a probabilistic or statistical nature.

In addition to considering the set of possible interpretations for the etch rate data as allowed by the above mentioned analysis we shall point out classes of unexpected but conceivable alternative interpretations for the etch rate data. These unexpected possibilities follow from the assumption of failure of some of the generally accepted assumptions regarding the physical significance of etch rate measurements.

We shall conclude that there is a wide range of alternative hypotheses that cannot be eliminated by the etch rate data. We will, however, be able to cast considerable doubt on the possibility that the unusual track was made by a Dirac monopole.

Since we find the data from the photographic Cerenkov detector unconvincing, we will be forced to conclude that without convincing data from the nuclear emulsions, there can be no hope of establishing the identity of the particle. In particular, we shall find that it is quite unlikely that this particle will ever be established as some unique object. It will here be useful first to consider the history of the controversy surrounding this event.

The cosmic radiation observed at the surface of the Earth and in balloon-borne experiments such as those of Price *et al.* is due to the incidence of extraterrestrial particles.[8] These so-called primary cosmic rays originate in part from the Sun, but there is a component of the primary cosmic radiation which is far too energetic to be originated by any conceivable mechanism consistent with known facts about the Sun. This primary cosmic radiation is observed to be highly isotropic in observations at the Earth, consistent with the widely held belief that the primary cosmic rays have their origins well outside the Solar System.

There are several puzzling aspects of the primary cosmic radiation as it has been measured. In particular, there is the energy content of the primary cosmic radiation which is believed to be huge under the assumption that observations at the Earth are typical of what would be measured anywhere within the Galaxy. Recent measurements offer further interpretations which imply that the primary cosmic radiation is absorbed by matter within the Galaxy on a relatively rapid time scale, indicating that the cosmic radiation must arise from some energy source of prodigious strength and efficiency. Thus, knowing the location and description of the source of the primary cosmic radiation has great fundamental physical interest as well as great astronomical and cosmological significance.

The primary cosmic radiation as observed so far consists principally of positively charged nuclei and various leptons. Present day observations are sufficient to allow the belief that the primary cosmic radiation contains every stable nuclide observed under laboratory conditions on Earth. In addition, it is widely believed that long-lived unstable isotopes including uranium and possibly curium are present in the primary cosmic radiation. Because of the large energies available in the primary cosmic radiation, there has been a number of exotic objects observed as secondary reaction products initiated by the primary cosmic radiation. In addition, there is the possibility of the introduction of exotic particles into the primary cosmic radiation from the present source of the cosmic radiation or from some primordial origin. It is thus conceivable that there may be some Dirac monopoles among the primary or secondary cosmic radiation.

The concept of the Dirac monopole needs little introduction. Such a particle would be the site of a net magnetic charge.[9] By analogy to the case of electric charges (electric monopoles) a

magnetic charge would have a radially-directed magnetic field whose intensity decreases with distance as $1/r^2$. It was observed by Paul Dirac[9] that quantum mechanical consistency arguments suggest that the magnitude of allowable magnetic charges would be integral multiples of $\frac{1}{2}e/\alpha$. Because of the great theoretical simplicity of the concept of magnetic charges, many scientific and technological uses have been proposed should such objects be discovered and become available. The discovery of such an object would rank as one of the most profound observations in the history of science.

There have been intensive experimental searches for Dirac monopoles. These searches can be classified by their assumptions regarding the origins of the particles. Many experiments have examined the reaction products from high energy particle accelerators, while many other have searched for monopoles of cosmological origins. Because of the high confidence needed to put forward such an interpretation as the possible discovery of magnetic charges, these searches have relied upon unambiguous properties believed to apply to magnetic charges, such as: 1.) their acceleration in an applied magnetic field[10] 2.) their characteristic induction of circulating electrical currents,[11] 3.) their characteristic coupling to Cerenkov and synchrotron radiation,[12] 4.) their characteristic dependence of ionization rate with penetration distance as they come to rest.[13]

The experiment we shall be considering here was balloon-borne so as to have as little disturbance of the primary cosmic radiation by passage through the atmosphere as practical. The Price particle was asserted to be identified as a Dirac monopole on the basis of the fourth scheme mentioned in the previous paragraph. The particle in question did not come to rest within the experimental device so that the arguments needed to assure the identification are somewhat obscured. During the early stages of analyzing their detector packages, Price *et al.* found the anomalous track that they thought could be explained only as a Dirac monopole of strength e/α [1]. This interpretation was published immediately,[1] but received little favorable response. For convenience we will refer to this particle as the Price particle from now on.

The monopole interpretation was disputed by several authors who found fault with the then current, but incomplete, published descriptions of the Price particle. Coincidently with the preparation of the responses of the critics, certain aspects of the earlier reported experimental claims were being revised by Price *et al.* These revised claims were published by Price in a reply to the critics.[6] The details of the critical responses to the original interpretation by Price *et al.* differ somewhat among the various commentators, but the conclusions of the critics Price *et al.* were unanimous: The original publication of Price *et al.* had not properly taken into account a certain class of normal-nuclei that might explain the experimental data.

In order successfully to put forward their explanations, each of the critics needed to deny some of the claims made in Ref. 1. In particular, Friedlander[2] rejected the interpretation of the Cerenkov detector of Pinsky, together with both of the nuclear emulsion measurement schemes of Osborne. He proposed that the Price particle might be a fragmenting curium nucleus. Alvarez[4] disallowed certain of the etch rate data points of Price and Shirk and rejected the nuclear emulsion halo radius measurement of Osborne and proposed that the Price particle might be a doubly fragmenting platinum nucleus. Alvarez also disallowed the quoted thickness of materials in the experimental package of Price *et al.* Fowler[3] partially challenged the Cerenkov detector of Pinsky and rejected the halo radius measurement of Osborne to propose, quite independently of Alvarez, the alternative interpretation of the particle in question as a doubly fragmenting platinum nucleus.

Fleischer and Walker,[5] in a joint publication, disallowed certain of the polycarbonate data of Price and Shirk and then formulated a spectrum of alternative interpretations of the Price particle, in terms of various nuclei fragmenting various numbers of times. Fleischer and Walker did not take a stand regarding the Cerenkov or nuclear emulsion data; instead their results were presented in terms of specific conclusions should the controversy surrounding those two measurement schemes ever be sufficiently settled to allow useful data.

Our discussion will delimit the set of normal-nucleus explanations that are consistent with the etch rate data of Price and Shirk together with the photographic Cerenkov detector data of Pinsky. Again, our treatment will be incomplete since we are unable to discuss the nuclear emulsion data. Our procedure will be, in this respect, similar to that followed by Fleischer and Walker. On the other hand, we approach the etch rate data differently from Fleischer and Walker.

In reaching our conclusions, we will critically evaluate the merits of the detector packages and their interpretation.We will adopt a highly conservative and openly skeptical standard of judging the experimental data. Our conclusions regarding the dependability of the measurements in Ref. 1 will be that every important reservation of each of the published criticisms was justified. In some cases our standards of judging the data will not allow us even to accept data that was unchallenged by previous critics. In particular, we will completely discard the data from Pinsky's Cerenkov detector and accept data only from 28 of the 35 polycarbonate sheets.

2. Description of the Balloon Experiments of Price *et al.*

The Price particle was observed in a balloon-borne package of experimental equipment flown from Sioux City, Iowa on September 18, 1973.[1] This flight was the second in a series of three similar experiments. The first balloon was launched on September 4, 1970 from Minneapolis, Minnesota[14] and the third balloon launched on September 25, 1973 from Sioux City.[6]

Each of the three balloon flights carried a detector package consisting of a thick polycarbonate stack, at least one nuclear emulsion, and at least one photographic Cerenkov detector. The Cerenkov detectors were untested and flown as an attempt at developing a new experimental technique. The differences between the detector packages in the three flights were small (see Table 1). When we specify details, they apply to the second flight, in which the Price particle was observed. The detector array is shown schematically in Fig. 1.

Let us interpret the differences among the three balloon flights represented in Table 1. The differences affect the detectors in different ways. Balloon flight 1 was aloft far longer than is customary for such missions because of certain mechanical malfunctions; the bulk of the extra time aloft was, however, spent at altitudes considerably below the region for clear-cut study of primary cosmic radiation. The time spent at electromagnetic shower altitudes can be regarded as detrimental to the quality of the emulsion based data, i.e. the nuclear emulsions and the photographic Cerenkov detectors. Time spent in ground storage before exposure must be considered to be particularly detrimental to the fast recording emulsion in the Cerenkov detector. Likewise, the time lag between exposure and development processing is most detrimental to the Cerenkov detector data. The effect of a time lag between exposure and development of the polycarbonate data is not well know. The time spent in ground storage before and after exposure is known to be somewhat detrimental to nuclear emulsions.

Although there were two extra nuclear emulsions and one extra photographic Cerenkov detector present in balloon flights 2 and 3, there was less matter above the thick polycarbonate stack in flights 2 and 3 than in flight 1. This difference was first pointed out by Alvarez[4] who noticed that the detector thickness reported in Ref. 1 coincided with those from the much earlier first flight, indicating that Price *et al.* might have been making unfounded assumptions of equivalence between flights 1 and 2 and 3.

Another crucial difference, which was not at first known by the experimenters, was the difference in the chemical composition of the polycarbonate detectors between flight 1 and flights 2 and 3. The ultraviolet dye customarily put in Lexan to retard deterioration was not present in the polycarbonate stacks in balloon flights 2 and 3.. The subsequent discovery of this chemical difference by the experimenters led them to revise their estimate of the particle's ionization from 137 to 114 after the publication of Ref. 1.

3. Etch Rate Detectors: Theory and Interpretation

The interpretation of the tracks in the polycarbonate detectors is a cornerstone of any discussion of the Price particle. The polycarbonate detectors provide a measure of the penetrating properties of the incident particles. As we shall see, these etch rate data describe heavier nuclei as being more penetrating than lighter nuclei. The etch rate data suggest that the Price particle

was the most penetrating particle ever observed with any detector.

In the following discussion, we will cover the theory of etch rate detectors, the nature of the data they yield, and the problems associated with the standard statistical interpretation of the data. Again, our goal in all of this is to apply rigor to the interpretation of the Price particle.

Track etchable detectors made of materials such as polycarbonates have been widely used since damage tracks were observed by Silk and Barnes.[15] Simply stated, a heavily ionizing particle displaces electrons as it passes through the polycarbonate, altering the chemical properties of the plastic around the path of the particle. When the polycarbonate is treated with the proper etching chemical, cones develop in the plastic. The dimensions of the cone are measured and used to infer the properties of the particle that made the track. A comprehensive discussion of the techniques of track etchable particle detectors is given in Ref. 16.

3.1. Interactions of Incident Nuclei within Polycarbonate Detectors

Ionization

When a nucleus passes through a material like Lexan polycarbonate, the electric fields from the nucleus' charge accelerate chemically-bound electrons from the polymer molecules. These electrons wander about within the plastic, in turn losing their kinetic energy through further ionization of the medium. Ultimately, much of the energy lost by the incident nucleus is degraded into thermal energy. Some of the deposited energy is stored in the form of permanently altered chemical structure, e.g. in the form of broken chemical bonds. This chemical damage provides the physical basis for later detection of the nuclear track. Although the chemical damage may, in principle, be at great lateral distances from the actual path of the incident nucleus, the chemical properties of the plastic are significantly altered only in a very narrow column (about 30 *Angstrom* radius) about the nucleus' actual path.[17]

Fragmentation

In addition to ionizing encounters with resting electons within the polycarbonate medium, the incident nucleus may undergo close encounters with the nuclei of the constituent atoms of the plastic. The consequences of such nuclear encounters can be drastic. Nuclear collisions can occasionally lead to complete destruction of the incident heavy nucleus, converting it into a shower of tiny fragments. On the other hand, nuclear collisions can occasionally lead to the

mildest elastic deflections of the incident nucleus, changing its speed and direction of motion by negligible amounts. It is believed that a considerable fraction of nuclear encounters between incident heavy nuclei and the constituent nuclei of the plastic lead to the stripping of a few nucleons from the incident nucleus. After undergoing such a so-called peripheral nuclear interaction, the nucleus continues along its way at essentially the same speed,[18] the only practical change being the decrease in the magnitude of its electric charge and mass.

Electron Pick-up

As an incident nucleus slows, it will have close encounters with the resting electrons of the polycarbonate medium. In some of these close encounters the electron may actually become attached into a bound state of the incident nucleus. The inverse process may also occur wherein the incident nucleus, when it has picked up electrons from the polycarbonate medium, may lose one or more of the attached electrons via some close electromagnetic encounter with the constituents of the plastic. The net effect of such electron attachment and stripping reactions is to alter the net electric charge on the incident nucleus (or, more properly, the incident ion) while leaving the speed and direction of the incident particle as well as its mass essentially unchanged.

3.2. Track Etching to Yield Etch-rate Measurements

Currently, there is no coherent theory that describes track etching. Empirical procedures for developing and interpreting track-etching data have been compiled in several different laboratories. Although there is some disagreement over the details of interpretation, there is a consensus as to the proper interpretation of etch rate data in cases where only the usual levels of certainty are needed.[16]

Polycarbonate detectors are etched by immersion in a caustic *NaOH* bath. Etching allows detection of the tiny cylindrical damaged regions because the damaged plastic is removed more rapidly than the surrounding undamaged plastic. To illustrate, let us consider the damaged cylinder to be damaged uniformly throughout its volume, while at the same time we allow for no damage whatsoever outside the cylinder. The process of etching such a track is indicated schematically in Fig. 2. We can see that the sub-microscopic cylinder of damaged plastic can be the source of two easily-measurable cones. The width (minor axis) of the ellipse defining the intersection of the etch cone and the surface of the plastic is principally determined by the duration of etching and the etch rate in undamaged plastic, provided the cone is much wider than the cylinder. The length of the cone axis is determined principally by the duration of the

etching.[16] The most readily measured parameter is the cone half-opening angle, θ_c, which is interpreted as

$$\theta_c = \sin^{-1}\left(\frac{v_b}{v_t}\right), \qquad \text{(Eq.1)}$$

where: θ_c=*half−opening angle of the etch cone,*

v_b=*etch rate in undamaged plastic,*

v_t=*etch rate in damaged plastic of track cylinder.*

The simplified model of Fig. (2) essentially reproduces the observed behavior because all dimensions of the actually measured cones are much larger than the diameter of the cylinder where appreciable chemical damage has occured.

That the damaged region is very small has been verified via two independent determinations.[17] Both of these studies show the damaged region to be less than 200 *Angstrom* in diameter, while the measured cones are typically more than $30\mu m$ long. The tiny size of the damaged region allows a further important simplification; the etch rate measurements reflect the electromagnetic scattering from the incident particle by the electrons in the medium only for the very lowest momentum transfers, i.e. only for very small equivalent center-of-mass scattering angles. For this reason it is customary to assume that the etch rate data points reflect the value of the parameter $|Q/\beta|$ where Qe is the effective charge of the incident particle and β is its speed.

Let us be quite specific in our definition of the parameter Q : We hypothesize that the measured etch rates reflect the parameter $|Q/\beta|$ regardless of the speed of the incident particle. This assumption *defines* Q as a function of the true atomic number, Z and the speed β of the incident nucleus. Thus, we can think of Q as a function, $Q(Z,\beta)$. This shows that our initial assumption (that the Lexan records $|Q/\beta|$ independently of β) was actually quite empty: Any functional dependence of the measured etch rates on the parameters Z and β of the incident nucleus can be expressed by a judicious choice of the function $Q(Z,\beta)$.

We shall make an important assumption, however, when we deal with Lexan measurements of $|Q/\beta|$, namely, that the numerical value of Q is not greatly different from the atomic number, Z, of the incident nucleus. This important assumption will be used throughout our discussion unless explicitly stated to the contrary. Our motivation for introducing the function $Q(Z,\beta)$ instead of simply using the incident particle's atomic number, Z, is because there is no firm consensus of opinion regarding the response of polycarbonate etch rates to the charge and speed of the incident particle. It is our opinion that the proper form for the function $Q(Z,\beta)$ yields values of Q systematically lower (by amounts varying in the region of interest from 0 to

10%) than the true Z of the incident nucleus. This effect is, in our belief, a consequence of the reduction of the average net charge of the slowing ion by its attachment of electrons from the slowing medium. The beliefs of this author aside, we must acknowledge our assumption that Q does not differ materially from Z, as being a hypothesis subject to doubt so that we present in Appendix D an assessment of how much our present conclusions may be affected by the possible failure of this assumption.

Although we have agreed that each Lexan cone angle reflects the value of $|Q/\beta|$ for the particle it records, this does not allow us directly to translate from cone angles to $|Q/\beta|$. We only can assert that the cone angles are some (as yet unknown) function of the physical parameter $|Q/\beta|$. To the best of our knowledge, no one has yet been able to predict beforehand the actual response of any track etchable dielectric to nuclei with known $|Q/\beta|$ either theoretically or empirically. The response depends upon the details of the chemical kinetics of etching radiation damaged plastic. That such a complicated process should be imperfectly understood is hardly surprizing. This ignorance necessitates a lengthy and thorough calibration of each etch rate experiment on some fiducial set of nuclear tracks to determine the sensitivity and response of the etch rates to various values of $|Q/\beta|$. The customary functional form used to describe, phenomenologically, the etch rate response and sensitivity is:[6]

$$v_t = v_0 \left| \frac{Q}{\beta} \right|^p , \qquad \text{(Eq.2)}$$

where: v_t= *the etch rate along the track,*

v_0= *some phenomenological parameter,*

p= *some phenomenological parameter.*

Recalling the functional form, Eq.(1), allows us to describe the cone angles in terms of the parameter v_t .

The power law form of function (2) also has not been predicted from any theoretical model; the parameters v_0 and p are not even found to be constant from batch to batch of Lexan. The parameter p varies from values below 3.0 to values as high as 5.0 or above depending upon as yet unknown systematics in the manufacture and etching of the plastics.[6] The corresponding values of the parameter v_0 also show variability. This variability no doubt arises in part from the fact that Lexan is itself a vaguely specified commercial plastic, its chemical composition varying considerably from batch to batch. Thus, we repeat, it is absolutely necessary to measure some set of fiducial nuclear tracks before making any quantitative estimates of the numerical values of $|Q/\beta|$ for any tracks through an uncalibrated batch of Lexan. The accuracy of the calibration procedure of Price *et al.* represents another assumption which will

underpin our conclusions; a discussion of the possible failure of the accuracy of the calibration will be given in Appendix C. We will temporarily accept the calibration parameters v_0 and p as reported by Price in Ref. 6 until taking up this question again in Appendix C.

3.3. Difficulties in Applying Statistical Analysis to Etch Rate Data

Granted that we may now use formulae (1) and (2) to estimate $|Q/\beta|$ from any given etch-cone angle, we must still know the random variability of that estimate. Very little is known about the variability of etch cone formation in Lexan polycarbonate. For this reason the proper statistical treatment of etch rate data is problematical. Let us consider, for purposes of understanding the variability of response, the etch cones resulting from the passage of many absolutely identical particles each having the same value of $|Q/\beta|$. Let us assume for concreteness that we have 200 such sheets of Lexan, 100 each from two separate manufacturer's production batches. If we were to etch 50 sheets from each production batch in the identical etchant bath, we would necessarily expect that the etch rates measured would be grouped about separate means corresponding to the differing values of the calibration parameters v_0 and p of Eq. (2) for the separate manufacturing batches of Lexan. Of course, there would be no reason to expect that the scatter of the measured values of etch rates about the respective means should be the same.

If we were now to etch the remaining 100 Lexan sheets in another etchant bath and attempt to keep the conditions of etching as close to those of the first process as possible, we would again find that the measured values of the etch rates would be grouped about the same two means as before corresponding to the two different manufacture batches. In the case of this second etch bath, however, the scatter of the measured etch rates about the two means must not necessarily be expected to be the same as observed from the previous etch bath, no matter what precautions have been taken to assure that the two etch baths were equivalently administered.[19] Such variability has been experimentally observed although its origins are not perfectly understood. We cannot rule out the possibility that the techniques of track etching might someday become sufficiently repeatable to allow the variability of Lexan response to remain constant from etch bath to etch bath; this possibility has, however, not yet been demonstrated beyond doubt.[19]

In practice, the tracks of the heaviest nuclei analyzed by etch rate measurements are etched one at a time, perhaps in several etch baths. Since such tracks are available only from the cosmic radiation it is virtually impossible to obtain any sample of tracks which represent truly identical incident particles. It is, thus, quite unlikely that any great advances may be made soon in understanding the random variability of etch rate measurements on heavy nucleus tracks: the heaviest nucleus which can presently be accelerated to relativistic energies is Fe,

while the present Lexan experiments in the cosmic rays regard the Fe as an uninteresting background signal.

There exist standard statistical techniques, which allow us meaningfully to treat certain experimental data without *a priori* knowledge of their statistical errors. In particular, the F-test allows one to compare quantitatively the quality of fit from two hypotheses to a set of data without knowledge of the statistical errors in the data.[20] It is our belief, however, that the F-test as used by Price and Shirk in the analysis of their etch rate data is not properly applicable to the generation of high confidence statistical arguments. One basis for our doubts about the applicability of the F-test is that the measured etch rates of any given particle may show considerable correlation within the magnitude of the experimental dispersion between successive cones. These sheet-to-sheet correlations may, in fact, represent intrinsic variations in the ionization of nuclei as they traverse a Lexan stack. Of course, the F-test is strictly applicable only when the data are independent, normally-distributed random variables.

3.4. Assigning Hypotheses to Etch Rate Data by "Curve-fitting"

Let us now turn to the general problem of assigning nuclei to tracks in Lexan. Let us briefly describe the assignment of hypotheses to etch rate data as practiced by Fleischer and Walker.[5] These workers generally accept or reject hypotheses on the basis of the quality of agreement of predicted smooth curves and the corresponding measured data points, i.e. by "curve fitting". Let us anticipate our case by considering the etch rate data from the Price particle. The etch rate data on Fig. (3) are of high quality when compared to other etch rate data now available.[21] Nevertheless, even the best etch rate data are so unruly that considerable judgment need be exercised. We will systematically take an approach more conservative than customary in applying our judgment, i.e. we do not disallow any normal-nucleus hypothesis unless it is very far from providing a good fit.

Let us briefly recall the significance of the F-test and how this statistic relates to the χ^2 statistic that is more commonly used in physics. The χ^2 statistic allows us to assign confidence levels to the quality of fit to data by some hypothesis provided that the magnitudes of the probable errors of measurement are known *a priori*. The statistic χ^2 is computed for the hypothesis as follows:

$$\chi^2 = \sum_{n=1}^{N} \frac{(x_n - y_n)^2}{\sigma_n^2} \qquad \text{(Eq.3)}$$

where: x_n= *the outcome of measurement n,*

y_n= *the hypothesis* for *measurement n,*

σ_n= *the experimental error known a priori.*

and tables are used to assign numerical levels of significance to the hypothesis. Because the F-test requires no *a priori* knowledge of the probable errors of measurement, it is no surprise that the F-test cannot be used to assign confidence levels which are intrinsic to any one hypothesis, as can be done with the χ^2 statistic. The F-test can be used to assign the numerical significance to the quality of fit to the data by one hypothesis relative to another hypothesis. This is apparent from the formula for F:

$$F = \frac{M\sum_{n=1}^{N}(x_n - y_n)^2}{N\sum_{m=1}^{M}(x_n - z_n)^2}, \qquad \text{(Eq.4)}$$

where: x_n= *the outcome of the* n^{th} *measurement,*

y_n= *the prediction of hypothesis number* 1

for *the* n^{th} *measurement,*

z_n= *the prediction of hypothesis number* 2

for *the* n^{th} *measurement.*

The confidence level from the χ^2 statistic can be thought of as an estimate for the likelihood that the tested theory should actually have a given quality of fit to the data. The confidence level from the F statistic can be thought of as the likelihood that hypothesis number one may actually provide a better fit to the data than does the hypothesis number two.

For the F-test to provide meaningful estimates of confidence levels, the observations, $\{x_n\}$, in Eq. (4) must be independent, normally-distributed random variables. For the χ^2 statistic to provide meaningful estimates of confidence levels, the observations, $\{x_n\}$, in Eq. (3) must be independent, normally-distributed random variables and the experimental errors, $\{\sigma_n\}$, must be precisely known *a priori.* We note in passing that *many* experiments are performed without *a priori* knowledge of the experimental errors but which are subsequently (incorrectly) interpreted via the χ^2 statistic.

4. Analyzing the Etch Rate Data from the Price Particle

4.1. Selecting Polycarbonate Sheets for Analysis

Each of the polycarbonate sheets in the detector stack has been etched and the results reported by Price.[6] Figure 1 shows the detector package and the Lexan sheets used. The large stack consisted of 33 sheets of thickness $0.987 g/cm^2$. In addition to this thick stack, there were several extra sheets of Lexan not primarily intended for high-quality data taking, but rather to indicate if a particular track originated on the ground before the flight. In addition, certain of the sheets in the thick stack were used solely as an aid in following the tracks from the emulsions into the thick Lexan stack; the etch cones from these sheets are unavoidably lost for purposes of data taking. We thus have no data from sheets 5 and 12.

Within the thick Lexan stack itself, the top three sheets and the bottom sheet have had histories somewhat different from the rest of the sheets. On the basis of our earlier observations regarding the unpredictability of the magnitude of the experimental scatter of etch rate measurements under carefully controlled conditions, we are unwilling to consider data from the sheets which have had treatment differing from the bulk of the stack. We would grant that these outer sheets may be providing a few extra measurements of the quantity $|Q/\beta|$, but we would be at a loss to assign these data equal significance compared with the measurements based upon the sheets from the interior of the stack. We thus do not accept data from Lexan sheets 4 and 35.

Similar objections may be raised against inclusion of data from Lexan sheets 1, 2, and 3, but we take a more certain stance regarding data from these sheets. Sheets 1 and 2 were placed in a package completely separated from the rest of the polycarbonate sheets; these two sheets were displaced with respect to each other at altitude to ensure that the studied tracks originated in the cosmic radiation. Certainly these two polycarbonate sheets have had histories considerably different from the sheets in the interior of the thick stack. Furthermore, sheets 1 and 3 are reported to have thicknesses different from the other Lexan sheets in this experiment; this implies that these sheets were manufactured under conditions different from the sheets in the interior of the thick stack. We conclude, therefore, that the etch rate data from polycarbonate sheets 1, 2, and 3 properly should not be included in any rigorous discussion of the etch rate data from the Price particle.

In summary, we take the stance that the exclusion of etch rate data from Lexan sheets 1, 2, 3, 4, 5, 12, and 35 has a positive overall impact on the quality of the interpretations of the Price particle, and that there is no obvious reason to exclude data from any of the other sheets.

The notation of expressing thickness of absorbing materials in units of g/cm^2 is very convenient. If the thickness of some material (in cm) is multiplied by its mass density (in g/cm^3) we obtain a measure of the true amount of matter in the layer. Otherwise we would necessarily need to specify the linear thickness and density separately.

Omitting the questionable etch rate data points reduces the usable number of sheets from 35 to 28 and the total usable thickness from $1.373 g/cm^2$ to $0.856 g/cm^2$. To date, none of the critics[2-5] of Price *et al.* have published substantial objections to any Lexan data other than the questionable sheets which we have excluded. The exclusion of the questionable sheets coincidentally has the advantage of avoiding the complications of extrapolating particle trajectories through the miscellaneous material above the thick polycarbonate stack.

In our diminished stack, we believe all of the plastic sheets are from the same manufacture batch and all had approximately similar histories. Thus we can use one pair of parameters, p and v_0, from Eq. (2) to translate measured cone angles to expected value estimates of $|Q/\beta|$ for all nuclei incident upon the stack.

4.2. Calibration of the Polycarbonate Sheets

Price calibrated the Lexan detectors by using the copious stopping iron tracks as the necessary fiducial set of calibration tracks, together with a consistency check based upon the relatively well-established platinum peak in the cosmic ray abundances. We summarize the result by restating his formula in our notation:

$$v_t = 0.900\left(\frac{Q}{90.18\beta}\right)^{5.07} \mu/hr. \qquad \text{(Eq.5)}$$

A few comments are in order with respect to this calibration. The exponent of 5.07 is above the range usually quoted from other Lexan etch rate experiments.[6] Price and Shirk attribute the difference in part to the absence of the ultraviolet absorbing dye in the Lexan.[6] As Price noted, this unexpected occurrence represents an advance for the discrimination of heavy nuclei with etch rate detctors.[6] We recall here that the initial publication in Ref. 1 assumed that the calibration parameters v_o and p were "$\approx 10^{-8}$" and "≈ 3.5" ,respectively, just as they were for the etch rate data from balloon flight No. 1.

The experimental procedure for determining the polycarbonate calibration parameters v_o and p is not completely clear-cut. In particular, the experimenters relied somewhat on certain theories of cosmic-ray abundances. These theories are, in large part, confirmed by the etch rate measurements. The calibration procedure is discussed in some detail in Ref. 6. This potential circularity in the process of assigning the polycarbonate calibration parameters is somewhat hard to assess without accompanying data for ordinary nuclei seen simultaneously in another independent detector, such as nuclear emulsions. Since the emulsion data of Osborne have not been published, we cannot independently verify the Lexan calibration procedure of Price and Shirk. Thus, we must accept as a hypothesis the calibration parameters as reported in Ref. 6.

It is worthwhile to point out that the values of V_o and p which we will use here are different from the values used by the critics[2-6] of Price *et al.* The initial report of Price *et al.* was issued without any calibration of the Lexan response whatsoever; somewhat later a preliminary report of the calibration was informally issued by Price and, in Ref. 6, the final calibration parameters were released. These three reports were mutually inconsistent beyond the stated probable errors. Each of the critical analyses were based upon various interpretations of the earlier, incorrect, versions of the calibrations. As we shall observe later, these differences of calibration assumptions do not produce much difference in the final conclusions regarding interpretations of the Price particle.

4.3. Examination of the Etch Rate Data from the Price Particle

We have considered the problem of treating etch rate data in general terms (see Etch Rate Detectors: Theory and Interpretation) and, in the present chapter, we have identified those polycarbonate sheets from the experiment of Price *et al.* that will provide high quality data. We are now in the position to deal with the actual etch rate data from the Price particle. Figure (3) represents the experimental data reported by Price after we have omitted the questionable polycarbonate sheets and removed the "error bars" (which can only be justified via the statistical arguments of the F-test as applied by Price and Shirk to their data).

Let us develop some intuitive , qualitative, understanding of the trends in these data. First, notice that the zero of the scale on the etch rates has been displaced and that the data lie roughly within a band about a line of constant measured etch rate near $2.9 \mu m/hr$. The dispersion about this hypothetical line of constant etch rate versus penetration depth into the Lexan stack is about $\pm 5\%$ of the mean value of the etch rate. Thus the principal behavior of the data can be identified as : etch rate roughly unchanging with position. Especially with the shifted zero on Fig (3), it is clear that there may be some structure in the dependence of measured etch rate versus position. In particular, there is a possible downward jog in the etch rate at about $1.1 g/cm^2$ after which the etch rates might be thought to rise steadily. The overall magnitude of this possible discontinuity is comparable to the random scatter of the measurements about the mean, however, so that it is impossible to assign much significance to its interpretation. Such apparent structure in the behavior of measured etch rate versus position is frequently seen in etch rate data.[6,16]

It is unjustified to read much significance into the local, point-to-point, variations of any set of experimental data from etch rate measurements. Although we believe that the etch rates reflect the parameter $|Q/\beta|$ as the particles traverse the stack, there are reasons why the form of the dependence of etch rate upon position may not accurately reflect changes in the speed of the incident particle:

a.) The value of the nuclear charge need not remain constant while a particle traverses the polycarbonate stack. Non-catastrophic nuclear interactions or electron-pickup reactions frequently decrease the nuclear charges of incident heavy nuclei by one or two units of charge. We would expect the etch rate data from the track of a nucleus that undergoes such reactions within the Lexan material itself to reflect, on average, some small discontinuity which could be very easily masked by the inherent variations between successive points in the data.

b.) The Lexan itself shows variability within the general statistical dispersion of the measurements from sheet to sheet in its response to ionization. We recall that each polycarbonate sheet provides two of the data points represented on Fig. (3). The two cones on each sheet show correlations in their response. This intra-sheet correlation can be readily seen by examining the etch rate data as represented in Fig. (3) for the tendency of successive data points to become paired.

4.4. Assigning Normal Nuclei to the Price Particle by "Curve-Fitting" to the Etch Rate Data

As previously indicated, we will include into our curve-fitting exercises a "confidence level" computation on the basis of the F-test. These computations must of course be based on some "standard hypothesis." We use the "standard hypothesis" of Price, *et al.* that the particle in question held a constant etch rate throughout the polycarbonate stack. This "straight-line" hypothesis does not correspond to the behavior expected from any known particle; however, it does match the expected behavior of certain conceivable undiscovered particles. It will become clear in our later discussions that this "straight-line" hypothesis does provide the best fit of any particle, discovered or otherwise, which we will be considering. Figure (4.) shows the etch rate data with the "straight-line" hypothesis represented as a solid curve.

Now let us consider how the etch rate data from the Price particle can be matched with the tracks of normal nuclei. The general behavior of $|Q/\beta|$ for normal nuclei, slowing without interacting, can be predicted from the standard stopping power formulae; $|Q/\beta|$ increases as the particle slows. For example, when a nucleus slows to the point that $|Q/\beta| \approx 114$ (the mean value of $|Q/\beta|$ inferred from the etch rate data for the Price particle, $|Q/\beta|$ should be markedly increasing with depth into the polycarbonate stack. Of course, in order for a heavier nucleus to have $|Q/\beta| \approx 114$, it will necessarily be moving faster than a light nucleus.

Trivial calculations using the range-energy relations for nuclei show that, for a fixed initial value of $|Q/\beta|$, heavier nuclei have longer residual ranges in Lexan than lighter nuclei. (Note that this behavior is reversed when the $|Q/\beta|$ qualification is replaced by equating the initial speeds.) Thus, we should expect that heavier nuclei will better fit the etch rate data than will lighter nuclei. Therefore, we want to compare the data to smooth curves which predict the

variation of $|Q/\beta|$ as a function of depth into the Lexan stack for heavy nuclei.

As indicated earlier, we believe that the parameter Q does not change appreciably for nuclei of interest as they slow so that the variations of $|Q/\beta|$ principally reflect variations in the speed, β, of the incident nucleus. Thus, in order to compute the desired smooth curves we need to know the quantitative slowing behavior of heavy nuclei in the polycarbonate stack.

There exist standard formulae which accurately describe the energy loss rate, $\frac{dE}{dx}$, for heavy singly charged particles slowing in media.[22] Knowledge of the energy loss rate, or the stopping power as it is called, and the mass of the incident particle is sufficient to determine the variations of the speed of a particle as a function of its depth into the polycarbonate stack. The customary treatment of stopping powers for heavy nuclei principally involves a simple scaling hypothesis:[23]

$$\left(\frac{dE}{dx}\right)_{Z,\beta} = Z^2\left(\frac{dE}{dx}\right)_{1,\beta}, \qquad \text{(Eq.6)}$$

where: $\left(\frac{dE}{dx}\right)_{a,v}$ = *the stopping power of a nucleus with charge ae, moving at speed v.*

The customary treatment of stopping powers is, however, almost certainly in substantial error when applied as above to heavy nuclei. As discussed in Appendix B, the customary treatment assumes that the first Born approximation is accurate for computing energy transfers to electrons. Since the Born approximation is not strictly valid in this case, we use the corresponding exact theory for the scattering of Dirac electrons from the incident nuclei instead. The details of our improved stopping-power calculations are outlined in Appendix B.

In order to calculate the desired smooth curves, $|Q/\beta(x)|$, for a particle, given its speed and stopping power, we need to know its mass as well. Throughout this section, we employ the phenomenological relation:

$$A = 2.0Q + 0.015Q^{1.8}, \qquad \text{(Eq.7)}$$

where: A = *the mass of the incident nucleus in A.M.U.*

Inherent in this relation is the assumption that the value of Q is close to the atomic number of the nucleus in question, *e.g.* that there are few electrons attached to the nucleus as it traverses the Lexan stack.

4.5. Non-Fragmenting Nuclei "Curve-Fit" to Price Particle

Figs. (5)-(9) compare the Lexan data with various other normal nuclei as hypotheses. Let us briefly consider how well the various normal-nuclei hypotheses agree with the etch rate data. The heaviest element widely believed to be present in the primary cosmic radiation is curium (Q = 96). Examining Fig. (5), we can see that the curium hypothesis appears to agree with the etch rate data; the solid curve does not clash with the data points. In line with our previous comments, we must expect that the hypotheses of normal nuclei for elements heavier than curium, should such particles be present in the cosmic radiation, allow even better fits to the etch rate data than that illustrated on Fig. (5). Figs. (6)-(9) show the hypotheses of various nuclei, all lighter than curium. We can see that for lead (Q = 82) and lighter nuclei, the fit to the Lexan data is quite unconvincing. There might be some debate about the quality of fit to the data by a uranium (Q = 92) nucleus. The F-test confidence level indicates that the fit is not excellent while the solid curve does not appear to clash too badly with the data points to make this to be an unacceptable explanation. Following our policy of treating experimental claims conservatively, we cannot rule out the possibility of a non-fragmenting nucleus with Q above 85.

4.6. Fragmenting Nuclei "Curve-Fitted" to the Price Particle

Of course, as mentioned earlier, nuclei can undergo interactions while traversing the Lexan stack. With the inclusion of nuclear fragmentation, we will also need to augment the confidence level estimates. We can still calculate the F-test confidence level to compare the quality of fit of any saw-tooth curve relative to our "standard hypothesis", however, this confidence level must be multiplicitively diminished by the probability for the fragmentation reactions. This procedure for calculating confidence levels is widely used by Lexan experimenters, and was used by Price in Ref. 6.

To estimate the fragmentation probabilities for normal nuclei, we will use the geometrically computed cross sections as estimated by Fleischer and Walker.[5] Caution is in order because the cross sections needed for the present work fall within a region of parameters Q and β , which must be extrapolated from actual experimental data.[5] Since the actual cross sections show smooth dependence upon the parameters, such an extrapooation procedure is not fraught with more than the usual difficulties. The probability for interaction of the appropriate nuclei can be variously estimated in the range between 0.10 and 0.03 , depending upon the extrapolation procedure used.[5] All estimates of the interaction probabilities yield values which are less than 0.10, so that we will be following conservative procedure by adopting this as the probability for any interaction in computing our confidence levels.

With the inclusion of enough nuclear interactions, we can now, in principle, describe the etch rate data in terms of almost any incident nucleus; if the nucleus is so light as to fit the data poorly on its own right, we would allow it to fragment succesively through the polycarbonate stack. The fragmentations will always allow a better match to the etch rate data in terms of a new saw tooth curve lying more closely within the dispersion of the data points than without the fragmentation. The confidence level does not always increase, however, because the confidence level must always be multiplied by the probability for the fragmentations.

Figures (10) and (11) illustrate the fits to the etch rate data of various singly fragmenting nuclei. We can now see that, whatever the objections to the previous non-fragmenting uranium nucleus, the uranium hypothesis is excellently matched to the Lexan data when one fragmentation is allowed. The singly fragmenting normal-nucleus hypothesis also makes a normal lead nucleus a possibility.

We can proceed toward lighter nuclei, allowing more and more nuclear fragmentations to broaden even further the range of normal nuclei that provide acceptable fits to the etch rate data. Figures (12)-(15) illustrate various attempts to fit multiply fragmenting nuclei to the etch rate data. Hypotheses describing nuclei with more than five fragmentations are poorly matched to the data and need not to be explicitly treated in this manner. Each of these figures represents a critical value of Q. For instance, Fig. 13 shows a Q=74 nucleus, triply fragmenting. We assert that this is the critical value of Q for triply fragmenting nuclei. All nuclei with Q below 74 must have more than three fragmentation interactions to fit the data acceptably.

4.7. "Curve-Fitting" to the Price Particle: Summary and Comparison to Earlier Work

The above essentially duplicates the alternative treatments of the etch rate data by the critics of the original interpretation of Price *et al.* Our results so far can be summarized as follows: Many normal nuclei can be considered to fit the etch rate data of Price and Shirk, especially when nuclear fragmentation is considered. Thus, our conclusions in this respect are in virtually complete agreement with the conclusions of each of the critics. One difference between our conclusions and those of the critics is that we have allowed no more data points than any of the critics so that the set of normal nuclei that we cannot eliminate is larger than the corresponding range for each of the critics.

It is interesting to note that the conclusions reached by each of the critics are borne out by our present analysis irrespective of the differences in the assumed calibration parameters: Each of the critics used values of the power, p, from Eq. (2) which were considerably smaller than the value used here, 5.07 . There are two offsetting effects when the value of p is taken too small. First, the apparent mean value of $|Q/\beta|$ becomes larger (137 for Ref. (2) and $\approx$121 for Refs. 3-5). The practical effect of assuming a value of $|Q/\beta|$ which is, all other effects

aside, too high is to make the etch rate data *harder* to fit with any normal-nucleus hypothesis. The offsetting effect is that, when too small a value of p is assumed, the fractional dispersion of the several etch rate estimates of $|Q/\beta|$ becomes larger. In terms of the equivalent $|Q/\beta|$ values on Figure (3), the mean etch rate is effectively increased, but the spread of the data points away from the mean becomes more significant. The net effect is that the set of permissible nuclei is virtually independent of the details of the polycarbonate calibration. This observation is important because it suggests that our previous conclusions regarding the interpretation of the etch rate data are insensitive to the specific details of the calibration.

4.8. Criticism of "Curve-fitting" Etch Rate Data Points

In the preceding sections, we have assigned certain normal-nucleus hypotheses to the etch rate data from the Price particle. In many cases, the confidence levels for these hypotheses are apparently quite small. It would be conceivable to define the set of normal nuclei that are compatible with the etch rate data to be those whose confidence levels are computed to be greater than some set value, say greater than 10^{-9}, and to disregard all other normal nuclei as hypotheses. If this approach is to be useful we must believe that the numerical values of the confidence levels have the desired significance. For our confidence level calculations to be applicable, we need to know that the data points represent independent, normally distributed values and we need to have accurate estimates of the probability for nuclear interactions to occur. As previously remarked, it is evident from the data points themselves that the etch rate measurements may have some correlation with nearby measurements; this casts doubt on any confidence level calculation based upon "curve fitting" to the etch rate data.

There is some reason even to doubt our estimates for the probability of fragmentations to occur. The estimates that we have used are based on extrapolations from observations of interactions of primary incident nuclei.[5] When we estimate the probability for several such interactions to occur, we are in effect assuming that the nucleus which emerges from a previous interaction has the same interaction length as the same species would have were it of primary origin, i.e. that secondary nuclei have the same interaction cross sections as do primary nuclei. This hidden assumption of ours has been challenged by several observers outside the context of the Price particle. These workers make a case that secondary nuclei have considerably shorter interaction lengths than do primary nuclei. This possibility is somewhat non-intuitive and we find the experimental techniques of these workers to be equivocal; there has been at least one publication which has questioned their experimental techniques and has arrived at conflicting conclusions.[25] We cannot, however, clearly settle this controversy here, so that there may be reason for some observers to question our estimates for the probabilities of nuclear interactions to occur.

As mentioned earlier, it is possible for nuclei incident upon the polycarbonate stack to pick up electrons as they slow. The practical effect of such electron pickup is similar to nuclear collisions; the net charge on the ion is reduced and its speed is essentially unchanged. Unlike the case in nuclear fragmentation, the cross sections for electron pick-up are not even known to within an order of magnitude in the realm applicable to the Price particle. Data do not exist for electron pick-up by nuclei with $Z>26$ moving with relativistic speeds, and the reliability of an extrapolation from existing measurements is clouded by the rapid variation of the cross sections with the charge and speed of the incident ion. Our knowledge of this process is so incomplete that we are reluctant to begin creating the curves which would be appropriate to repeat our previous curve-fitting procedure, allowing for electron pick-up.

For the reasons stated above, we believe that curve fitting to etch rate data points can provide conclusions of only moderate certainty. We are led to formulate for the etch rate data points for the Price particle a novel interpretation which depends solely upon the measured thickness of the polycarbonate stack and the inferred mean value of the parameter $|Q/\beta|$. This technique will allow us to arrive at conclusions which are completely independent of the variation of the measured etch rates with depth into the stack; completely independent of the probabilities for nuclear interactions or electron pick-up to occur, and completely independent of statistical arguments.

5. Treating Etch Rate Data in a Non-Statistical Way

We will now develop a new method for treating the etch rate data for the Price particle. This method is based on our relatively well-founded estimates for the total rates of energy loss by the incident particle. The only aspect of the data needed for this method to be applied is the mean value of the measured etch rate together with the thickness of the experimental stack. In particular, there is no need to deal with statistical arguments regarding the response of the various polycarbonate sheets to the incident particle. This method allows conclusions to be drawn completely independently of the possible sequences of nuclear fragmentation collisions and the possible sequences of electron attachment to the incident nucleus. This method allows us to state with high confidence that the particle in question could not have been any normal nucleus whose initial speed was less than $0.55c$.

In any slowing medium, the energy loss rate for a nucleus as it decelerates is nearly proportional to $|Q/\beta|^2$. In particular, the energy loss rate increases faster than linearly with $|Q/\beta|$. It is easily verified by a simple variational calculation that among all functional forms for $|Q/\beta|(x)$ subject to the restriction that $<|Q/\beta|(x)>=114$, the straight line at $|Q/\beta|(x)=114$, independent of x, leads to the smallest total energy loss by the incident particle. That the straight line functional form for $|Q/\beta|(x)$ happens to fit the etch rate data well is a coincidence

and is in no way related to the above conclusion.

This simple observation allows us to place a rigorous bound upon the initial speed of the nuclei which could ever be conceived compatible with the etch rate data for the Price particle. It is conceptually simplest to work from the bottom of the polycarbonate stack upwards. At the bottom of the stack the particle in question certainly had some kinetic energy; it penetrated the disallowed sheet, sheet 35. We certainly know that the particle had kinetic energy at the bottom of sheet 34; we thus may place a lower bound on the kinetic energy of the particle at each position within the polycarbonate stack by appealing to our above observation:

$$KE(x) \geqslant KE_{\min}(x), \qquad \text{(Eq.8)}$$

where: x= *the distance "above" sheet number* 35,

$KE(x)$= *the kinetic energy of the particle in question,*

$KE_{\min}(x)$= *a function which satisfies the following*

differential equation:

$$\frac{dKE_{\min}}{dx} = -\left(\frac{dE}{dx}\right)_{Q(x),\beta(x)} \quad ; \quad KE_{\min}(0)=0,$$

where: $\beta(x)$ = *the speed of the nucleus*

when it has kinetic energy $KE_{\min}$,

and $|Q/\beta|(x)=114$ *exactly.*

Any particle which starts at position x above the bottom of Lexan sheet 34 with energy less than $KE_{\min}(x)$ will necessarily come to rest before reaching the bottom of the stack *regardless* of its fragmentation behavior, provided that it meets the restriction that $<|Q/\beta|(x)> = 114$.

5.1. Treating the Etch Rate Data from the Price Particle in a Non-Statistical Way

It is interesting to note the implied behavior of a nucleus which obeys the optimal solution $KE(x) = KE_{\min}(x)$. This nucleus would penetrate thickness x of the stack, come to rest at the bottom of the stack having lost only $KE_{\min}(x)$ of energy while maintaining $<|Q/\beta|(x)>=114$ this nucleus would also have $|Q/\beta(x)|=114$ precisely for all x. Since the particle would come to rest at $x=0$, $Q(x)$ would necessarily also vanish as x approached zero to maintain the ratio $|Q/\beta(x)|=114$. Therefore, in conclusion, we see that for a nucleus to exhibit the optimal energy loss behavior, that nucleus must successively lose every one of its charges via interactions.

Of course, we do not seriously mean to propose that it is reasonable to describe the Price particle as, for instance a $Z=70$ nucleus which underwent 70 separate nuclear interactions, losing one unit of charge in each collision; that is, in our opinion, quite an absurd possibility. Our intention, however, is to use the variational calculation and its optimal solution to place a bound upon the speed of the particle in question when it was at the top of the polycarbonate stack. We will specify this bound by computing the initial speed of the unrealistic optimal solution which we have described above. All other nuclei, regardless of their fragmentation behavior will necessarily have greater initial speeds (provided that these nuclei penetrate the stack and maintain $<|Q/\beta|(x)>=114$ Given that we have used an accurate energy loss formula and that we correctly know the thickness of the material traversed, our resulting lower bound upon the initial speed of the incident particle will be correct.

One certainly may wonder whether we are being too wasteful by computing our bound upon the speed with such an unrealistic optimal behavior; one cannot doubt that the lower bound upon the initial speed is a correct lower bound. There are, for instance, many ways that physical nuclei differ from the optimal behavior: The optimal solution represents a particle which decreases continuously in charge as it penetrates the stack while, in fact, the physical charge is in units of e. The optimal solution exhibits precisely the straight-line dependence of $|Q/\beta(x)|$ while the actual measurements show some scatter away from the straight-line behavior. The optimal solution loses every one of its charges via interactions while it is unlikely that a physical nucleus undergoes very many interactions. The optimal solution comes to rest above polycarbonate sheet 35 while a physical nucleus would probably emerge with considerable residual kinetic energy. Each of these inaccuracies of the optimal solution implies that we could be too conservative by accepting only our proposed lower bound upon the incident speed computed from the optimal solution. We shall see in a later section that our apparent conservatism in this matter has not greatly modified the quantitative conclusions based upon the etch rate data.

To compute our rigorous lower bound on the initial speed of the Price particle as a normal nucleus, let us define the effective thickness of the experimental stack over which the particle has been measured to have $<|Q/\beta|>=114$. We certainly must include those sheets of Lexan that were allowed into our restricted data set in the previous sections. In addition to the sheets from which dependable data may be obtained, we add sheet 12. No data were taken from sheet 12. Sheet 12 is represented in Fig. (3) as a gap among the data points at about $0.65 g/cm^2$ depth into the polycarbonate stack. We believe that the measured etch rates for the 12 data points above sheet 12 and the 44 data points below sheet 12 show that the particle had a smooth behavior of etch rate above as well as below sheet number 12. These two smooth sections appear to match up quite well across the gap so that we think it appropriate to assume that the

particle had smooth behavior in the missing sheet, 12. Therefore, we consider it appropriate to include the interpolation through the 4% of that total depth which lies within sheet 12. Of course, the length of path must be calculated to take into account the 11^{o} angle of inclination of the track from the vertical.

We will want to anticipate the possible outcomes of the unpublished $|Z/\beta|$ measurements in the nuclear emulsions of Osborne: It is well known that accurate measurements of the physical parameter $|Z/\beta|$ for incident nuclei can be obtained from properly calibrated nuclear emulsions.[21] If the assessment of $|Z/\beta| \approx 114$ is substantiated in the thick nuclear emulsions, the thickness over which the ionization rate remained constant will be expanded from $0.897 g/cm^2$ to $1.104 g/cm^2$. If the thin nuclear emulsions were to be added, the thickness would be further increased to about $1.25 g/cm^2$.

Calculated values of β_{min} are summarized in Table (2). For $<|Q/\beta|>=114$, we calculate $\beta_{min}=0.561$. These rigorous bounds on the class of normal nuclei are seemingly close to our earlier class of normal nuclei which could easily enough be imagined to fit the etch rate data. For instance, we calculate, for penetrating the $0.897 g/cm^2$ of the polycarbonate stack, that the optimal solution with $<|Q/\beta|>=114$ has initial speed equal to $\beta=0.561$. This optimal solution describes the behavior of a $Z=64$ nucleus which enters the top of the stack with $\beta=0.561$ and which, as it slows to a stop progressively loses each one of its charges via nuclear interactions. For Figure (15), we calculated by means of curve-fitting to the same etch rate data that a $Z=68$ nucleus with initial speed $\beta=0.62$ could penetrate the same thickness of the polycarbonate stack needing to lose only 10 of its charges via nuclear interactions. Thus, there is a drastic increase in the necessary number of charges to be lost when the initial speed is changed from $\beta=0.62$ to $\beta=0.561$.

This increase occurs because of the progressive steepening of the function $|Q/\beta|(x)$ as β assumes smaller values. Examining Fig.(15), we consider the behavior of each of the smooth segments of the sawtooth curve as they cross the value $|Q/\beta|=114$. On Fig.(15) there are six such segments, each successive segment corresponds to a nucleus of lower charge than its predecessor. Thus, at the point where each curve crosses the value $|Q/\beta|=114$, each successive nucleus is slower than was its predecessor. We can see on Fig.(15) that the slopes of the smooth curves are becoming successively steeper. If we were to imagine a $Z=64$ nucleus incident with $\beta=0.561$, the successive smooth segments would become so steep that the nucleus would necessarily dissipate all of its charges before penetrating to the bottom of the polycarbonate stack.

We have mentioned that nuclei may have other than nuclear interactions while penetrating the polycarbonate stack. Incident nuclei may pick up electrons as they slow in the polycarbonate medium. It has been suggested in an unpublished pre-print that electron pick-up may

be responsible for the apparent penetrating behavior of the Price particle.[26] As we have mentioned before, it is very difficult to estimate the probabilities for any sequence of electron pick-up. Fortunately, our present non-statistical way of treating the etch rate data makes no reference to the probabilities for nuclear interactions so that we may equally well apply our present formalism to the case of electron attachment. The only practical difference between the two cases is that we must assume different formulae for the stopping power of the incident ions together with a different assumed rate of mass loss: As an ion attaches charges, its mass does not change appreciably while its net charge is decreased. As a nucleus loses charges via nuclear interactions, its mass is diminished by approximately the same fraction as its charge is diminished.[47] We explicitly outline our energy loss rate calculations in Appendix B.

Table (3) shows the results of our calculations allowing for electron pick-up. The results are presented analogously to those of Table (2). We can see that in the limit of the optimal solutions, nuclear fragmentations allow a slightly slower initial speed than does electron pick-up. Thus, we conclude that the optimal solution for nuclei incident upon the polycarbonate stack is for nuclei with initial speed β=0.561. We can have the highest confidence in the conclusion that, if the Price particle is a normal nucleus, it necessarily must have had initial speed in excess of β=0.561, or, for a round number, β=0.55. This final estimate for β should also allow for the possibility of both nuclear fragmentation and electron pick-up occurring along the particle's path.

6. Can the Etch Rate Data Allow the Price Particle to be a Dirac Monopole?

In this work, we have considered only part of the data bearing upon the Price particle, we have not considered the nuclear emulsion data. On the basis of the data we have considered, we cannot rule out any of a rather broad class of normal nuclei as hypotheses to explain the event. It may, therefore, be premature even to discuss how well the data fit exotic hypothetical explanations. The possibility that this particle might actually be a Dirac monopole is, of course, the cause of its notoriety. Therefore, we feel that it is proper to show why the Price particle probably *cannot* be a magnetic monopole.

Since the polycarbonate detector is assumed to record the distant encounters for incident nuclei with resting electrons, we at first should expect that a Dirac monopole of strength e/α would leave etch cones corresponding to those from a nucleus which had $|Q/\beta|\approx 137$. The basis for this statement lies in the (relativistically correct, non-quantum mechanical) standard expression for the differential scattering cross section for scattering of spinless "electrons" from a static magnetic monopole potential center.[27] For the smallest center-of-mass scattering angles, the monopole scattering cross section becomes equal to the Rutherford scattering cross section for electrons scattering from a nucleus with the parameter $|Q/\beta|=1/\alpha$. Since this result obtains

regardless of the speed of the hypothetical monopole, we should naively expect to see in etch rate data a characteristic signature for monopoles.[28] The etch rate measurements would yield estimates corresponding to a nucleus which held its value of $|Q/\beta| \approx 137$ constantly throughout the depth of the stack regardless of the assumed initial speed or the slowing behavior of the monopole.

It, thus, might at first appear that a Dirac monopole could never be consistent with the measured value $|Q/\beta| \approx 114$. It was, however, quickly pointed out by S.P. Ahlen that one must expect that, as a Dirac monopole comes to rest, its apparent value of $|Q/\beta|$ drops continuously from the expected value of 137 to zero. Ahlen qualitatively calculated the behavior of the polycarbonate etch rate with respect to speed of Dirac monopoles. His calculation was based on the treatment of stopping powers by Fermi.[30] Table (4) summarizes the results of Ahlen's calculation. Taking his results at face value indicates that the Price particle must have a speed $\beta \approx 0.28$ to be interpreted as a Dirac monopole.

The calculation of Ahlen uses the following assumptions: First, that the Fermi theory of energy loss rates accurately estimates the amount of energy loss into a tiny cylinder in the polycarbonate detectors. These energy losses can then be computed in closed form for all nuclei moving at all speeds and for Dirac monopoles moving at all speeds. Second, that the measured etch rate in the polycarbonate is determined solely by the energy loss into a cylinder whose radius is of a certain size. This second assumption allows one to identify families of nuclei and monopoles which should produce the same mean values of measured etch rates. In particular, at each speed of a monopole of charge e/α it should produce the same etch rate as one family of nuclei. Third, the specific numerical estimates from the etch rate data (for instance, the number $|Q/\beta|=114$) are assumed to have a particular physical significance. More specifically, it is assumed that all particles that have etch rate measurements of $|Q/\beta|$ of any fixed value lie within the family of nuclei and monopoles which includes an ultra-relativistic nucleus with atomic number $|Z|=|Q|$ exactly. In particular, this latest assumption allows one to make quantitative predictions for the speed of an incident monopole which would be needed to produce etch rate measurements indicating $|Q/\beta|=114$.

Granted the three underlying assumptions stated above, the model of Ahlen allows, in the language of this present work, quantitative estimates of the behavior of the function $Q(Z,\beta)$. We have not included any such explicit model into our earlier efforts to define the set of normal nuclei which could explain the Price particle; our results regarding these normal nuclei are more general than could be obtained from the model of Ahlen because we did not make specific assumptions regarding the nature of track formation in polycarbonate detectors. Ahlen estimates the value of β for monopoles to produce the measured etch rate of the Price particle. His best estimate is $\beta=0.28$, while the monopole interpretation of the experimental data of

Price *et al.* requires a monopole with speed near $\beta=0.55$[1,6] (This restriction on the speed of monopole arises from certain interpretations of the nuclear emulsion data which we shall not be considering here.)

This apparent quantitative disagreement between the model predictions of Ahlen and the experimental claims of Price *et al.* is ascribed by Ahlen[29] and, later, by Price[6] to failings of Ahlen's model due to the uncertainty of its assumptions and calculations together with experimental uncertainties from the etch rate data. It is not surprising that models predicting such complex phenomena as chemical etch rates in polymeric media should have large inherent uncertainties. We think it appropriate to attempt to corroborate the calculations of Ahlen and, if possible, to try to clarify the origins of the apparent disagreement between the model of Ahlen and the experimental interpretation of Price *et al.*

We will calculate similarly to Ahlen, making certain discretionary changes in his model assumptions. Our assumptions can be outlined in parallel with our previous outline of Ahlen's assumptions. We assume: First, that the Bohr theory of energy loss may be used to calculate the energy lost into a tiny cylinder by incident nuclei and monopoles.[30] Thus, we do not use the Fermi treatment as does Ahlen; this difference is insignificant because the two theories agree quantitatively in the regions we shall be considering.[30] Second, we assume that the measured etch rates can be predicted by calculating the energy loss into the identical size of cylinder as does Ahlen. Thus, there is no difference whatever between the two models in this respect. Third, we assume that the specific numerical estimates from the etch rate data (for instance, the number $|Q/\beta|=114$) have a particular physical significance. More specifically, we assume that all particles having $|Q/\beta|$ measurements of any fixed value, say 114, lie within the family of nuclei and monopoles which contains an iron nucleus with $(Z=26)/\beta=|Q/\beta|$ exactly.

Our third assumption thus differs somewhat from Ahlen's third assumption; he chose to consider ultra-relativistic nuclei as the calibration standard while we choose iron nuclei. We choose iron for this purpose because Price reports that he has used iron in his calibration.[6] We note here that there exists no calibrated source of ultra-relativistic nuclei heavy enough to register etch cones in Lexan so that it seems to us unlikely that a convincing case could be made that Price *et al* have ever calibrated their detectors with respect to ultra-relativistic nuclei.

Let us now start our quantitative calculations. First we calculate the energy loss into an arbitrary tiny cylinder of the polycarbonate following the textbook treatment of Bohr's formalism by J.D. Jackson (complete details may be obtained from that reference.)[30] The electrons of the slowing medium are approximated as being harmonically bound at frequency determined by the Planck relation, $\omega_0=I$. Here I is the characteristic binding energy of electrons in the polycarbonate, $I=69.5eV$ The energy transfer to such a harmonically bound charge is precisely:

$$\Delta E = \frac{\pi}{m}|\tilde{F}(\omega_0)|^2, \qquad \text{(Eq.9)}$$

where: $\tilde{F}(\omega) = \frac{1}{\sqrt{2\pi}}\int_{-\infty}^{\infty} F(t)e^{-i\omega t}dt,$

F= the perturbing force on the electron.

The electromagnetic fields surrounding an electric charge moving along the $\hat{z}$ axis are

$$E_z = \frac{-Ze\gamma\beta t}{(b^2+\gamma^2\beta^2t^2)^{3/2}}, \qquad \text{(Eq.10)}$$

$$E_x = \frac{Ze\gamma\beta b}{(b^2+\gamma^2\beta^2t^2)^{3/2}},$$

$$B_y = \beta E_x,$$

all other components of $\overline{E}$ and $\overline{B}$ *vanish.*

where: *b= the impact parameter of the incident nucleus with respect to the electron.*

while those from a moving magnetic charge are:

$$B_z = \frac{-Ye\gamma\beta t}{(b^2+\gamma^2\beta^2t^2)^{3/2}}, \qquad \text{(Eq.11)}$$

$$B_x = \frac{Ye\gamma b}{(b^2+\gamma^2\beta^2t^2)^{3/2}},$$

$$E_y = -\beta B_x,$$

all other components of $\overline{E}$ and $\overline{B}$ *vanish,*

where: *Ye= the magnitude of the magnetic charge in esu.*

Performing the Fourier transforms yields:

$$\tilde{E}_z(\omega) = \frac{-iZe}{\beta\gamma b}\sqrt{\frac{2}{\pi}}\frac{\omega b}{\gamma\beta}K_0\left(\frac{\omega b}{\gamma\beta}\right), \qquad \text{(Eq.12)}$$

$$\tilde{E}_x(\omega) = \frac{Ze}{b\beta}\sqrt{\frac{2}{\pi}}\frac{\omega b}{\gamma\beta}K_1\left(\frac{\omega b}{\gamma\beta}\right),$$

for incident nuclei, and, for incident monopoles:

$$\tilde{E}_y(\omega) = -Ye\sqrt{\frac{2}{\pi}}\frac{\omega b}{\beta\gamma}K_1\left(\frac{\omega b}{\gamma\beta}\right) \qquad \text{(Eq.13)}$$

Thus we can compute the restricted energy loss for incident electric and magnetic charges as being:

$$\left(\frac{dE}{dx}\right)_{>b_{min}} = N_0\frac{4\pi}{m}\left(\frac{Z\alpha}{\beta}\right)^2\left(\frac{\omega_0}{\gamma\beta}\right)^2\int_{b_{min}}^{\infty}\left\{\frac{1}{\gamma^2}K_0^2\left(\frac{\omega_0 b}{\gamma\beta}\right)+K_1^2\left(\frac{\omega_0 b}{\gamma\beta}\right)\right\}b\ db, \qquad \text{(Eq.14)}$$

$$= N_0\frac{4\pi}{m}\left(\frac{Z\alpha}{\beta}\right)^2\left\{\xi K_1(\xi)K_0(\xi) - \tfrac{1}{2}\beta^2\xi^2\left[K_1^2(\xi)-K_0^2(\xi)\right]\right\},$$

$$\textit{where: } \xi=\frac{\omega_0 b_{min}}{\gamma\beta},$$

and,

$$\left(\frac{dE}{dx}\right)_{>b_{min}} = N_0\frac{4\pi}{m}(Y\alpha)^2\left(\frac{\omega_0}{\gamma\beta}\right)^2\int_{b_{min}}^{\infty}K_1^2\left(\frac{\omega_0 b}{\gamma\beta}\right)b\ db, \qquad \text{(Eq.15)}$$

$$= N_0\frac{4\pi}{m}(Y\alpha)^2\left\{\xi K_1(\xi)K_0(\xi) - \tfrac{1}{2}\xi^2\left[K_1^2(\xi)-K_0^2(\xi)\right]\right\},$$

respectively. These formulae represent the rates of energy loss only to those electrons of the slowing medium which originally lay outside distance b_{min} of the path of the incident particle. An assumption common to the two treatments of this problem is that $\left(\frac{dE}{dx}\right)_{>b_{min}}$ corresponds to the energy deposited within a tiny cylinder.

At each given speed we can now compute the apparent energy loss rate of a Dirac monopole in polycarbonate (I=69.5eV) in terms of the value of $\left(\frac{dE}{dx}\right)_{>b_{min}}$ for the monopole and compare this to the corresponding value of $\left(\frac{dE}{dx}\right)_{>b_{min}}$ for an iron nucleus. More specifically, at each given speed of monopole we find the particular value of $|Q/\beta|$ for an iron nucleus which will have the identical restricted energy loss rate as does the monopole. As stated earlier, we take the identical value for the parameter b_{min} as in Ref. 29, b_{min}=0.117 *Angstrom*. We thus can produce an alternative version of Table (4) based on our present treatment, Table (5). We can see that, according to our calculations, a Dirac monopole must be very slow indeed to produce the measured Lexan signature of $|Q/\beta|$=114 ; if our results are taken at face value, we must have β=0.14.

The magnitude of the difference between Ahlen's and our estimates of the speed needed for a Dirac monopole is due to the difference in our assumed set of calibration nuclei. We believe that our assumption that the polycarbonate data were calibrated with respect to non-relativistic iron nuclei is a more accurate description of the experimental procedures of Price *et*

al. than is Ahlen's assumption of calibration with resect to ultra-relativistic nuclei. We, therefore, believe that our estimate of $\beta=0.14$ for a monopole to fit the Price particle is more accurate than Ahlen's estimate of $\beta=0.28$. In any event, we must notice that both estimates of β, 0.28 and 0.14 are far below the value of $\beta\approx 0.5$ needed for the monopole interpretation of Price *et al.* We conclude that it is quite unlikely that the Price particle can be interpreted as a Dirac monopole because its measured etch rate differs so greatly from the values expected from monopoles with speed $\beta\approx 0.5$.

7. Etch Rate Data: Summary and Conclusion

We have proposed a large number of normal-nucleus hypotheses which can be considered compatible with the etch rate data for the Price particle. These hypotheses are summarized in terms of the permissible set of initial charges and speeds of incident nuclei which might ever give rise to etch rate data similar to those measured. The set of acceptable normal nuclei contains all nuclei with $Z\geqslant 63$, each having Z/β close to the value 114 . No normal nucleus with initial speed less than $\beta=0.55$ can ever be considered compatible with the etch rate data; this holds true regardless of any assumed sequence of nuclear fragmentation reactions and any assumed sequence of electron pick-up reactions.

We have briefly considered the possibility that the Price particle might have been a Dirac monopole. By pursuing an alternative calculation we have considered Ahlen's estimate that a monopole with speed $\beta=0.28$ could produce the etch rate data of Price *et al.* We estimate that the needed speed is $\beta=0.14$. The differences between our calculation and Ahlen's principally reflect differing assumptions about the set of calibration nuclei; we have taken iron nuclei as the calibration set while Ahlen has taken ultra-relativistic nuclei. We believe that our choice of iron as the calibration standard reflects the experimental procedures of Price *et al.* Independently of the proper choice of calibration standard, we observe that our model and Ahlen's model both estimate that a monopole should be slower than the speed $\beta\approx 0.5$ needed for interpretation of the Price particle as a monopole. We conclude that it is quite unlikely that the Price particle could be a Dirac monopole quite independently of the large apparent discrepancy of that interpretation with previous experimental searches.

Let us briefly compare our conclusions from the etch rate data to those of other authors.[1-6] Table (6) summarizes our interpretation of the results of the various authors when their analyses of the etch rate data alone are used. We find no conflict whatsoever between our results and the conclusions from Refs. 2-5; therefore, we find complete agreement with each of the critics of the original paper of Price *et al.* Of course, we do find unavoidable disagreement with the conclusions of Ref. 1. In addition, we find considerably stronger conclusions in Price's reply to the critics (Ref. 6) than we can support by our present analysis. We attribute these

differences to the higher level of certainty allowed by our analysis: the analysis of Ref. 6 is based upon "curve-fitting" with the use of confidence levels from the F-test.

In Ref. 5, Fleischer and Walker make statements which might be taken to imply that normal nuclei with initial speeds below β=0.60 are too improbable to fit the etch rate data. Fleischer and Walker use "curve-fitting" to draw this conclusion. By comparison, we have proved that initial speeds below β=0.55 are ruled out without regard to probabilities. These two conclusions are in agreement of course; we have simply taken a more conservative stance with respect to the desired level of certainty. We do not disagree with the possibility that $\beta < 0.6$ are completely unrealistic hypotheses for normal nuclei; it is, however, possible for us to prove only our stated limits.

8. Photographic Cerenkov Detectors

8.1. Introduction

Photographic Cerenkov detectors were in the detector packages of the balloon flights we have been discussing. Although this detector was still in the development stage at the time of the flights, the investigators hoped it would provide data that would allow accurate estimation of the speed of the incident particles. As we have shown, knowing the speed of the particles makes the interpretation of the polycarbonate tracks a relatively straightforward matter. In their identification of a magnetic monopole, Price *et al.* claimed that the absence of a Cerenkov image in the photographic Cerenkov detector indicated that the particle in question had a velocity less than 0.68 c. This velocity and the etch rate of the polycarbonate detector were important pieces of the evidence that led to the monopole claim. However, after a thorough evaluation of the Cerenkov detector we find that the technique has fundamental weaknesses and we believe it is doubtful that the photographic Cerenkov detector could ever have performed as intended.

Today, the photographic Cerenkov detector technique is still an unproved experimental tool. Complete specifications of the device and details of its interpretation are not published. Therefore, we must base our discussion of the limitations of this device principally on the manufacturer's specifications for the photographic recording emulsion. The reader is referred to Ref. 31 for a more complete and general description of the physical basis of photography. Our conclusions can be summarized: 1.) The photon signal available to produce images that are unambiguous is weak by a factor of 100 below the manufacturer's nominal sensitivity. 2.) The characteristic features, which need to be resolved in order unambiguously to identify the images as being originated by Cerenkov radiation, are so small that they would become obscured by vigorous chemical development. 3.) The photon signal from Cerenkov radiation in this device is so short that it might leave no permanent photographic image regardless of its intensity. 4.) There is far more energy deposited in all regions of the recording emulsion by the ionization accompanying the passage of any nucleus than by Cerenkov photons. 5.) It is possible that all of the images previously studied with this kind of detector could be due at least in part to sources other than Cerenkov radiation. In conclusion, it does not appear that this detector yields data good enough to warrant serious consideration.

8.2. Theory of Operation

The concept behind the Cerenkov detector is elegantly simple.[32] Figure 16 represents the photographic Cerenkov detector schematically. A fast nucleus impinging from above will cause Cerenkov radiation to be emitted as it traverses the transparent dielectric radiator material. These Cerenkov photons would be recorded by an ideal photographic emulsion as a conic section with the nuclear path as a focus. The size and shape of this ideal photographic image is determined solely by the speed and direction of the incident nucleus, independently of its charge. Thus, the photgraphic Cerenkov detector should ideally provide an excellent companion to ionization measurements, which record essentially the quantity $|Z/\beta|$ independently of speed, β.

8.2.1. Marginal Sensitivity

Let us consider the response of the Cerenkov detector to a vertically incident, fully stripped, nucleus of speed β and charge Ze. The expected Cerenkov photon energy flux impinging upon the recording emulsion is given by:

$$\frac{dE}{d\omega dA} = \frac{\omega Z^2 \alpha}{4\pi\rho} \sin 2\theta_c \qquad \text{(Eq.16)}$$

$$\textit{when:}\quad 0 < \rho < \Delta \tan\theta_c$$

where: ρ= *the cylindrical radius*

Ze= *the charge on the nucleus,*

β= *the speed of the nucleus,*

α= *the fine structure constant,*

θ_c= *the Cerenkov half−opening angle,* $\cos\theta_c = \frac{1}{n\beta}$,

$n(\omega)$= *the refractive index of the radiator medium,*

ω= *the angular frequency of the emitted photon,*

Δ= *the thickness of the radiator.*

We will want to find a rigorous upper bound to the photon energy flux. First, observe that there are rigorous estimates for the energy flux of expression (16). If we assume that the recording emulsion is insensitive outside some interval of photon frequency, $\omega_1 \leqslant \omega \leqslant \omega_2$, we

can compute the precise value of the relevant energy flux

$$\frac{dE}{dA} = \frac{Z^2\alpha}{4\pi\rho}\int_{\omega_1}^{\omega_2}\omega\sin(2\theta_c(\omega))\,d\omega. \qquad \text{(Eq.17)}$$

The function $\sin(2\theta_c)$ assumes its maximum value at some particular frequency, ω_o, in the interval $[\omega_1, \omega_2]$. We can now compute a rigorous upper limit on the energy flux

$$\frac{dE}{dA} \leqslant \frac{Z^2\alpha}{4\pi\rho}\sin[2\theta_c(\omega_0)]\left[\frac{\omega_2^2}{2} - \frac{\omega_1^2}{2}\right] \qquad \text{(Eq.18)}$$

We will want to estimate the appropriate values of ω_1 and ω_2 for the recording emulsion used in all cases by Pinsky, Eastman Kodak EK2485.[1,6,14,33,34] Figure (17) shows the spectral sensitivity of EK2485 as measured by the manufacturer.[35] We take the values of ω_1=1.6eV and ω_2=4.25eV from Figure(17). Also from Fig. (17) we estimate the nominal sensitivity of the recording emulsion to be 0.04 erg/cm^2 across the useful range of frequencies. To reduce the question of the relative sensitivity of the recording emulsion to dimensionless terms, we can divide our rigorous upper bound to the photon energy flux by the liberal estimate of the nominal sensitivity of the emulsion

$$\frac{1}{\Phi_0}\frac{dE}{dA} \leqslant 1.0x10^{-4}\frac{Z^2\sin[2\theta_c(\omega_0)]}{\rho} \qquad \text{(Eq.19)}$$

where: ρ *is measured in* μm.

As we shall soon see, there is a relatively prodigious competing source for formation of images on the recording emulsion, namely the ionization energy which is incidentally deposited with the passage of the nucleus to be observed. This ionization energy deposition must be expected to leave an image similar in appearance to those seen in nuclear emulsions; it should be relatively dark at the center with darkness tapering off gradually with increasing distance from the center, becoming indistinguishable from background at some large distance.

In order clearly to distinguish an image on the recording emulsion as being caused by Cerenkov radiation, it is necessary to observe the characteristic implied sharp demarcation of the edge of the illuminated region. It is, therefore, at the very least, necessary to observe the darkening somewhere at the edge of the image. The radial distance to the edge of the Cerenkov photo illumination is $\Delta\tan\theta_c$, so that we compute the relative strength of the energy flux at the position of the edge using Eq. (19):

$$\frac{1}{\Phi_0}\frac{dE}{dA} \leqslant \frac{2.x10^{-4}Z^2}{\Delta}\cos^2\theta_c(\omega_0). \qquad \text{(Eq.20)}$$

The thicknesses for the transparent radiator in the two Cerenkov detectors in balloon flight 2 have been reported to be $100\mu m$ and $200\mu m$, respectively.[6] We will use the thinner of the two thicknesses begause this choice is more optimistic with respect to the success of the detector. Furthermore, for purposes of this discussion, we will use $Z=105$, the highest charge seen on any nucleus to date, and we will also assume that $\theta_c(\omega_o)=45^o$, both very optimistic estimates. The final result of these calculations can be summarized as

$$\frac{1}{\Phi_0}\frac{dE}{dA} < 0.11 \qquad \text{(Eq.21)}$$

at the edge of the Cerenkov photon image.

In order to support the experimental claim that the detector of Pinsky could not miss Cerenkov radiation from any nucleus, it must be shown, at the very least, that a photon signal 100 times weaker than the nominal sensitivity of the recording emulsion could not have escaped detection!

8.2.2. Image Blurring

In addition to detecting the very weak Cerenkov photon signal, the experimenter must be certain that he has not missed any discontinuity in the image darkness which would indicate the edge of the Cerenkov photon signal. The edges of the images must be clearly resolved before they can be attributed to Cerenkov radiation with certainty.

Especially when photographic emulsions are vigorously developed, such features as the edges of an image become blurred; the more heavily processed a film is, the more blurred its images become. Figure (18) shows the modulation transfer function for EK2485 under two processing procedures.[35] The modulation transfer function can qualitatively be interpreted as the ratio of the amplitude of the variations in developed darkness to the amplitude of the variations in exposure intensity from a spatially modulated photon signal. Figure (18) clearly shows the tendency for increasingly vigorous processing to obscure larger features of the emulsion. For purposes of orientation, the largest possible Cerenkov image would be $200\mu m$ wide, while the typical Cerenkov image should be about $50\mu m$ wide. Remembering that it is essential to be able to resolve the edges of a Cerenkov image, one must be able to resolve features not much wider than $5\mu m$. Such a feat would be very difficult even with the gentler processing technique indicated on Fig. (18), and becomes more difficult for any processing technique more vigorous than that indicated on Fig. (18).

8.2.3. Short-time Reciprocity Failure

One very important consideration is the so-called short-time reciprocity failure of the photographic emulsion. A related phenomenon, *long-time* reciprocity of failure, is known in astronomic photography.

In common practice, the response of photographic emulsions depends only upon the total energy deposited in the recording emulsion and is independent of the duration of the exposure to the photons. When the emulsion is exposed beyond a certain time duration, however, the recording efficiency of the emulsion drops so that a higher *total* of energy deposition is needed to achieve any specified level of emulsion darkening. This is the familiar reciprocity failure, or more accurately, long-time reciprocity failure. At the opposite extreme, when the exposure becomes very short, there is a similar drop in the effective efficiency of the recording of photographic emulsions. This so-called "short-time reciprocity failure" has long been known; specifications for this behavior are routinely provided with high speed photographic emulsions.

Cerenkov photon pulses are notably brief, being very close to theoretical bounds in the optical frequencies. For the photographic Cerenkov detector as described, the Cerenkov photon pulse certainly is shorter than $10^{-12}s$, so that to get estimates of the effect, one must extrapolate from published measurements. Figure (19) shows present measurements of the reciprocity characteristics of EK2485 photographic emulsion.[35] The vertical scale can be interpreted as the relative efficiency of an erg/cm^2 deposited by photons. The relevant extrapolation is to estimate where the solid curve will pass through the shaded region. While this cannot be reliably done, we can see from the measured data that the relative efficiency is falling for pulses briefer than $10^{-6}s$. It is conceivable that the curve may make a dramatic drop between $10^{-6}s$ and $10^{-12}s$.

Another critical point which can be raised on the basis of Fig. 6 of Ref. 35 is that, for faint images, the effects of short-time reciprocity failure are apparently more extreme than for strong images; the desired Cerenkov radiation images certainly must be quite faint on the basis of our Eq. (21), so that we might be led to believe that our conclusions on the basis of Fig. (19) may be optimistic in comparison to the actual performance of the detector.

Another factor to consider with respect to reciprocity failure in the photographic Cerenkov detector is that reciprocity failure and marginal sensitivity are frequently exacerbated by low temperatures[31] of the sort frequently encountered at balloon altitudes.

One might think that short-time reciprocity failure would preclude the possibility of ever recording Cerenkov photons in all cases. Of course, Cerenkov photons have been frequently observed photographically in charged accelerator beams. The short-time reciprocity failure problem is irrelevant in these cases because the photographic emulsion records the

superposition of many individual Cerenkov pulses.

Because the manufacturer of the recording emulsion regards its composition as proprietary information, we were forced to do a very approximate calculation in compiling Fig. (20). We have modeled the recording emulsion medium as polyethylene plastic adjusted to have density $2.5 gm/cm^3$. The thickness of the emulsion layer was taken to be $12 \mu m$ and we have used the crude model of Fowler[5] to estimate the ionization energy deposition about the track of the incident nucleus. In computing the Cerenkov photon energy deposition into the recording emulsion, we have assumed 100% absorption of the photons.

8.3. Competing Ionization Signal Possibly Responsible for all Images Seen to Date

At this point in our discussion, we might wonder if any images at all were observed in the photographic Cerenkov detector of Pinsky. There has not been any publication of photomicrographs which depict the images in the recording emulsion in either flight 2 or 3. Half-tone reproductions of photomicrographs of the images of five nuclei observed in flight 1 have been published.[33,34]

One must wonder how those images originated since the Cerenkov photons provide so little signal. There is at least one obvious competing source of darkening of the photographic emulsions. Images, which might be mis-identified as being due to Cerenkov photons, may actually be due to the ionization energy, which necessarily accompanies the passage of each nucleus. Fig.(20) shows the energy deposition expected due to delta-rays ejected from the nucleus' track in the recording emulsion of the photographic Cerenkov detector from a vertically-incident nucleus at β=0.75 and, separately, due to Cerenkov photons. Since both processes, ionization and Cerenkov radiation, occur with amplitudes nearly proportional to Z^2, the ratios indicated on Fig.(20) hold for any charge of the incident nucleus. The units are in terms of the nominal photon sensitivity of the emulsion. Even in the thickest Cerenkov detector of this design flown to date, the Cerenkov images are narrower than $400 \mu m$ so that all of the images reported to date have been within regions where there has been more ionization energy deposited than Cerenkov photon energy.

The presence of a well-defined boundary of the proper shape about the darkened region is about the only convincing signature for origins of the image from Cerenkov photons. None of the reported images appears to differ obviously from the continuously diminishing darkness vs. distance relation characteristic of nuclear emulsion tracks, which are due solely to ionization. What might be identified by the present author as a blurred edge of an ellipse in the image in Ref. 14 has the wrong orientation, being rotated about 30^o from the described trajectory projection onto the plane of the image.

The basis of Pinsky's interpretation of the origins of his images as Cerenkov photons depended on a modified design of the detector, including an extra recording emulsion (see Fig. 21). The Cerenkov photons are directed along the direction of the nucleus' motion so that they should typically illuminate only the bottom recording emulsion. Thus, we would expect to find no image or, at most, only a small image in the upper emulsion even when a large Cerenkov image was left in the lower emulsion. There have been only two photos of the upper images published corresponding to the tracks which have been seen to date, both, of course, from flight 1.[33]

These published half-tone reproductions indicate upper images which are smaller than the corresponding lower images. However, one may easily see, for instance in Ref. 14, that the top emulsion sheet has a much lower level of background as indicated in the periphery of the published photomicrographs. The apparent difference in background level, if due to processing differences, is so great as to make comparison quite obscure.

Even more significant in undermining the usefulness of the differences between the upper and lower images to identify the Cerenkov origins of the images is that the claimed differences are not unequivocal: It is well known that the ionization energy deposition about a nuclear track is selectively depleted near the point of entry of the nucleus into a medium.[36] This is due to the selective loss of the knock-on electrons from the medium through its surfaces before they have surrendered all of their kinetic energy. We thus expect that nuclei *should* leave smaller ionization images, especially at relatively large lateral distances from their tracks, in the top emulsion.

There is, furthermore, the definite possibility that the registration between the top and the bottom recording emulsion sheets was not correctly measured; no details of the image location scheme on the Cerenkov films from balloon flight 1 have been published. There would certainly be dozens of darkened images on the upper recording emulsions within any likely area of experimental imprecision due to the ionization of unrelated stopping nuclei unless some elaborate location scheme were used. We remain uncertain whether the published images from the upper emulsion were actually made by the same particle as were the published lower images.

8.4. Difficulties in Comparing Photographic Cerenkov Detector Data from Different Flights

Even if we were to accept for purposes of argument that the photographic Cerenkov detector of Pinsky did work as claimed in the balloon flight 1, we may still entertain doubts regarding its interpretation in respect to balloon flight 2. The recording emulsion on flight 1 was certainly from a different manufacturer's batch than that in flight 1. Since the recording emulsion necessarily is expected by the experimenters to perform in a manner outside its specifications, there is little reason to believe that the same performance would be obtained in

both cases. In particular, we must re-open questions regarding the sensitivity, image blurring, reciprocity failure, and response to ionization with respect to the new batch of recording emulsion regardless of its assumed behavior in balloon flight 1. In addition there is the imponderable effect of the six-months' pre-flight ground storage and possible subsequent post-flight storage before the emulsion was developed. It is the experience of this author that EK2485 recording emulsion degrades in image quality even under the best storage conditions. Before any clear-cut interpretation can be obtained for the Price event the conditions of storage of the emulsions for balloon flight 2 should be carefully examined.

8.5. Photographic Cerenkov Detectors: Conclusions

In response to an inquiry from this author, Price et al. have recently stated a modified position regarding the size of the image of the particle in question in the Cerenkov detector recording emulsion. They say: "At this point in the re-analysis of the previously reported Cerenkov data, no definitely proved limits on the size of the Cerenkov spot can be supported. Continuing analysis of this detector may lead to claims in the future."[37] It seems to us that there are good reasons to doubt even the possibility of obtaining a convincing physical interpretation of whatever claims might be made for the size of the images in question. We are certainly forced to exclude from this present discussion the possibility of using the Cerenkov detector to support any claims for the uniqueness of the particle in question.

Let us briefly consider a possible explanation for why our conclusions regarding the potential performance of the photographic Cerenkov detector differ so greatly from Pinsky's conclusions. In Fig. (22) we compare two versions of the spectral sensitivity of EK2485 recording emulsion. One of the smooth curves is from Fig. B-1, page 195 of Ref. 32. This is the only version of the spectral sensitivity published by Pinsky to date. The other smooth curve is the Kodak specification for the spectral sensitivity for D = 1.0 above background from Ref. 35. There is a general agreement between the form of the curves of Figs. (22A) and (22B), but the scales are labeled differently. To translate from Kodak specification to Pinsky's curve, one might assume a re-labeling of Pinsky's vertical scale. By comparison to the Kodak specification, Pinsky's curve indicates a factor of 10 increase in sensitivity and a square root compression of the peak-to-valley ratios in the spectral sensitivity. The precise resolution of this discrepancy is not yet known.

9. Conclusions

We find that the etch rate data of Price and Shirk allow one conclusion of the highest certainty, namely that, if the Price particle actually were a normal nucleus, it must have had initial speed greater than $\beta=0.55$ when incident upon the thick polycarbonate stack. Our conclusion obtains independently of any assumed sequence of interactions of the particle within the polycarbonate stack. This conclusion is in complete agreement with the conclusions of each one of the published criticisms[2-5] of the original interpretation of Price *et al.* This conclusion is, therefore, in disagreement with the original interpretation of Ref. 1.

We also find some disagreement with the spirit of Price's reply to the critics (Ref. 6). Ref. 6 can be read to imply that it is unacceptably remote to consider the possibility that the etch rate data can be matched to any incident nucleus with charge lower than platinum ($Z=78$). We have found even by curve fitting that many such hypotheses are viable. The apparent disagreement between our conclusions and those in Ref. 6 principally reflects the higher level of certainty which our analysis allows. We find severe limitations for the photographic Cerenkov detector as built by Pinsky. We find that this detector is expected to perform far beyond the manufacturer's specifications for its sensitivity, image quality, and reciprocity characteristics. We find that there is more energy deposited within the recording emulsion by the ionization incident to the passage of a heavy nucleus than is available from the desired Cerenkov photons. It is conceivable that all images seen in this detector to date may be due to this ionization energy and not to Cerenkov photons alone. We conclude that this detector cannot provide data of sufficient quality to be useful at our desired level of certainty.

We recall that the nuclear emulsions have not been treated here. We thus have not exhausted the possibilities for the experimental data of Price *et al.* to show that the Price particle may be unique. We have, however, defined the task which must lie upon the nuclear emulsion interpretation: To make any such claim, the particle must be shown to be incompatible with any normal nucleus hypothesis that has $\beta \leqslant 0.55$ at the top of the thick polycarbonate stack. Even the most rigorous interpretation of experimental data can be misleading when there are questions of systematic effects and freak occurrences unaccounted for. We will briefly discuss some of these issues in the Appendices.

Appendix A: Equations for Coulomb Scattering of Electrons

To compute energy loss rates, we must have the formulae that describe Coulomb scattering. The reader is referred to the review article by Motz, Koch, and Olsen[38] for a thorough discussion of this issue. Throughout this section, we neglect the effects of binding the electrons. The starting point in our discussions of Coulomb scattering is the Rutherford cross section:

$$\frac{d\sigma}{d\Omega} = \left(\frac{Z\alpha}{2p\beta \sin^2 \frac{\theta}{2}} \right)^2, \qquad \text{(Eq.A1)}$$

where: p=*momentum of "electron"*,

β=*speed of "electron"*,

θ=*scattering angle of "electron"*.

This equation describes the scattering of non-relativistic , spinless electrons from a static Coulomb potential of magnitude Ze at rest in the laboratory frame. If we now take the point of view that the incident nucleus is a static Coulomb potential moving with respect to the laboratory frame at speed β, we can re-express Eq.(A1) in terms of the spectrum of kinetic energies transferred to the electrons initially at rest in the laboratory frame (i.e. "knock-on" energies):

$$\frac{d\sigma}{dE} = \frac{2\pi}{m} \left(\frac{Z\alpha}{\beta} \right)^2 \frac{1}{E^2}; \qquad \text{(Eq.A2)}$$

when: $0 < E < 2m\beta^2\gamma^2$.

where: Ze= *incident nucleus charge,*

β= *incident nucleus speed,*

E= *electron knock−on kinetic energy.*

The Rutherford formula is the first Born approximation to the Coulomb scattering problem for the case of spinless particles scattering from a static Coulomb potential. The Rutherford formula ignores particle production effects, real or virtual, all effects due to finite size of the nucleus and effects due to higher electric and magnetic moments residing on either the nucleus or the scattered electron. All of these conditions are approximately met for the relatively large impact parameter (small center-of-mass scattering angle, small knock-on energy) collisions with free electrons. Thus we must expect that, no matter how much we refine Eq.

(A2), the correct formula must approach Eq. (A2) for small knock-on energies. Thus, it will be convenient to express the improved versions of Eq. (A2) as a ratio to the Rutherford result (Eq. A2). Another aspect of Eq. (A2) is also preserved: all improved versions of the Coulomb scattering treatment contain the same (kinematic) upper energy cut-off.

As it turns out, Eq. (A2) is correct even relativistically for spin-zero electrons in the first Born approximation. When the first Born approximation is applied for Dirac electrons, Mott's well known formula for scattering cross section is obtained:

$$\frac{\left(\frac{d\sigma}{dE}\right)_{First\ Born}}{\left(\frac{d\sigma}{dE}\right)_{Rutherford}} = \left(1-\frac{E}{2m\gamma^2}\right) \qquad \text{(Eq.A3)}$$

Note that this inclusion of the electron spin always diminishes the scattering cross section relative to the Rutherford scattering. Note also that the scattering cross section is independent of the sign of the charge of the nucleus. This latter condition is true only in the first Born approximation, and will certainly be violated in the next order of perturbation, while the former prediction depends upon the supposed validity of the first Born approximation. That the Coulomb scattering cross sections for electrons is not independent of the sign of Z, can be seen explicitly by examining the second Born Approximation:[38]

$$\frac{\left(\frac{d\sigma}{dE}\right)_{Second\ Born}}{\left(\frac{d\sigma}{dE}\right)_{Rutherford}} = \left[1-\frac{E}{2m\gamma^2}+\pi Z\alpha\sqrt{\frac{E}{2m\gamma^2}}\left[1-\sqrt{\frac{E}{2m\gamma^2}}\right]\right] \qquad \text{(Eq.A4)}$$

It is a matter of experience that the Born series for the problem of Coulomb scattering is poorly convergent and awkward to calculate term by term. Another approximation method yields results more easily.

The problem of computing exact phase shifts (relative to the problem of non-relativistic Schrodinger Equation Coulomb scattering) also was first solved by Mott.[40] The scheme is to separate the Dirac equation in polar coordinates as usual and solve the radial wave equations explicitly in terms of hypergeometric functions. Knowing the explicit asymptotic behavior of these radial wave functions allows exact calculations of the various phase shifts. The phase shifts can be reconverted into the exact scattering cross section by doing a somewhat awkward numerical summation:

$$\frac{\left(\frac{d\sigma}{dE}\right)_{Mott}}{\left(\frac{d\sigma}{dE}\right)_{Rutherford}} = \left\{\frac{2E}{m\beta^2\gamma^4}|F|^2+\frac{E^2}{(Z\alpha m\beta\gamma^2)^2\left[1-\frac{E}{2m\beta^2\gamma^2}\right]}|G|^2\right\}, \qquad \text{(Eq.A5)}$$

where: m= *electron mass,*

E= *electron knock−on energy,*

β= *nucleus speed,*

$\gamma=(1-\beta^2)^{-1/2}$,

Ze= *nucleus charge,*

$$F=\sum_{l=-1}^{\infty} F_l,$$

$$G=\sum_{l=-1}^{\infty} G_l,$$

$$F_l=\begin{cases} \frac{1}{2}\dfrac{\Gamma\left(1-\dfrac{iZ\alpha}{\beta}\right)}{\Gamma\left(1+\dfrac{iZ\alpha}{\beta}\right)} e^{\left[i\left(\frac{Z\alpha}{\beta}\right)\ln\left(\frac{E}{2m\beta^2\gamma^2}\right)\right]}; & l=-1 \\ \frac{1}{2}\left[lD_l+(l+1)D_{l+1}\right]P_l\left(\dfrac{E}{m\beta^2\gamma^2}-1\right); & l\geqslant 0 \end{cases}$$

$$G_l=\begin{cases} \left(\dfrac{Z\alpha}{\beta}\right)\left[\dfrac{2m\beta^2\gamma^2-E}{E}\right]F_{-1} & l=-1 \\ \dfrac{i}{2}\left[l^2D_l-(l+1)^2D_{l+1}\right]P_l\left(\dfrac{E}{m\beta^2\gamma^2}-1\right); & l\geqslant 0, \end{cases}$$

where: $$D_l=\frac{e^{-i\pi l}}{\left[l+i\left(\dfrac{Z\alpha}{\beta}\right)\right]}\frac{\Gamma\left(l-\dfrac{iZ\alpha}{\beta}\right)}{\Gamma\left(l+\dfrac{iZ\alpha}{\beta}\right)}-\frac{e^{-i\pi\rho_l}}{\left[\rho_l+i\left(\dfrac{Z\alpha}{\beta}\right)\right]}\frac{\Gamma\left(\rho_l-i\dfrac{Z\alpha}{\beta}\right)}{\Gamma\left(\rho_l+i\dfrac{Z\alpha}{\beta}\right)},$$

$\rho_l=\sqrt{l^2-(Z\alpha)^2}$,

P_l= *Legendre polynomial of order l,*

$\Gamma(z)$= *Gamma function of complex argument.*

We use, for $E\leqslant 0.017m\beta^2\gamma^2$, the result of Bartlett and Watson[41] to approximate the above cross section as follows:

$$\frac{\left(\dfrac{d\sigma}{dE}\right)_{Mott}}{\left(\dfrac{d\sigma}{dE}\right)_{Rutherford}}\approx\left|1+\frac{\pi Z\alpha}{\gamma}\sqrt{\frac{E}{2m}}\cos\chi\right| \qquad \text{(Eq.A6)}$$

$$\text{where: } e^{i\chi} = \frac{\Gamma\left(\tfrac{1}{2}+\frac{iZ\alpha}{\beta}\right)\Gamma\left(1-\frac{iZ\alpha}{\beta}\right)}{\Gamma\left(\tfrac{1}{2}-\frac{iZ\alpha}{\beta}\right)\Gamma\left(1+\frac{iZ\alpha}{\beta}\right)}.$$

and find expression to be accurate to better than 2% compared with the tabulations of Doggett and Spencer. The function $\cos\chi(Z\alpha/\beta)$ is plotted in Fig. (23).

Examination of formula (A6) shows the somewhat surprising result that the first Born approximation cross section for Coulomb scattering of electrons is smaller than the Rutherford cross section, whereas the exact scattering cross section (from positive nuclei) for electrons exceeds the Rutherford cross section at the smallest scattering angles. This simple fact does have some consequences for experimental situations. In particular, the standard, so-called Bethe-Bloch stopping power formula is theoretically based solely upon the first Born Approximation Eq. (A3), to account for the effects of close collisions and most attempts to improve this treatment have relied upon the second Born Approximation,[36] Eq. (A4) instead of formula (A5). Appendix B presents modification to the Bethe-Bloch treatment of stopping powers including formula (A5) together with formula (A6).

In order to use the cross sections implied by Eq. (A5), we need numerical values. We use for this purpose the numerical tabulations of Doggett and Spencer,[42] interpolating their widely-accepted results according to the instructions of that reference.

Appendix B: Calculating Energy Loss Rates for Heavy Nuclei

Unfortunately, there is no completely suitable theoretical treatment for the problem of calculating the total energy-loss rate of various heavy nuclei. We follow the general approach of the review article of Uehling[43] to compute energy-loss rates. In doing so, we consider only the Coulomb encounters between the resting electrons of the stopping medium and the incident nucleus, neglecting all other modes of energy loss. We can, as Uehling has done, divide Coulomb encounters into two classes, the close and distant collisions. This division is necessary to allow sufficient simplification of the problem for numerical calculations to be done.

Close collisions are those in which the chemical binding of the electrons can be neglected. For close collisions, the effective scattering cross section is given by the Mott scattering formulae, Eqs. (A4) and (A5), and the energy-loss rate can be computed simply by

$$\left(\frac{dE}{dx}\right)_{Close\ collisions} = N_0 \int_I^{2m\beta^2\gamma^2} E\left(\frac{d\sigma}{dE}\right)_{Mott} dE, \qquad \text{(Eq.B1)}$$

where: N_0= *Number density of electrons in stopping medium,*

I= *Characteristic binding energy of electrons in the stopping medium.*

This can be considered to be a classical treatment of the close collisions in the energy-loss problem. Energy loss rates for the distant collisions can be treated via semi-classical computation schemes such as the Bohr treatment or the Fermi treatment of stopping powers. In the case of the standard, so-called Bethe-Bloch stopping power formalism, the entire energy-loss rate can be computed in the first Born approximation:[43]

$$\left(\frac{dE}{dx}\right)_{"Bethe-Bloch"} = \frac{4\pi N_0'}{m}\left(\frac{Z\alpha}{\beta}\right)^2\left\{\ln\left(\frac{2m\beta^2\gamma^2}{I}\right)-\beta^2\right\}. \qquad \text{(Eq.B2)}$$

We may apply our exact form for the contribution due to close collisions by simply adding the right-hand side of Eq. (B1) to the right-hand side of Eq. (B2) and subtracting the contribution due to the close collisions as calculated in the same context as Eq. (A3), namely the first Born approximation. Eq. (B3) is the result.

$$\left(\frac{dE}{dx}\right) = \left(\frac{dE}{dx}\right)_{"Bethe-Bloch"} + \qquad \text{(Eq.B3)}$$

$$\left(\frac{dE}{dx}\right)_{Close\ collisions} -$$

$$\frac{2\pi N_0}{m}\left(\frac{Z\alpha}{\beta}\right)^2\left\{\ln\left(\frac{2m\beta^2\gamma^2}{I}\right)-\beta^2\right\}.$$

This result is very near to that of Eby and Morgan,[44] except their treatment formally includes several terms to allow for shell effects of the stopping medium, the density effects, etc., which are frequently applied to the problem of stopping unit-charged particles. It is not clear how these latter computations (which depend on various calculational schemes) should be modified for the cases that we shall be considering, namely for high charges of the slowing particle. We will, therefore, neglect such detailed considerations, restricting our formulae to nucleus speeds in the range $0.4 < \beta < 0.99$.

We can, however, make one minor improvement to the calculation of the stopping of highly charged nuclei. Ashley, Ritchie, and Brandt[45] have computed, by semi-classical means, the equivalent of the second Born approximation calculation for the energy-loss rate due to distant collisions. Their result is stated in terms of a correction (of order Z^3) to the usual stopping power formula. This correction is of minor importance in the overall magnitude of the total stopping power calculation, and it is included only to verify that we have not erred too far by being unable to compute any exact formula for the stopping power due to distant collisions.

Our resulting expression for the stopping power of a bare nucleus of charge Ze moving with speed β is

$$\left(\frac{dE}{dx}\right)_{Z,\beta} = \left(\frac{dE}{dx}\right)_{\text{"Bethe-Bloch"}} + \left(\frac{dE}{dx}\right)_{\text{Close collisions}} + \left(\frac{dE}{dx}\right)_{\text{Distant collisions}} - \frac{4\pi N_0}{m}\left(\frac{Z\alpha}{\beta}\right)^2\left\{\ln\left(\frac{2m\beta^2\gamma^2}{I}\right)-\beta^2\right\}. \qquad \text{(Eq.B4)}$$

Equation (B4) is our calculation for the energy-loss rate for a nucleus of charge Ze moving with speed β having no attached electrons. We will also want to calculate the stopping powers for nuclei with arbitrary numbers of attached electrons. The customary elementary treatment of stopping powers[30] will be sufficient to verify the magnitude of these modifications.

In this elementary treatment of stopping powers, it is assumed that the classical impulse approximation relation between impact parameter, b , and energy transfer, δE, applies for all relevant impact parameters:

$$\Delta E = \frac{2}{m}\left(\frac{Z\alpha}{\beta}\right)^2 \frac{1}{b^2}; \quad \text{for } b_{\min} < b < b_{\max}, \tag{Eq.B5}$$

$$\frac{dE}{dx} = N_0 \int_{b_{\min}}^{b_{\max}} \Delta E(b) 2\pi b db,$$

where: N_0= *number density of electrons in medium.*

The inner impact parameter, $b_{\min}$, is determined to be $1/(m\beta\gamma)$, while $b_{\max}$ is determined to be $b_{\max}=(2\beta\gamma)/I$, where I is the characteristic binding energy of the electrons in the medium. Although these estimates are crude, it should be understood that the dependence on the impact parameters is masked by the weak (logarithmic) dependence of the stopping power on their numerical values. The resulting estimate for $\frac{dE}{dx}$ happens to be correct to order $\frac{\beta^2}{ln(\frac{2m\beta^2\gamma^2}{I})}$.

$$\frac{dE}{dx} = \frac{4\pi N_0}{m}\left(\frac{Z\alpha}{\beta}\right)^2 \ln\left(\frac{2m\beta^2\gamma^2}{I}\right). \tag{Eq.B6}$$

To modify the above treatment to allow for the presence of N electrons around the nucleus of charge Ze, which electrons reduce the net charge on the ion to Qe, we will divide the region of integration over impact parameter into two separate regions, $[b_{min}, b_o]$ and $[b_o, b_{\min}]$. In the region $[b_{min}, b_o]$, the effective charge of the ion for collisions with electrons is taken to be Ze while, in the region $[b_o, b_{\max}]$, the effective charge is taken to be Qe. This procedure yields an estimate for the stopping power:

$$\frac{dE}{dx} = \frac{4\pi N_0}{m}\left\{\left(\frac{Z\alpha}{\beta}\right)^2 \ln\left(\frac{b_0}{b_{\min}}\right) + \left(\frac{Q\alpha}{\beta}\right)^2 \ln\left(\frac{b_{\max}}{b_0}\right)\right\}. \tag{Eq.B7}$$

The numerical value for the cross-over parameter b_o can be phenomenologically picked as

$$b_0 = \frac{0.95}{m\alpha} \frac{1}{Z^{1/3}\left|1+Q\right|^{2/3}}. \tag{Eq.B8}$$

It can be seen that this result is intuitively correct by examining the limiting cases when only one electron is attached:

$$b_0 = \frac{0.95}{m\alpha Z}, \quad \textit{near } \frac{1}{m\alpha Z}, \tag{Eq.B9}$$

and when the ion is completely neutralized in the usual Fermi-Thomas approximation:

$$b_0 = \frac{0.95}{m\alpha Z^{1/3}}, \quad \textit{near the usual } \frac{0.885}{m\alpha Z^{1/3}}. \tag{Eq.B10}$$

Of course, our final result depends only logarithmically upon the exact numerical value of b_o chosen. Our final estimate of the stopping power of any ion with net charge Qe and atomic number Z is obtained by taking the ratio of Eqs. (B6) and (B5) and multiplying this ratio times the correct stopping power formula as computed earlier for a fully stripped nucleus with atomic number Z.

$$\left(\frac{dE}{dx}\right)_{Q,Z,\beta} = \left\{\frac{Z^2\ln\left(\frac{b_0}{b_{\min}}\right)+Q^2\ln\left(\frac{b_{\max}}{b_0}\right)}{Z^2\ln\left(\frac{b_{\max}}{b_{\min}}\right)}\right\}\left(\frac{dE}{dx}\right)_{Z,Z,\beta}, \qquad \text{(Eq.B11)}$$

$$\textit{where:}\ \left(\frac{dE}{dx}\right)_{Z,Z,\beta} = \textit{our (Eq.B4)},$$

$$b_{\max}=\frac{2\beta\gamma}{I},$$

$$b_{\min}=\frac{1}{m\beta\gamma}.$$

Appendix C: Sensitivity of Our Conclusions to Systematic Errors in Calibration of the Etch Rate Data

Throughout the body of the text, we have adopted as hypotheses the numerical values of the etch rate based estimates for $|Q/\beta|$. Here, we will show that our conclusions for the Price particle do not depend very sensitively on the precise values of these numerical estimates. An error in the estimates for $|Q/\beta|$ from the etch rate data could arise from some unknown systematic error in the calibration procedure of Price and Shirk. Thus, we will assume for the sake of argument that the values of v_o and p from our earlier Eq. (2) were erroneously estimated; we will now, therefore, be assuming that our much used mean value of $|Q/\beta|$, 114, was actually in error. To test the sensitivity of our conclusions to this assumed error, we simply repeat our previous calculations using arbitrarily assumed values for the mean of $|Q/\beta|$, equal to 110 and 118, respectively. These results are summarized in Table (2) and Table (3). We easily can see that our estimates for the minimum speed of incident nuclei are not greatly changed when the value of $|Q/\beta|$ is changed by 4 units. We do not, of course, know the true magnitude (or even the true sign) of any likely systematic errors in the Lexan calibration procedure of Price and Shirk, so that we cannot say absolutely that the systematic calibration errors can have no significant effect upon our conclusions, but the sensitivity of our conclusions to such systematic errors is at least relatively small.

Appendix D: Consequences from Failure of Our Assumed Form for the Lexan Response

We have explicitly assumed throughout this work that the measured etch rates accurately reflect the physical parameter $|Q/\beta|$, independently of the speed of the incident nucleus. This assumption was seen to be rather empty when we noted that the parameter Q was not assumed to be the atomic number of the incident particle. In fact, Q was assumed to be an unknown function of the speed β and the atomic number Z of the incident nucleus. What we have in effect assumed at various places in the bulk of the text is that Q does not depart too far from being numerically equal to the atomic number of the incident nucleus. We will now examine the possible consequences of this assumption not being true.

The basis for proposed uniqueness of the Price particle must lie within its apparently highly-penetrating behavior in the polycarbonate stack. We are, therefore, interested in studying systematical errors in our assumption that $|Q/\beta| \approx |Z/\beta|$ for this particle. We are most interested in systematic errors which might allow $|Q/\beta|$ to overestimate $|Z/\beta|$ considerably. Thus, it will be of interest here to assume that there might be some means by which the value of Q may actually *exceed* the atomic number of the incident nucleus.

The most reasonable means by which the value of Q may become larger than Z for a certain class of nuclei would be if the etch rates actually were determined by the total energy lost within the sub-microscopic cylinder in the plastic. This model is not unreasonable. It is, in fact, the model used by Ahlen[29] in computing his estimates for the expected behavior from slow Dirac monopoles.

The overall trend of energy deposition into the tiny damage cylinder is shown, as calculated after the model of Ahlen, in Fig. (24). Notice that there is a rather steady rise in the energy deposition with increasing values of the speed of the incident nucleus even when the value of $|Q/\beta|$ is held fixed. Thus, if we were to accept the hypothesis that the polycarbonate actually records the restricted energy loss according to Ahlen's model, we should consider what effects this would have on our conclusions. Instead of our previous assumption that Q nearly equals Z for the incident nucleus, we now have Q a slowly rising function of β for each fixed value of Z .

Now let us consider, within the context of Ahlen's model, the set of nuclei that can be responsible for the formation of any given measured etch cone. In the bulk of our text we have assumed that all such nuclei should have very nearly the same values of $|Z/\beta|$, quite independently of their speed. With the assumptions of this Appendix, however, the slow nuclei in our set must have higher value of the $|Z/\beta|$ than the faster nuclei in our set. Our conclusions depended only indirectly on the measured values of $|Q/\beta|$ and directly on another parameter, the total energy-loss rate. Figure (25) illustrates the variation of the total energy-loss rate among all nuclei with their expected etch rates equal to the mean of the measured etch rates

for the particle in question according to Ahlen's model. Notice that the total energy-loss rates are systematically higher for the faster nuclei in the set.

This makes it more difficult to match the polycarbonate data with slow nuclei and easier to match them with fast nuclei. The thrust of the arguments in the main discussion is that the etch-rate data provide no undeniable guarantee that the particle was not a fast nucleus, but that the particle in question could never have been a very slow nucleus, β=0.55 or less. Thus, both of the conclusions reached in the main discussion are *strengthened* by assuming that the value of Q exceeds the value of Z for fast nuclei.

Appendix E: Less Conventional Explanations for the Price Particle

We have dealt in the body of the text with a restricted class of potential normal nucleus explanations of the Price particle and its behavior in the polycarbonate stack. These explanations centered around the possibility that normal nuclei might fragment several times or capture electrons with in the polycarbonate plastic. In this appendix we will list several additional possibilities for explaining the data. These possibilities must be regarded as freak occurrences whose likelihoods, though very small, cannot easily be estimated. These possibilities will be simply listed; we will not discuss their possible experimental resolution. We do not assert that these explanations may or may not be excluded by careful interpretation of Price's experimental data. The explanations with an asterisk are not original with the present author.

I.) The interpretation of Price *et al.* can be qualitatively understood as describing a particle that is slower at the top of their experimental stack than it is at the bottom. The particle might be considered as a normal nucleus incident from below.* II.) We have assumed throughout this discussion that the track was made by a single nucleus. If several highly relativistic heavy nuclei were to hit the detector package, there might be effects which we have not allowed for. We might assume that more than one nucleus traversed the Lexan stack in close proximity, giving rise to a single etch cone and an etch rate of some unexpected value. There are two separate ways in which we might imagine that nuclei might traverse the Lexan stack in close proximity. It is possible that the nuclei of the atoms in some incident molecule incident upon the stack might traverse the stack in close proximity.* There is evidence that cosmic particles of extremely high energies are present at the top of the atmosphere. Such particle initiate very large electromagnetic showers as they penetrate the atmosphere. The effects of such an imagined electromagnetic shower of charges upon the polycarbonate stack is not easily predicted. IV.) The particle might in fact be a negative nucleus which particle may or may not need to have fragmentation collisions depending upon its initial speed and charge. V.) There may be a massive failure of the assumed response of the etch rate for ultra-relativistic incident particles. It may be that the measured mean value of $|Q/\beta|=114$ corresponds to ultra-relativistic nuclei with $|Z/\beta|$ assuming a much smaller value. The possibility of such an effect is qualitatively suggested by the literal interpretation of the model of Lexan response used by Ahlen and later quoted by Price. This hypothetical failure of the response seems to this author to be particularly difficult to rule out since there exist no unequivocal experimental data with which to identify the response of Lexan to ultra-relativistic particles.

In the context of this last possibility, we offer a quantitative example of the possible consequences. Figure (25) represents the consequences from our interpretation of the response model of Ahlen. The results are expressed in terms of the true values needed by the parameter $|Z/\beta|$ to mimic the mean value of $|Q/\beta|=114$ measured for the Price particle. Keep in mind

that Ze is the true charge on the incident nucleus, while Qe is an artifact of etch rate data. We can see from Fig. (25) that the slower incident nuclei need larger true charges than is necessary to have $|Z/\beta|=114$, while faster speeds imply that the particles actually have smaller true charges than corresponding to $|Z/\beta|=114$. The question is, at what speed does the calibration procedure of Price and Shirk make $|Q/\beta|$ equal to $|Z/\beta|$? For purposes of preparing Fig. (25), we have taken $\beta=0.45$, a speed typical of the speeds of the slowing iron nuclei, which are actually used by Price and Shirk to calibrate their Lexan.

Let us now consider what the charge of an ultra-relativistic incident nucleus would have to be for $|Q/\beta|= 114$. Referring to Fig. (25) we can see that for $\beta=1.0$, the corresponding value of $|Z/\beta|$ is invitingly near 92, so that we might expect that the etch rate data could be explained in terms of an ultra-relativistic uranium nucleus if the Lexan response model of Ahlen is actually correct.

We note in passing that it is our opinion that the emulsion track expected from an ultra-relativistic uranium nucleus should be considerably smaller than the emulsion tracks expected from most normal nuclei that would have Lexan estimates of $|Q/\beta|=114$. This possibility may prove to be the most appealing hypothesis for the ultimate explanation of this very interesting cosmic ray event.

References

1. P.B. Price, E.K. Shirk, W.Z. Osborne, and L.S. Pinsky, Phys. Rev. Lett. 35, 487 (1975).
2. M.W. Friedlander, Phys. Rev. Lett. 35 ,1167 (1975).
3. P.H. Fowler, in *Proceedings of the Fourteenth International Conference on Cosmic Rays, Munich, West Germany, 1975* (Max-Planck-Institut fur Extraterrestrische Physik, Garching, West Germany, 1975), p. 4049.
4. L.W. Alvarez, in *Proceedings of the International Symposium on Lepton and Photon Interactions, High Energies, Stanford, California, 1975,* edited by W.T. Kirk (Stanford Linear Accelerator Center, Stanford, Calif., 1975), p. 967, and Lawrence Berkeley Laboratory Report No. 4260, 1975 (unpublished).
5. R.L. Fleischer and R.M. Walker, Phys. Rev. Lett. 35 , 1412 (1975).
6. P.B. Price, *New Pathways in High Energy Physics, I* (Plenum, New York, 1976), p. 167.
7. *Physics Today,* October, 1975, p. 17.
8. For a general discussion of the primary cosmic radiation see: R.R. Daniel and S.A. Stevens, *Space Science Reviews,* 17 , 45 (1975).
9. For a general discussion of monopoles with many references, see: R.A. Carrigan, Jr., Fermilab Report No. 77/42 (unpublished).
10. See, for example, W.V.R. Malkus, Phys. Rev. 83 ,899 (1951).
11. See, for example, R.R. Ross, P.H. Eberhard, L.W. Alvarez, and R.D. Watt, Phys. Rev. D 698 (1973).
12. See, for example, V.P. Zerlov, *et al.* JINR-P1-7996 (1974) (unpublished).
13. See, for example, R.L. Fleischer, H.R. Hart, G.E. Nichols, P.B. Price, Phys. Rev. D 7, 24 (1971).
14. E.K. Shirk, P.B. Price, E.J. Kobetich, W.Z. Osborne, L. S. Pinsky, R.D. Eandi, and R. B. Rushing, Phys. Rev D 7, 3220 (1973).
15. E.C.H. Silk and R.S. Barnes, Phil. Mag. 23 449 (1959).
16. R.L. Fleischer, P.B. Price, and R.M. Walker, *Nuclear Tracks in Solids: Principles and Applications* (Univ. of California Press, Berkeley, 1975).
17. There are two independent measurement schemes which yield similar estimates of the radius of chemical damage regions:

Electron Microscopy:

P.B. Price and R.M. Walker, J. Appl. Phys. 33, 3407 (1962).

Electrical Conductivity:

C.P. Bean, M.V. Doyle, and G. Entine, J. Appl. Phys. 41, 1454 (1970).

18. See, for instance, P.J. Lindstrom *et al.*, Lawrence Berkeley Laboratory Report No. 3650 (unpublished).

19. H.J. Crawford, private communication (1977).

20. For a general discussion of the use of the F-test, see W.A Wallis and H.V. Roberts, *Statistics: A New Approach* (The Free Press, New York, 1974).

21. See, for instance, Fig. (4) of Ref. 3.

22. W.H. Barkas and M.J. Berger, *Nuclear Science Series Report No. 39* p. 103 (1964).

23. See, however, J.D. Jackson and R.L. McCarthy, Phys. Rev. B 6, 4131 (1972).

24. B. Judek, Can. J. Phys.

50, 2082 (1972),

E. Friedlander and M. Spirchez, Nucl. Sci. Abstracts 15, 3457 (1961),

H. Yagoda, Geophys. Res. Papers 50 (1958).

25. P.S. Freier and C.J. Waddington, Astro. Phys. Space Science, 38, 419 (1975).

26. N. Durgaprasad and N.K. Rao, unpublished preprint.

27. See, for instance, E.F. Carter and H.A. Cohen, Am. J. Phys.

41, 994 (1973).

28. "They would appear as heavily-ionizing particles and would be distinguishable from ordinary charged particles by the property that the ionization they produce would not increase towards the end of their range but would remain roughly constant".

P.A.M. Dirac, Phys. Rev. 74, 817 (1948).

29. S.P. Ahlen, Phys. Rev. D 2935 (1976).

30. For a summary of the Bohr and Fermi theories of stopping power calculations, see:

J.D. Jackson, *Classical Electrodynamics,* Wiley, New York (1975).

31. V.M. Fridkin, *The Physics of the Electrophotographic Process,* The Focal Press, London (1973).

32. L.S. Pinsky, NASA Technical Memorandum, MSC-07561, NASA TM X-58102 (1975).

33. L.S. Pinsky, R.D. Eandi, W.Z. Osborne, and R.B. Rushing, *Proceedings of the Twelfth International Conference on Cosmic Rays, Hobart, Australia, 1971,* Univeristy of Tasmania Press, Hobart, Australia, Vol. 4, p. 1630.

34. L.S. Pinsky, R.D. Eandi, R.B. Bushing, L.F. Thomson, and W.Z. Osborne, *Proceedings of the Eighth International Conference on Nuclear Photography and Solid State Detectors, Bucharest,* Institute of Atomic Physics, Bucharest, 1972, p. 526.

35. Kodak Technical Publication No. P-94 (1971).

36. P.H. Fowler *et al.,* Proc. Roy. Soc. London, Ser. A 318, 1 (1970).

37. P.B. Price, E.K. Shirk, L. S. Pinsky, and W.Z. Osborne, private communication.

38. J.W. Motz, Haakon Olson, and H.W. Koch, Rev. Mod. Phys. 36, 881 (1964).

39. N.F. Mott, Proc. Roy. Soc. London, Ser. A. 124, 425 (1929).

40. N.F. Mott, Proc. Roy. Soc. London, Ser. A 135, 429 (1932). Note that there are certain misprints in this early article. The proper formulae are clearly derived in N.F. Mott and H.S.W. Massey, *The Theory of Atomic Collisions,* Oxford University Press, London (1949).

41. J.H. Bartlett and R.E. Watson, Proc. Am. Acad. Sci. 74, 53 (1940).

42. J.A. Doggett and L.V. Spencer, Phys. Rev. 103, 1597 (1956).

43. E.A. Uehling, *Ann. Rev. Nucl. Science,* 10, 315 (1955).

44. P.B. Eby and S.H. Morgan Jr., Phys. Rev. A 5, 2536 (1972).

45. J.C. Ashley, R.H. Ritchie, and W. Brandt, Phys. Rev. B 5, 2393 (1972).

46. P.J. Lindstrom and E.M. Friedlander, private communication.

TABLES

Comparison of balloon flights			
	Flight 1	Flight 2	Flight 3
Area of array	17.8sq.m	10.sq.m	20.sq.m
Time aloft Time at altitude	350Hr. ~60Hr.	60Hr. (60Hr.)	60Hr. (60Hr.)
Altitude reached	(6 gm)	3 gm	5 gm
Time on ground before launch	?	(>6Months)	(>6Months)
Time at shower altitudes	(~250Hr.)	(~3Hr.)	(~3Hr.)
Number of Cerenkov Detectors Type of Cerenkov Detectors	1 2 Layers	2 1 Layer	2 1 Layer
Nuclear emulsions 200 micron G.5 10 micron NTA	 1 0	 1 2	 1 2
Matter between Cerenkov and polycarbonate stack	0.8 gm	0.4 gm	0.4 gm
Thickness of polycarbonate stack Number of sheets in polycarbonate stack Number of Polycarbonate sheets not in thick stack	.9 gm 30 10	1.0 gm 33 2	1.0 gm 33 2
Total thickness of package	1.7 gm	1.4 gm	1.4 gm
Time lag to processing polycarbonate data	?	20 Mo.	20 Mo.

TABLE 1 Comparison of the experimental packages flown on the balloon borne experiments of Price *et al.* Entries in parentheses must be considered approximately known. All thicknesses quoted in units of gm are in Lexan equivalent g/cm^2.

Lower limits to initial speeds of normal nuclei			
ionization rate	Lexan only v/c minimum	Lexan and thick emulsion v/c minimum	Lexan and all emulsions v/c minimum
110	0.555	0.591	0.609
114	0.561	0.596	0.614
118	0.568	0.602	0.619

TABLE 2 Lower limits to the speed of normal nuclei which can be thought to fit the etch rate data from the Price particle. Regardless of the number of nuclear interactions, no nucleus slower than the stated limits could fit the data. The "ionization rate" refers to the equivalent mean value of the paramater $|Q/\beta|$ while the stack description defines the thickness over which the mean ionization rate might be measured. In the present work, we assert only that the ionization rate has been measured through the Lexan.

Lower limits to initial speeds of normal nuclei			
ionization rate	Lexan only v/c minimum	Lexan and thick emulsion v/c minimum	Lexan and all emulsions v/c minimum
110	0.573	0.609	0.627
114	0.579	0.614	0.632
118	0.585	0.619	0.636

TABLE 3 Lower limits to the speed of normal nuclei which can be thought to fit the etch rate data from the Price particle. Regardless of the number of electron attachments, no nucleus slower than the stated limits could fit the data. The "ionization rate" refers to the equivalent mean value of the paramater $|Q/\beta|$ while the stack description defines the thickness over which the mean ionization rate might be measured. In the present work, we assert only that the ionization rate has been measured through the Lexan.

Predicted speed of monopole	
ionization rate	v/c monopole
80	-
90	0.05
100	0.10
110	0.21
114	0.28
120	0.44
130	0.66
135	0.93

TABLE 4 Equivalent values of $|Q/\beta|$ for slow monopoles of strength e/α. These relationships are computed directly after the model of Ahlen.

Predicted speed of monopole	
ionization rate	v/c monopole
80	-
90	-
100	0.07
110	0.12
114	0.14
120	0.17
130	0.24
135	0.29

TABLE 5 Equivalent values of $|Q/\beta|$ for slow monopoles of strength e/α. These relationships are computed by modifying the model of Ahlen to conform to the calibration procedures described by Price for his experimental data.

Published estimates for initial speeds	
Interpretation	Author
v/c<1.00 cannot fit	P.B.Price, et al. (ref.1)
v/c>0.75 do fit	M.W.Friedlander (Ref.2)
v/c>0.68 do fit	L.W.Alvarez (Ref.4)
v/c>0.69 do fit	P.H.Fowler (Ref.3)
v/c>0.60 may fit	R.L.Fleischer and R.M.Walker (Ref.5)
v/c<0.74 do not fit	P.B.Price (Ref.6)
v/c>0.55 may fit	Present work
v/c<0.55 cannot fit	Present work
v/c>0.60 do fit	Present work

TABLE 6 Comparison of published interpretations for the Price event. Various authors have published claims regarding the possible range of initial speeds for normal nuclei which might fit the reported experimental data. All of the claims of all of the authors with the exception of the claims in Refs. 1 and 6 are consistent with one another.

Figure Captions

Fig.1 Schematic representation of the experimental configuration of Price *et al.* All approximate thicknesses are given in units of so-called Lexan equivalent g/cm^2. Each material in the stack has it own stopping power for relativistic charged particles. When the stopping power is computed in each layer of the apparatus, the stopping power is the same as for a particular thickness of Lexan plastic expressed customarily in terms of its physical thickness times the mass density of the hypothetical Lexan layer. This figure is taken from Fig. 1 in Ref. 6.

Fig.2 Schematic depiction of dielectric track etching. Fig. 2A shows the column of damaged plastic due to the passage of a highly ionizing nucleus. Fig. 2B shows, in supermicroscopic scale, the removal of plastic during a very short initial time period after etching begins. The plastic removed in this interval is shaded. Notice that the damaged plastic is chemically eroded more quickly than the surrounding undamaged plastic, leading to the formation of a tiny pit centered about the nucleus' path. Fig. 2C shows the removal of plastic during the second infinitesimal time period. Notice that the walls of the damaged region continue to be etched, but at the slower rate characteristic of undamaged plastic, so that the etch pit is enlarged even beyond the region where any chemical damage has occurred to the plastic while the length of the etch pit grows at the enhanced etch rate characteristic of the damaged plastic. Fig. 2D shows the net effect of etching the plastic for a sufficiently long time period. The scale is now greatly increased to the microscopically visible. The etch pits have ideally become measurable cones. Notice that the mouths of the two cones on each Lexan sheet should be congruent conic sections, typically ellipses, their precise size and shape being determined principally by the erosion rate of the *undamaged* plastic, the inclination of the nuclear track and the total time spent in the etching bath and are therefore nearly independent of the ionization properties of the incident nucleus. Notice that the depth of the etch cone is determined principally by the erosion rate in the damaged plastic and the total time spent in the etching bath.

Fig.3 Estimated values of $|Q/\beta|$ as a function of depth through the Lexan stack for the track in question. This data set is edited so as to remove from consideration all Lexan sheets to which any objection can be made regarding their having had differing manufacture or handling from the rest as described in the text. This data set conforms to the most severe reservations raised by any of the critics of the original interpretation of Price *et al.* in regard to the unreliability of the data from any of the individual Lexan sheets. Also excised are the "error bars" of Price and Shirk, since these are unknown without the use of certain questionable statistical arguments. The data

represented in this figure are the totality of points from the Lexan which will be quantitatively used in our discussions.

Fig.4 Etch rate data of Price and Shirk with "straight-line" hypothetical fits imposed. This "straight-line" hypothesis provides the basis for confidence level estimates based upon the F-test in this work and in Ref. 6. We use these statistical tools only for purposes of discussion. This figure is Fig. 3 with the addition of the continuous curve.

Fig.5 Comparison of expected behavior for a non-fragmenting normal (Z = 96) nucleus with the etch rate data of Price and Shirk. Data are edited as per Fig. 3. Curium is the heaviest nucleus commonly believed to be present in the cosmic rays. This fit is deemed to be excellent.

Fig.6 Comparison of expected behavior for a non-fragmenting normal uranium (Z = 92) nucleus with the etch rate data of Price and Shirk. Data are edited as per Fig. 3. This fit is deemed to be acceptable.

Fig.7 Comparison of expected behavior for a non-fragmenting normal lead (Z = 82) nucleus with the etch rate data of Price and Shirk. Data are edited as per Fig. 3. This fit is deemed unacceptable.

Fig.8 Same as for Fig. 7. except that Z = 78.

Fig.9 Same as for Fig. 3 except that Z = 65.

Fig.10 Comparison of expected behavior for a singly-fragmenting normal uranium (Z = 92) nucleus with the etch rate data of Price and Shirk. This fit is deemed completely acceptable.

Fig.11 Comparison of expected behavior for a singly-fragmenting normal lead (Z = 82) nucleus with the etch rate data of Price and Shirk. The fit is quite good.

Fig.12 Comparison of expected behavior for a doubly fragmenting normal Z = 82 nucleus with the etch rate data of Price and Shirk. This fit to the data is deemed completely acceptable.

Fig.13 Same as Fig. 12 except that Z = 74 and triply fragmenting.

Fig.14 Same as Fig. 12 except that Z = 70 and quadruply fragmenting.

Fig.15 Same as Fig. 12 except that Z = 68 and five times fragmenting.

Fig.16 Schematic representation of the photographic Cerenkov detector of Pinsky. The particle under study, incident from above, passes through the transparent radiator medium emitting faint visible radiation via the Cerenkov effect. When the emitted photons impinge upon the recording photographic emulsion below the radiator, an extended image is formed which, under highly idealized conditions, would depend solely upon

the speed of the incident particle, independent of its charge.

Fig.17 Measured spectral sensitivity of Eastman Kodak EK2485. high speed photographic recording emulsion. This graph gives an upper bound of 0.04 erg/cm^2 over the bandwidth of photon energies ranging from 1.6 eV to 4.25 eV on the useful sensitivity and useful bandwidth of the recording emulsion used in Pinsky's Cerenkov detector. This figure is after Fig. 4 of Ref. 35.

Fig.18 Modulation transfer funciton for EK2485 photographic emulsion. Given a light pattern with amplitude varying sinusoidally with position, imperfect image rendition on the recording emulsion will tend to blur the image, reducing the amplitude of the sinusoidal variation. The abscissa of this figure corresponds to the wavelength of the spatial variations (not the wavelength of the source light) and the ordinate corresponds to the fractional reduction of the amplitude of response. The smaller the desired photographic image, the more of the higher spatial frequencies are needed to accurately record it. The inverses of the maximum sizes of needed features of the Cerenkov images in the two detectors are indicated. Figure taken from Fig. 5 of Ref. 35 with additions.

Fig.19 Measured reciprocity behavior of Eastman Kodak EK2485 high speed recording emulsion. The ordinate on this figure corresponds to the effective sensitivity relative to that obtainable under the conditions where the data of Fig.17 were taken. The data on this figure were obtained from Fig.6 of Ref.35 The shaded region represents the range of light pulse durations of the desired Cerenkov photon signal in the Cerenkov detector of Pinsky.

Fig.20 Comparison of ionization and Cerenkov energy deposition in the photographic recording emulsion. The energy deposition estimate must be considered approximate because of the unavailability of a description of the physical and chemical composition of the emulsion from the manufacturer. The energy deposited in the recording emulsion by knock-on electrons accompanying the passage of the nucleus ($Z = 80$, $\beta = 0.75$) far exceeds the energy deposited by the desired Cerenkov photon signal. The production of ionization and Cerenkov energy both are roughly proportional to Z^2 so that this figure accurately reflects the disparity between the two competing signals for all nuclei.

Fig.21 Schematic representation of the configuration of the Cerenkov detector as flown in balloon flight 1. The relatively diminished sizes of the upper recorded images reported on three nuclear tracks compared to their lower recorded images was used as evidence for the Cerenkov origins of the lower images. Alternative explanations are given in the text.

Fig.22 Comparison of spectral sensitivity curves for EK2485 recording emulsion as published by Pinsky and as published by the manufacturer. Curve A is from Pinsky, Curve B is from Kodak. We note the discrepancy in labelling of vertical scales. Figure after Fig. B1 of Ref. 32 and Fig. 4 of Ref. 35.

Fig.23 The function $\cos\chi$ as it depends on the variable $Z\alpha/\beta$. This function is useful for computing the small-angle approximation to the Mott scattering cross section.

Fig.24 Departure of Lexan response from constancy for nuclei with the same values of $|Z/\beta|$, but with differing speeds as calculated from the restricted energy loss model of Ahlen.[29]

Fig.25 Values of $|Z/\beta|$ needed to produce the measured mean etch rate giving $|Q/\beta|$=114 as calculated after the restricted energy loss model of Ahlen.[29] This plot is based on the model of Ahlen with our assumption that the value of $|Q/\beta|$ equals the value of $|Z/\beta|$ for iron nuclei.

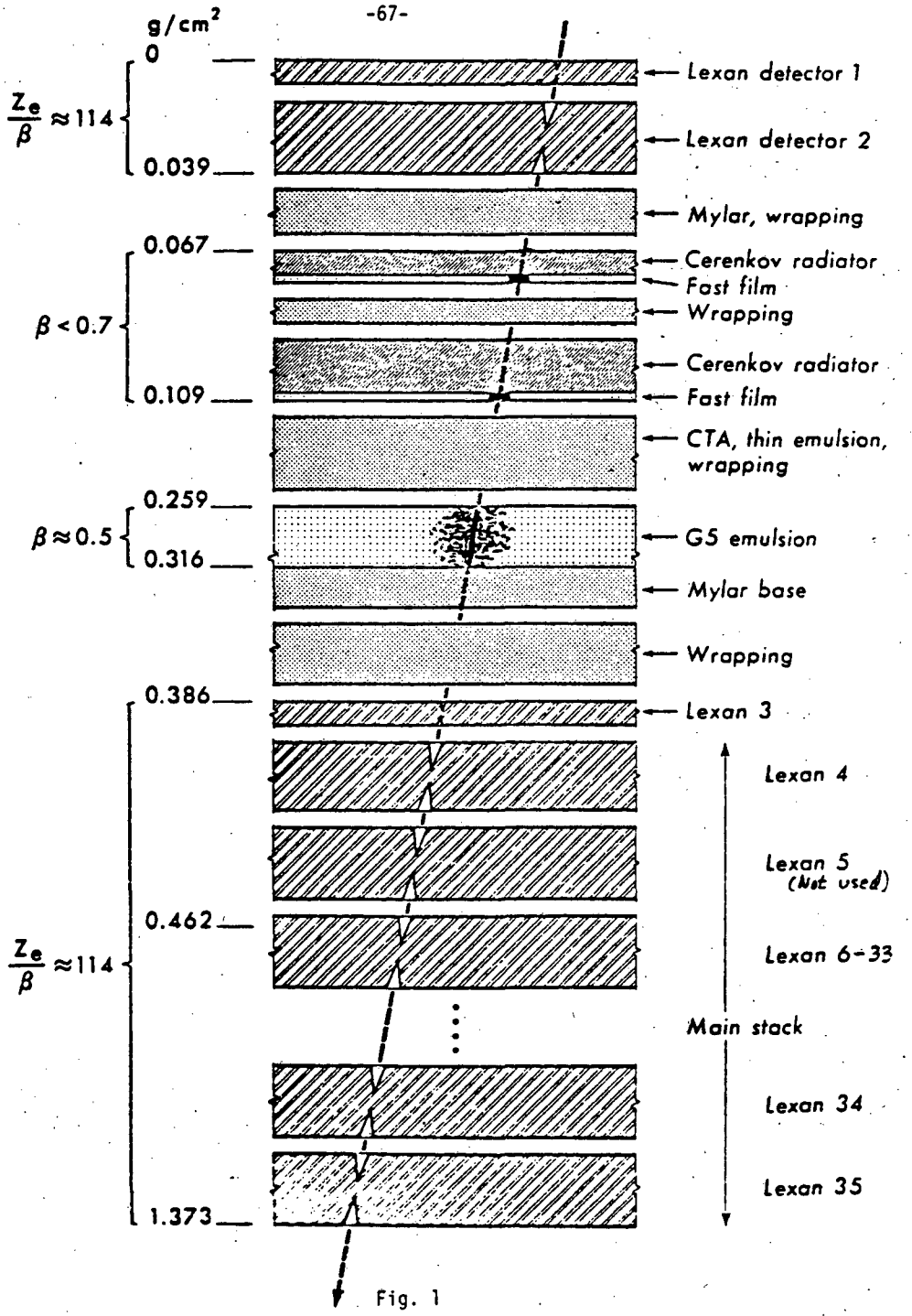
g/cm²
0
0.039
0.067
0.109
0.259
0.316
0.386
0.462
1.373
Ze/β ≈114
β < 0.7
β ≈0.5
Ze/β ≈114
Lexan detector 1
Lexan detector 2
Mylar, wrapping
Cerenkov radiator
Fast film
Wrapping
Cerenkov radiator
Fast film
CTA, thin emulsion, wrapping
G5 emulsion
Mylar base
Wrapping
Lexan 3
Lexan 4
Lexan 5 (Not used)
Lexan 6-33
Main stack
Lexan 34
Lexan 35

Fig. 1

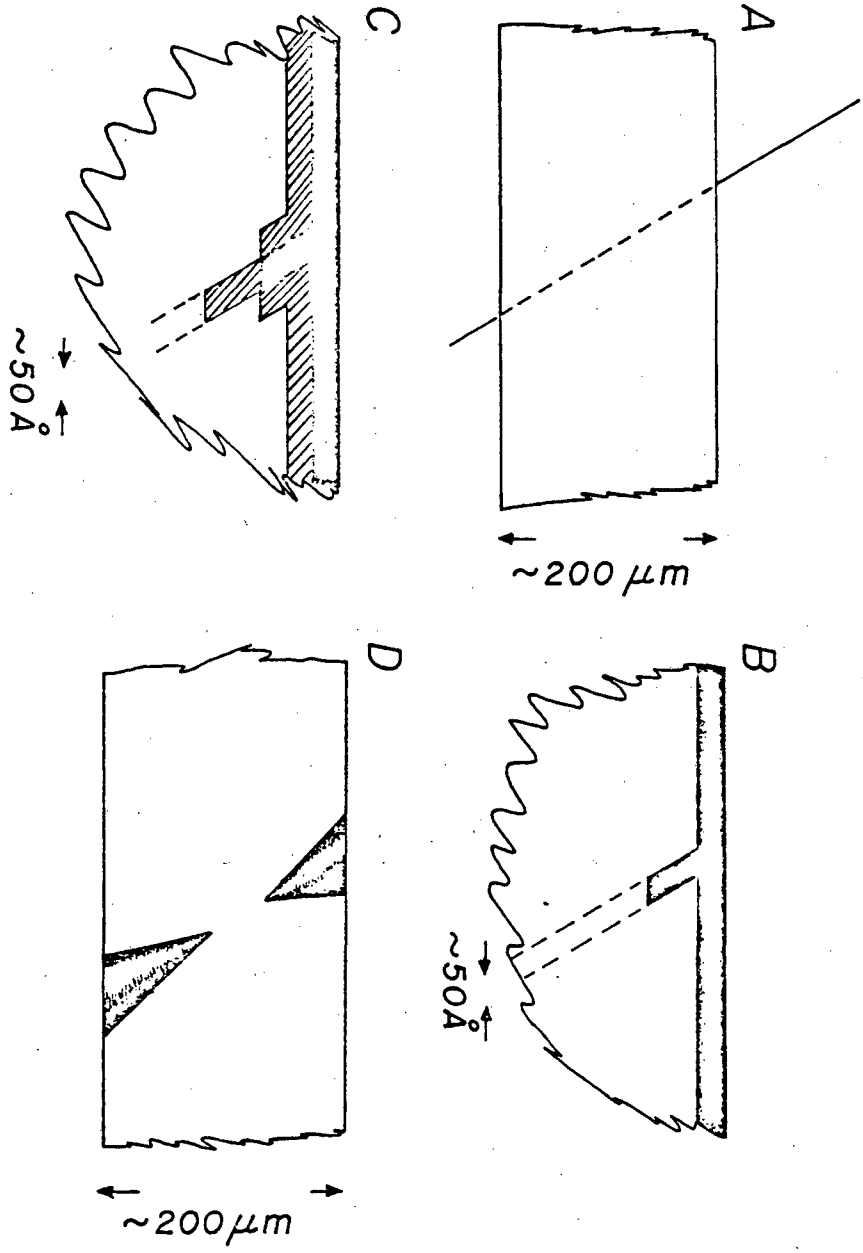

Fig. 2

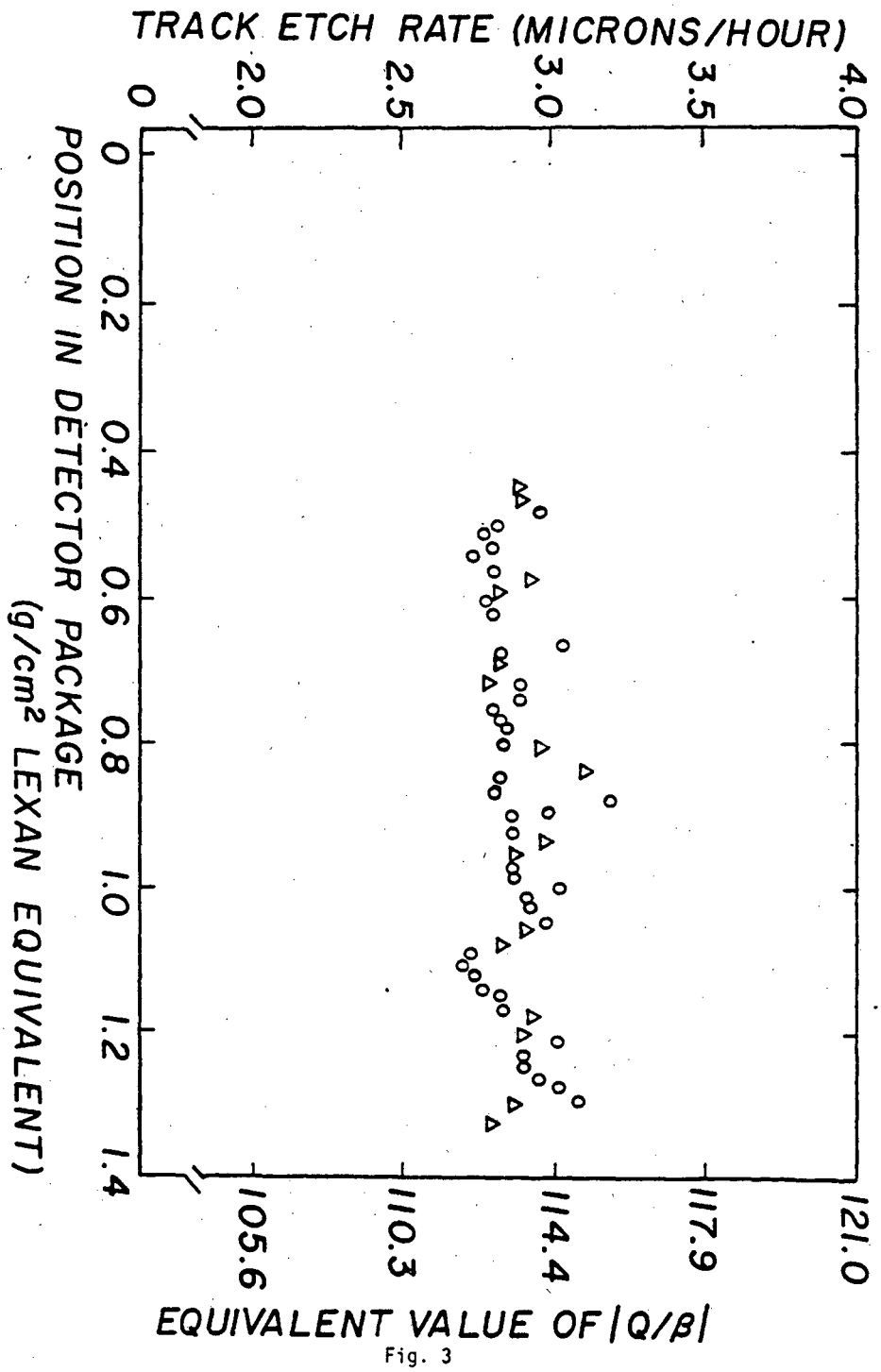
TRACK ETCH RATE (MICRONS/HOUR)
2.0
2.5
3.0
3.5
4.0
0
0
0.2
0.4
0.6
0.8
1.0
1.2
1.4
POSITION IN DETECTOR PACKAGE
(g/cm² LEXAN EQUIVALENT)
105.6
110.3
114.4
117.9
121.0
EQUIVALENT VALUE OF |Q/β|

Fig. 3

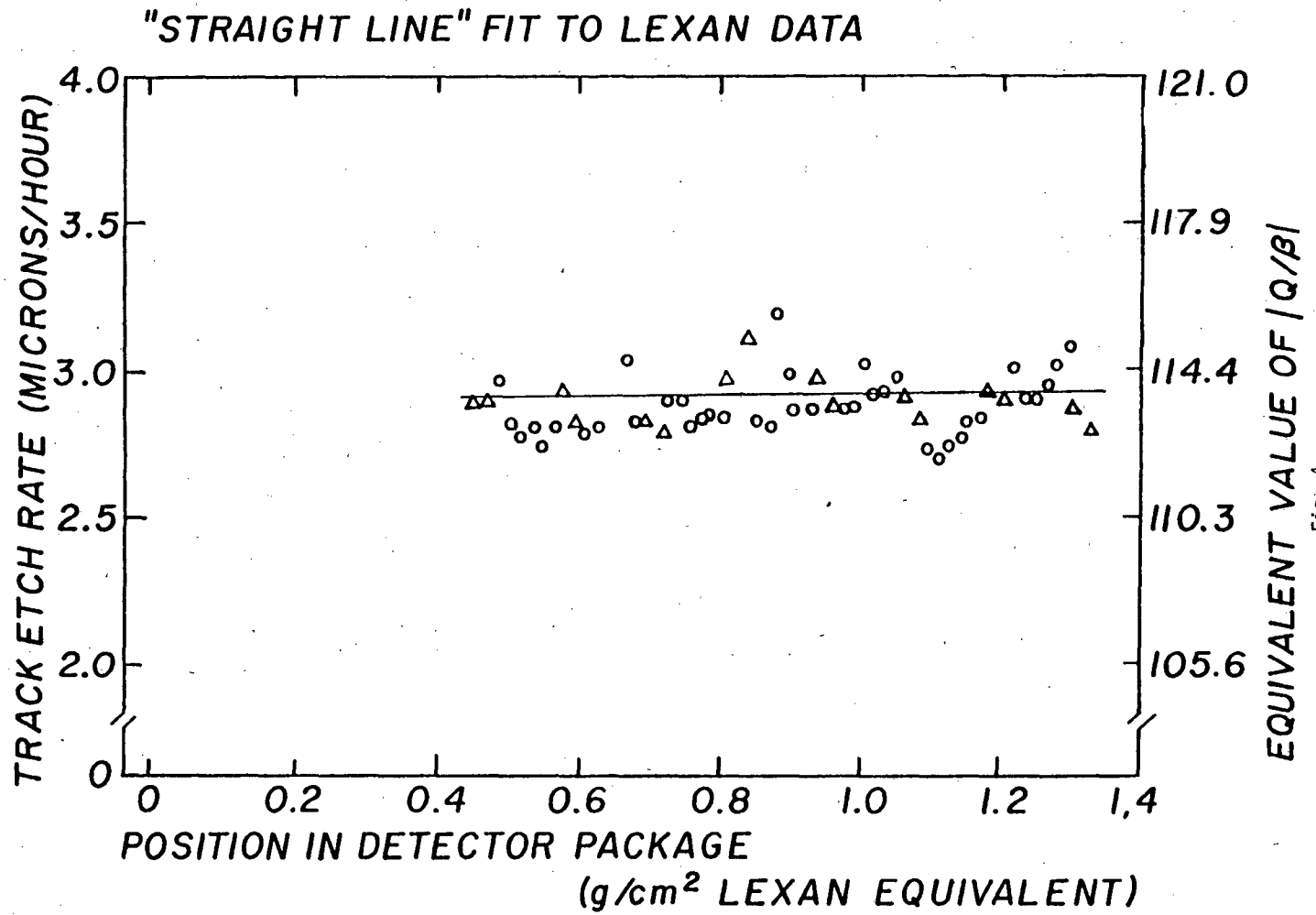
"STRAIGHT LINE" FIT TO LEXAN DATA
TRACK ETCH RATE (MICRONS/HOUR)
4.0
3.5
3.0
2.5
2.0
0
0
0.2
0.4
0.6
0.8
1.0
1.2
1.4
POSITION IN DETECTOR PACKAGE
(g/cm² LEXAN EQUIVALENT)
121.0
117.9
114.4
110.3
105.6
EQUIVALENT VALUE OF |Q/β|

Fig. 4

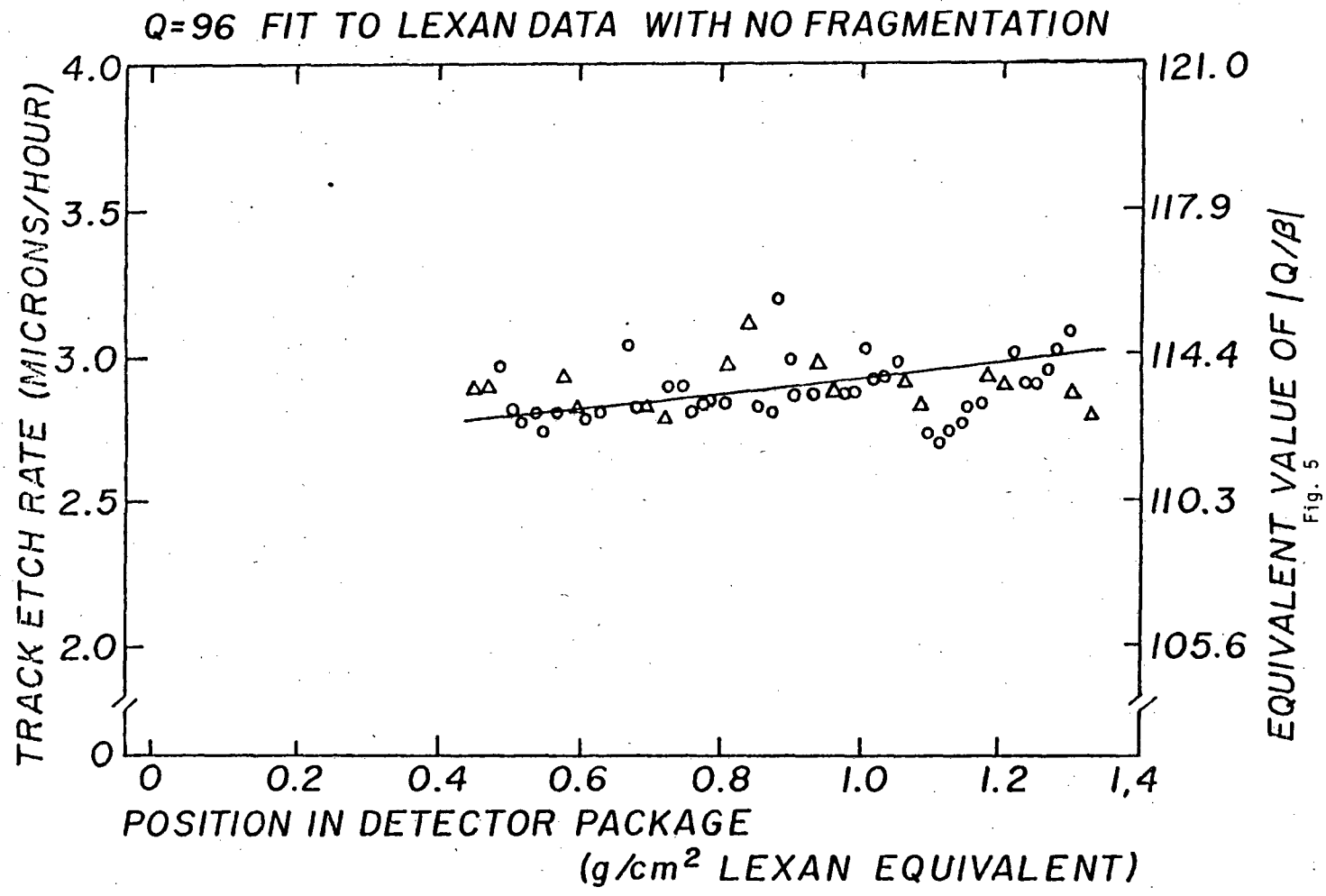
Q=96 FIT TO LEXAN DATA WITH NO FRAGMENTATION
TRACK ETCH RATE (MICRONS/HOUR)
EQUIVALENT VALUE OF |Q/β|
4.0
3.5
3.0
2.5
2.0
0
121.0
117.9
114.4
110.3
105.6
0
0.2
0.4
0.6
0.8
1.0
1.2
1,4
POSITION IN DETECTOR PACKAGE
(g/cm² LEXAN EQUIVALENT)

Fig. 5

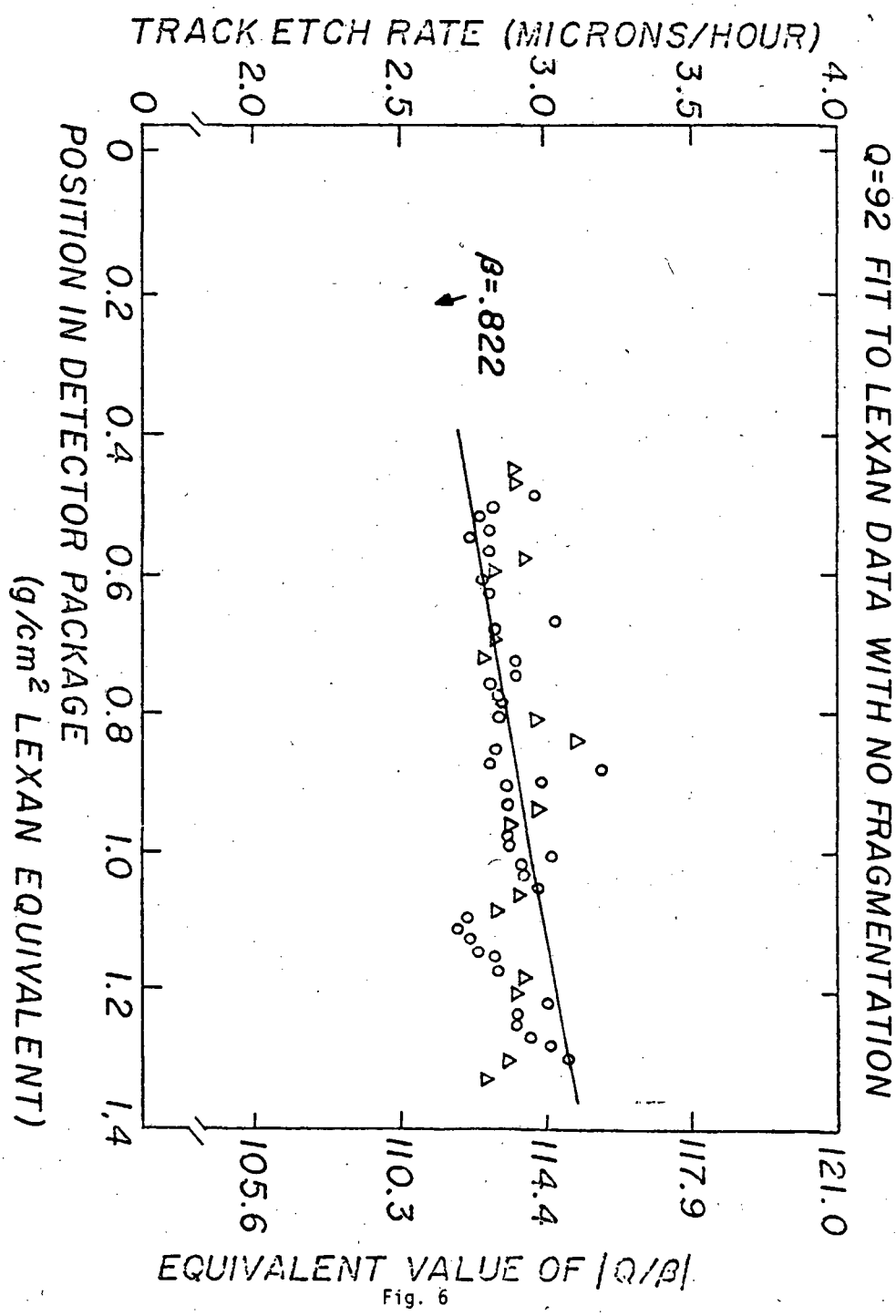
TRACK ETCH RATE (MICRONS/HOUR)
0
2.0
2.5
3.0
3.5
4.0
Q=92 FIT TO LEXAN DATA WITH NO FRAGMENTATION
β=.822
0
0.2
0.4
0.6
0.8
1.0
1.2
1.4
POSITION IN DETECTOR PACKAGE
(g/cm² LEXAN EQUIVALENT)
105.6
110.3
114.4
117.9
121.0
EQUIVALENT VALUE OF |Q/β|

Fig. 6

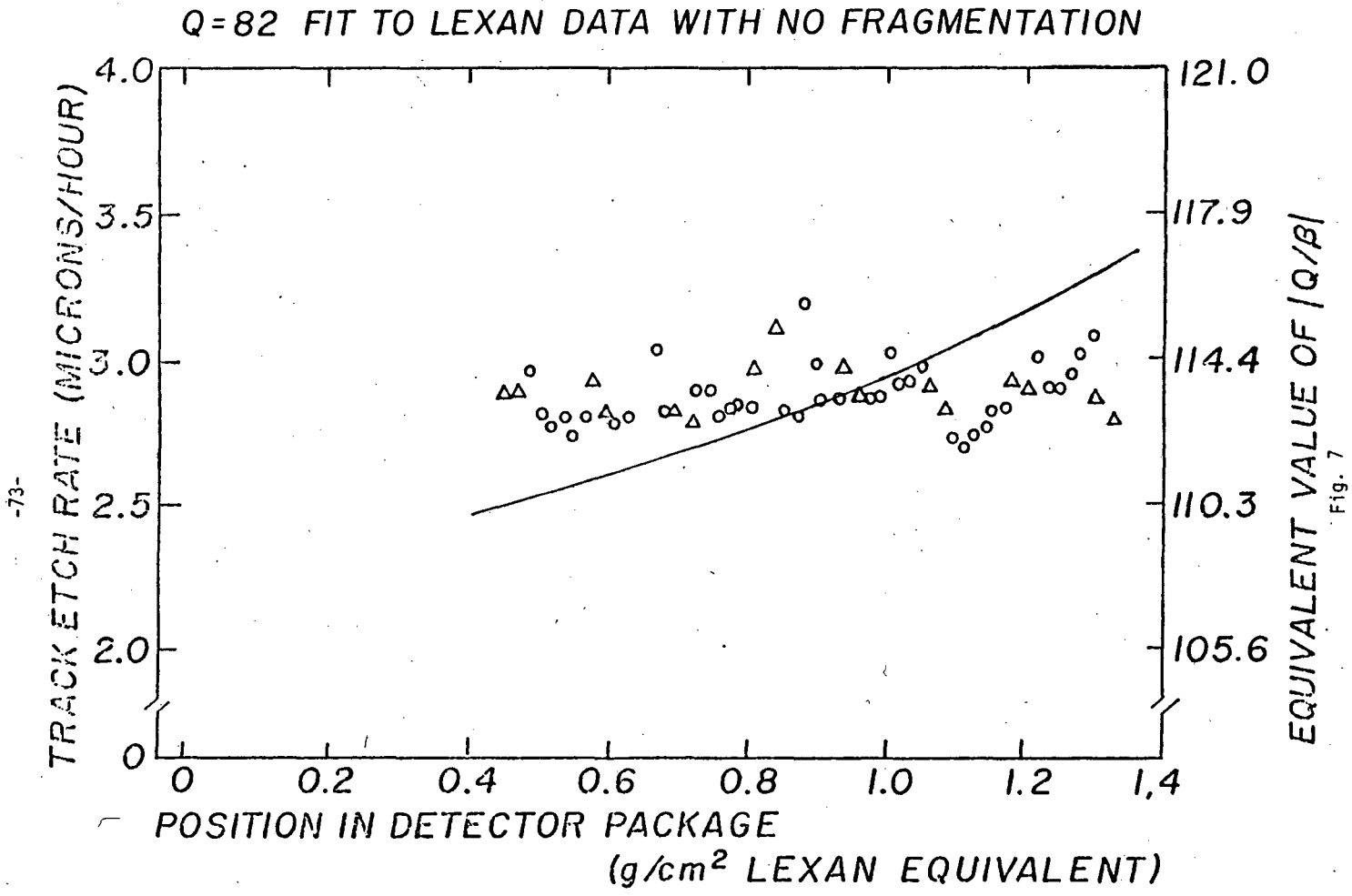
Q=82 FIT TO LEXAN DATA WITH NO FRAGMENTATION
TRACK ETCH RATE (MICRONS/HOUR)
4.0
3.5
3.0
2.5
2.0
0
0
0.2
0.4
0.6
0.8
1.0
1.2
1.4
POSITION IN DETECTOR PACKAGE
(g/cm² LEXAN EQUIVALENT)
121.0
117.9
114.4
110.3
105.6
EQUIVALENT VALUE OF |Q/β|

Fig. 7

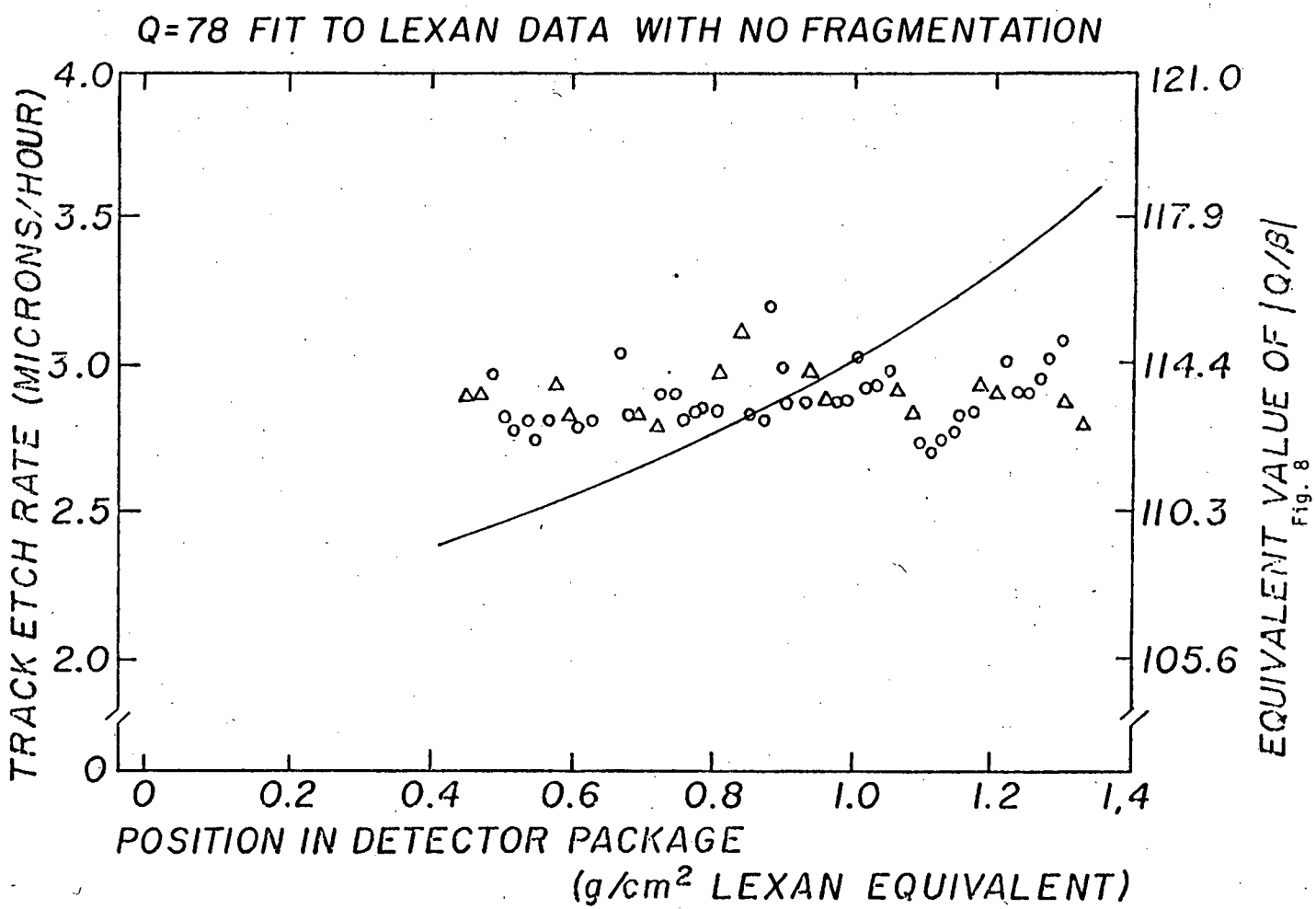
Q=78 FIT TO LEXAN DATA WITH NO FRAGMENTATION
TRACK ETCH RATE (MICRONS/HOUR)
EQUIVALENT VALUE OF |Q/β|
4.0
3.5
3.0
2.5
2.0
0
121.0
117.9
114.4
110.3
105.6
0
0.2
0.4
0.6
0.8
1.0
1.2
1.4
POSITION IN DETECTOR PACKAGE
(g/cm² LEXAN EQUIVALENT)

Fig. 8

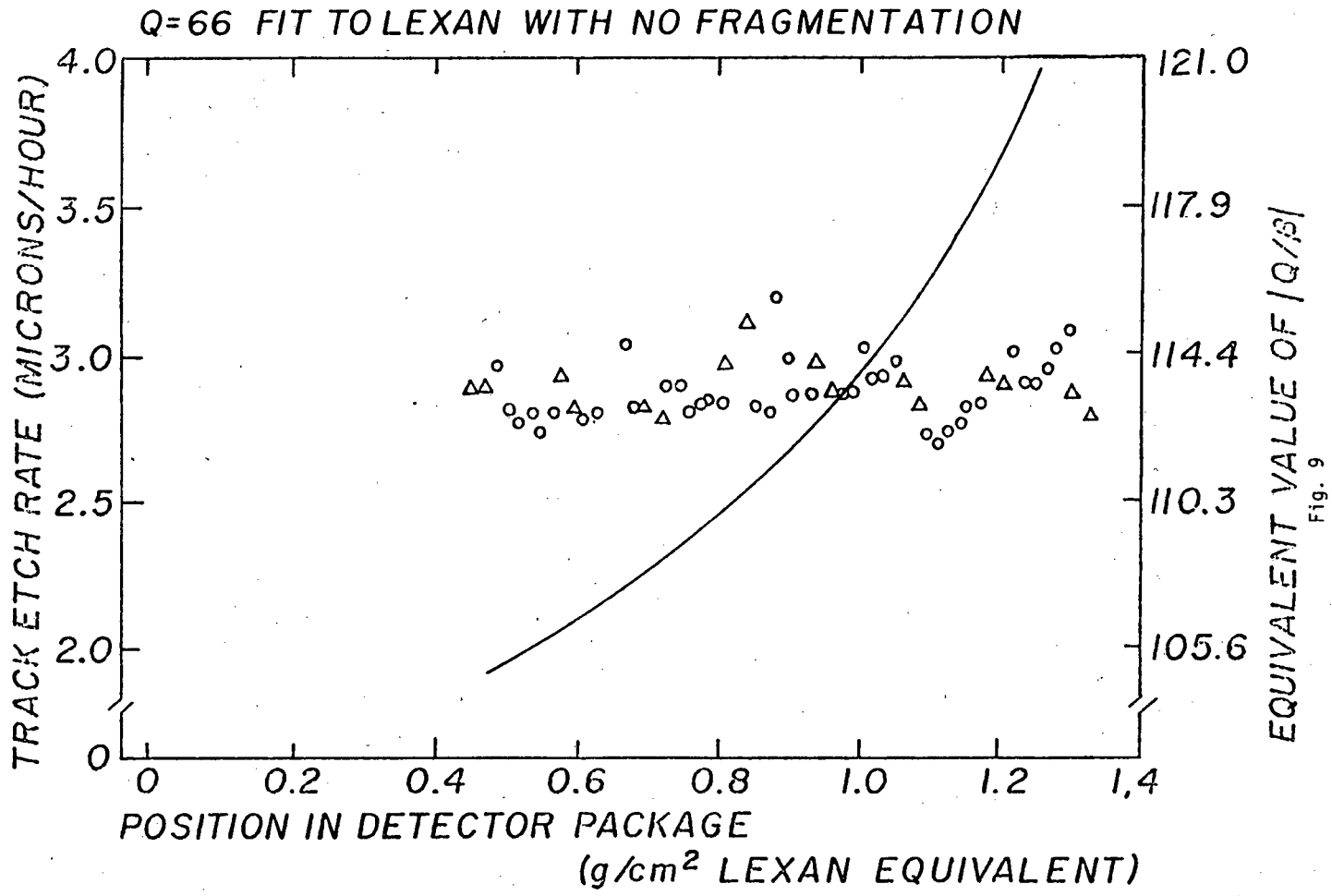
Q=66 FIT TO LEXAN WITH NO FRAGMENTATION
TRACK ETCH RATE (MICRONS/HOUR)
4.0
3.5
3.0
2.5
2.0
0
0
0.2
0.4
0.6
0.8
1.0
1.2
1.4
POSITION IN DETECTOR PACKAGE
(g/cm² LEXAN EQUIVALENT)
121.0
117.9
114.4
110.3
105.6
EQUIVALENT VALUE OF |Q/β|

Fig. 9

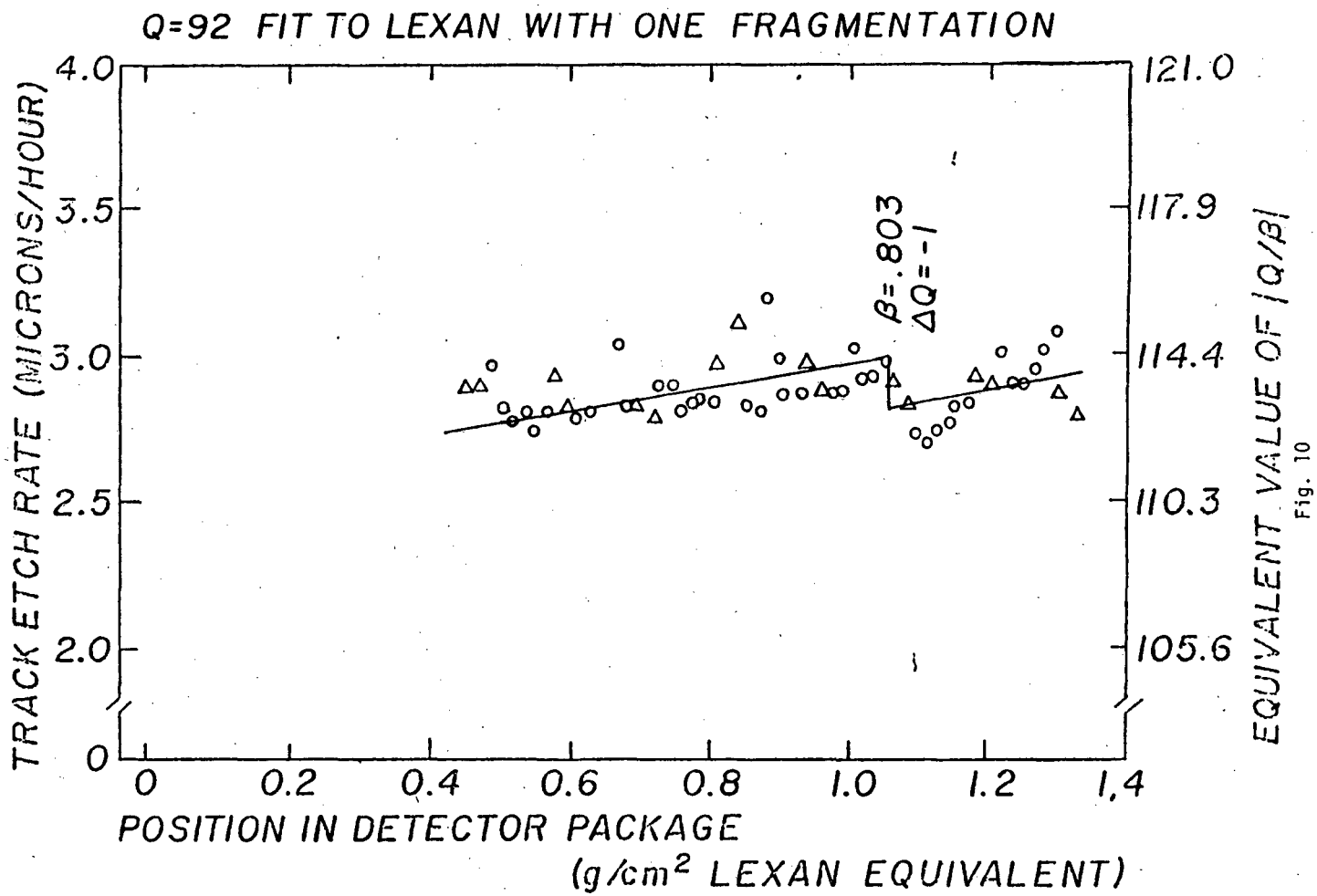
Q=92 FIT TO LEXAN WITH ONE FRAGMENTATION
TRACK ETCH RATE (MICRONS/HOUR)
EQUIVALENT VALUE OF |Q/β|
β=.803
ΔQ=-1
4.0
3.5
3.0
2.5
2.0
0
121.0
117.9
114.4
110.3
105.6
0
0.2
0.4
0.6
0.8
1.0
1.2
1.4
POSITION IN DETECTOR PACKAGE
(g/cm² LEXAN EQUIVALENT)

Fig. 10

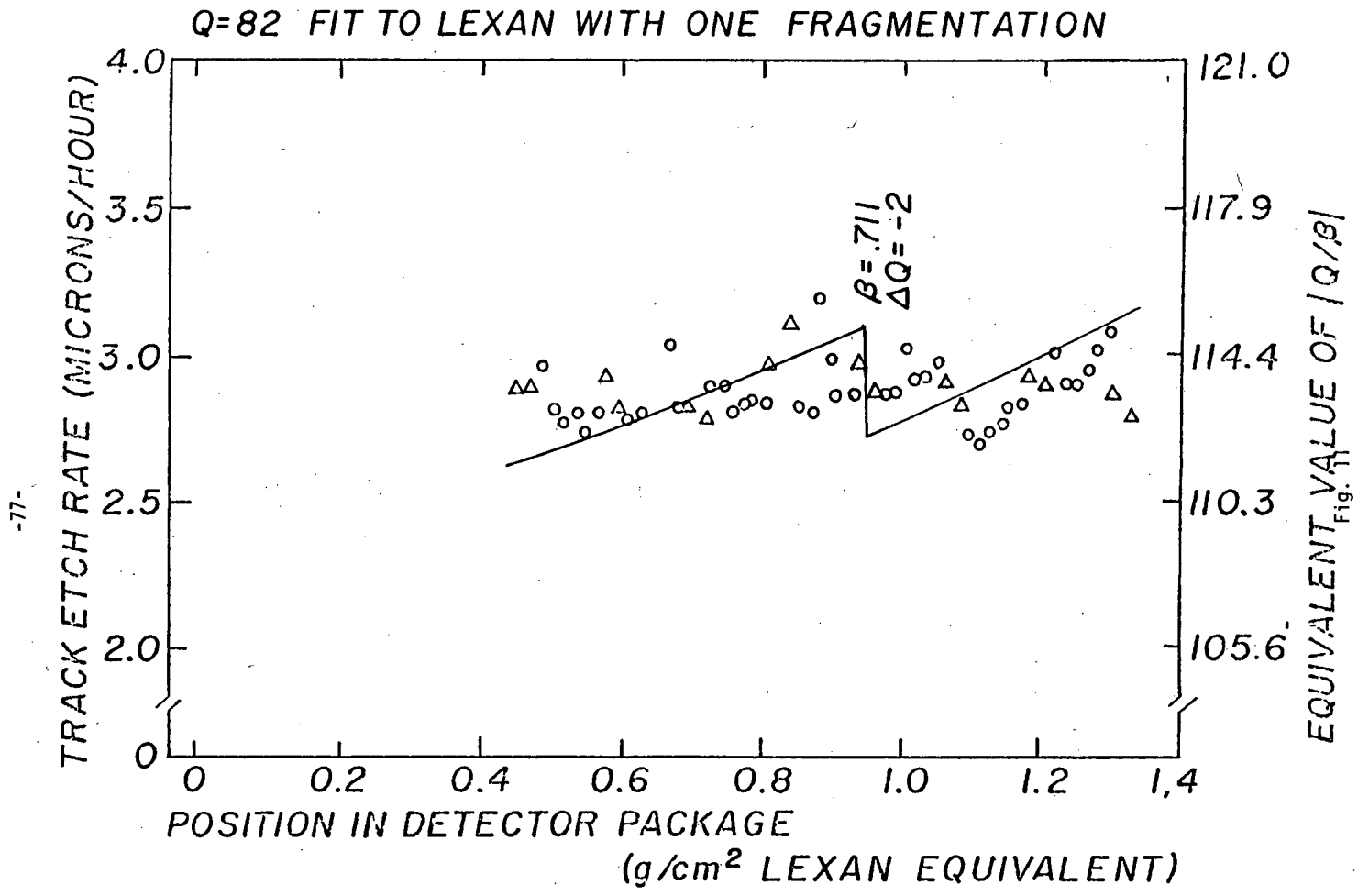
Q=82 FIT TO LEXAN WITH ONE FRAGMENTATION
TRACK ETCH RATE (MICRONS/HOUR)
EQUIVALENT VALUE OF |Q/β|
β=.711
ΔQ=-2
4.0
3.5
3.0
2.5
2.0
0
121.0
117.9
114.4
110.3
105.6
0
0.2
0.4
0.6
0.8
1.0
1.2
1.4
POSITION IN DETECTOR PACKAGE
(g/cm² LEXAN EQUIVALENT)

Fig. 11

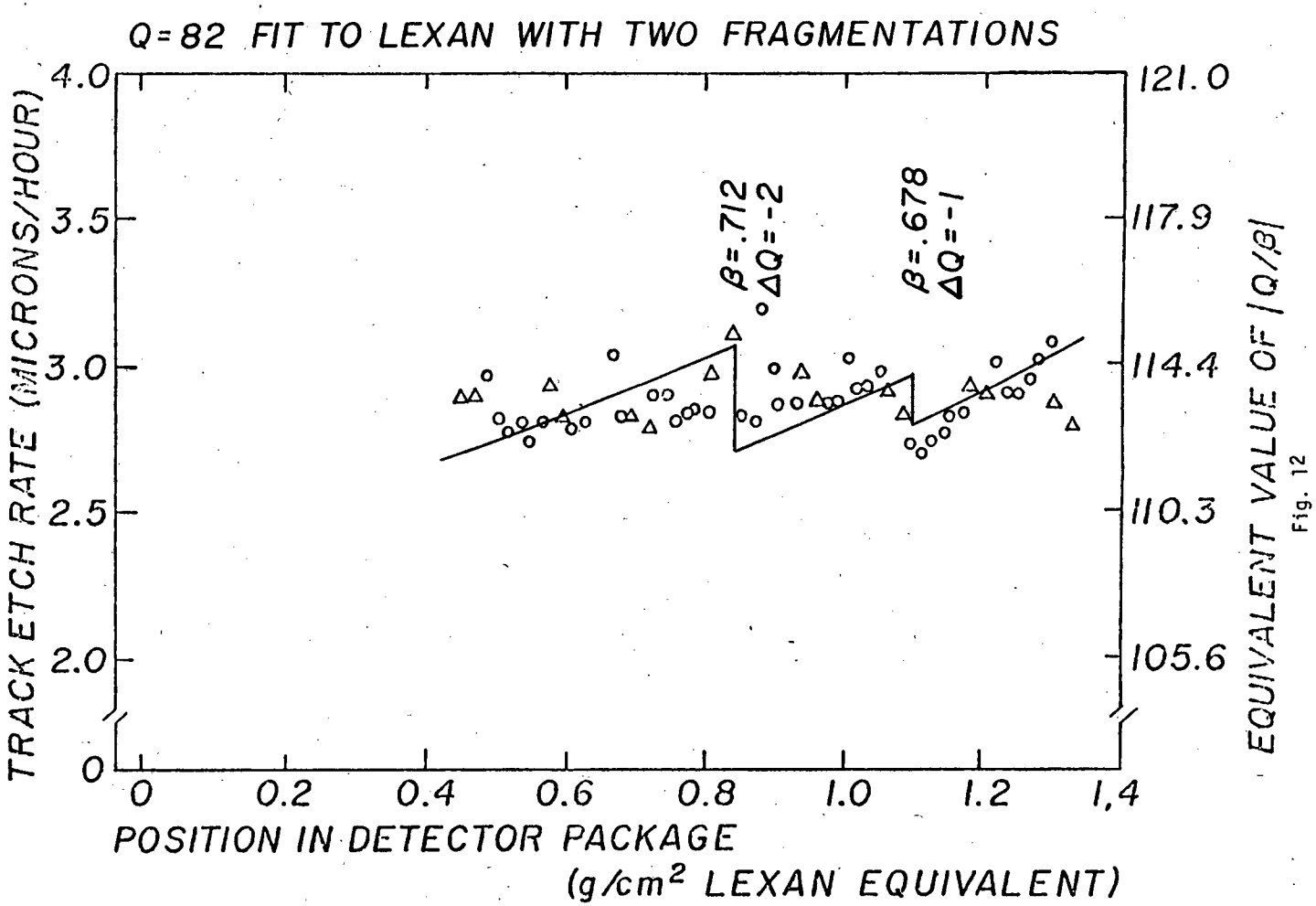
Q=82 FIT TO LEXAN WITH TWO FRAGMENTATIONS
TRACK ETCH RATE (MICRONS/HOUR)
EQUIVALENT VALUE OF |Q/β|
POSITION IN DETECTOR PACKAGE
(g/cm² LEXAN EQUIVALENT)
β=.712
ΔQ=-2
β=.678
ΔQ=-1
4.0
3.5
3.0
2.5
2.0
0
121.0
117.9
114.4
110.3
105.6
0
0.2
0.4
0.6
0.8
1.0
1.2
1.4

Fig. 12

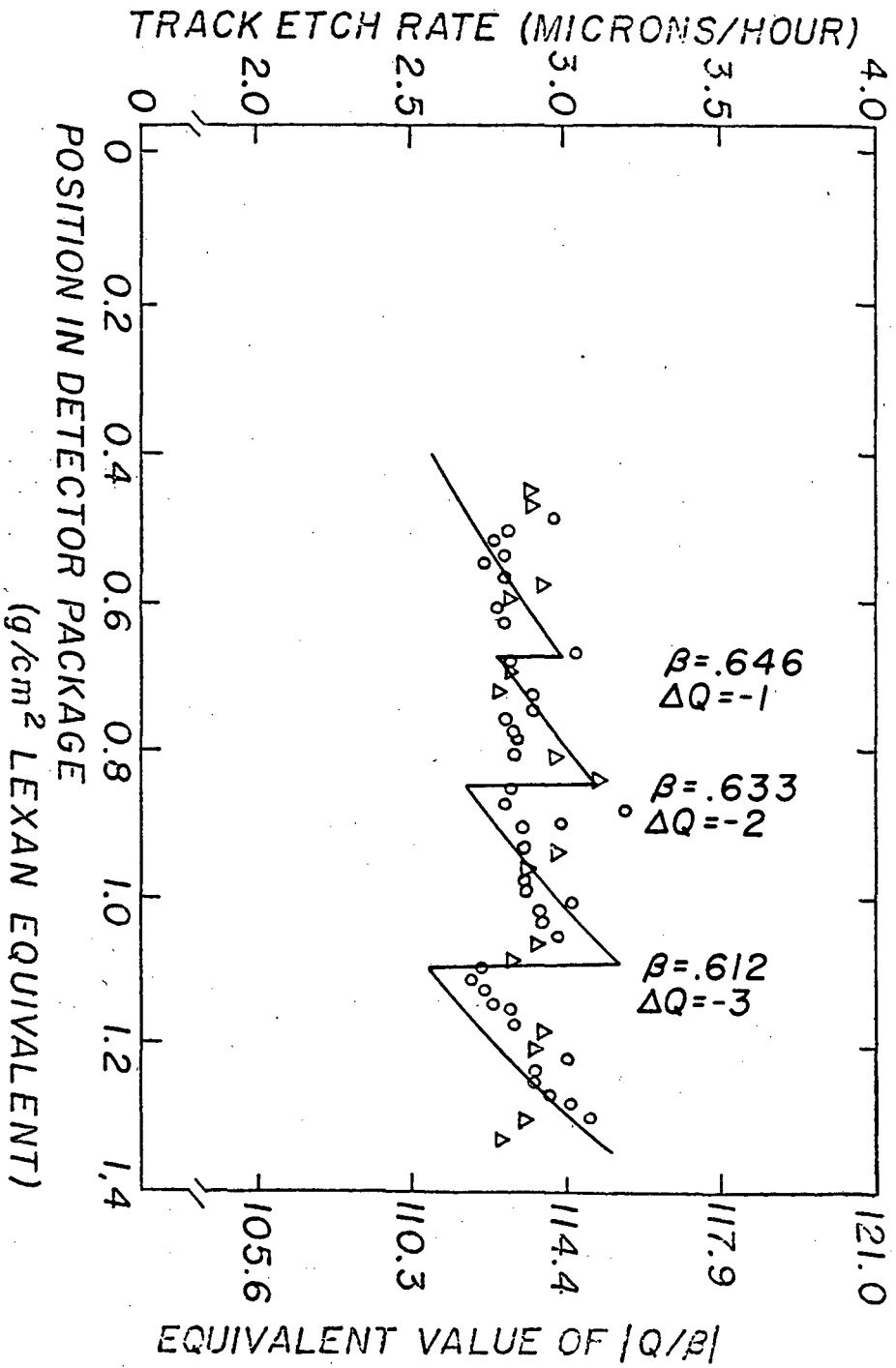
TRACK ETCH RATE (MICRONS/HOUR)
2.0
2.5
3.0
3.5
4.0
Q=74 FIT TO LEXAN WITH THREE FRAGMENTATIONS
0
0.2
0.4
0.6
0.8
1.0
1.2
1.4
POSITION IN DETECTOR PACKAGE
(g/cm² LEXAN EQUIVALENT)
β=.646
ΔQ=-1
β=.633
ΔQ=-2
β=.612
ΔQ=-3
105.6
110.3
114.4
117.9
121.0
EQUIVALENT VALUE OF |Q/β|

Fig. 13

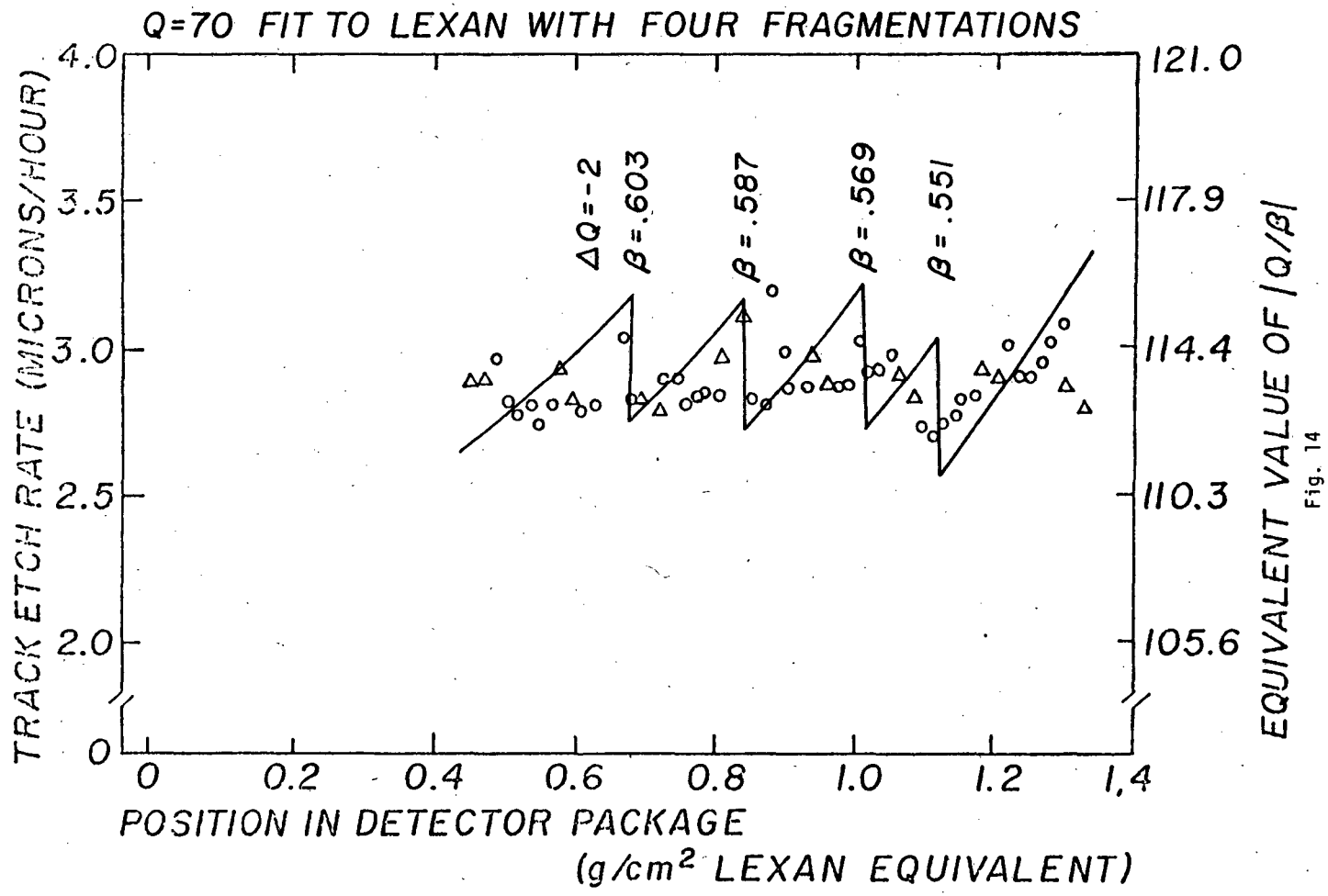
Q=70 FIT TO LEXAN WITH FOUR FRAGMENTATIONS
TRACK ETCH RATE (MICRONS/HOUR)
EQUIVALENT VALUE OF |Q/β|
ΔQ=-2
β=.603
β=.587
β=.569
β=.551
4.0
3.5
3.0
2.5
2.0
0
121.0
117.9
114.4
110.3
105.6
0
0.2
0.4
0.6
0.8
1.0
1.2
1.4
POSITION IN DETECTOR PACKAGE
(g/cm² LEXAN EQUIVALENT)

Fig. 14

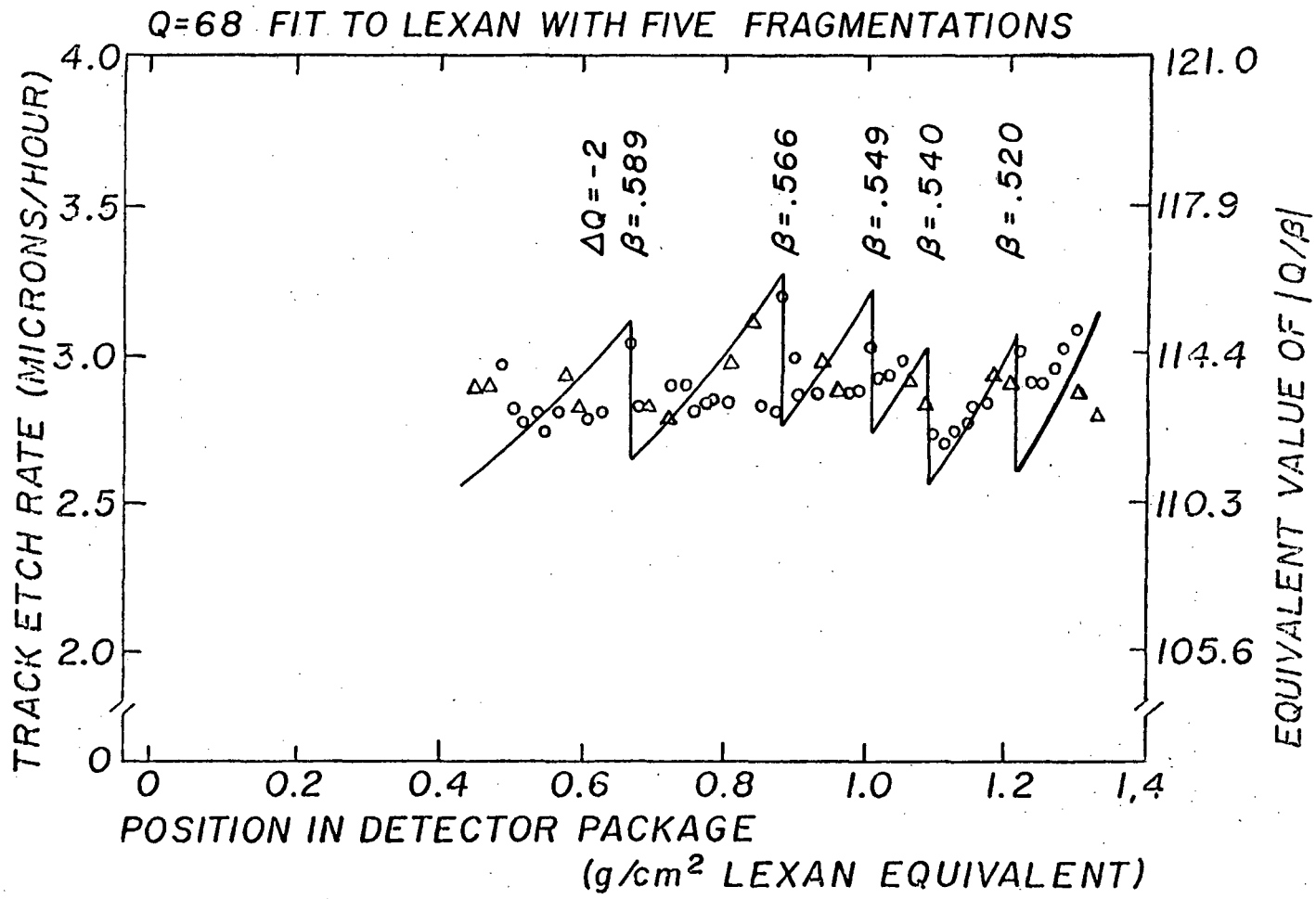
Q=68 FIT TO LEXAN WITH FIVE FRAGMENTATIONS
TRACK ETCH RATE (MICRONS/HOUR)
EQUIVALENT VALUE OF |Q/β|
POSITION IN DETECTOR PACKAGE
(g/cm² LEXAN EQUIVALENT)
ΔQ=-2
β=.589
β=.566
β=.549
β=.540
β=.520
4.0
3.5
3.0
2.5
2.0
0
0
0.2
0.4
0.6
0.8
1.0
1.2
1.4
121.0
117.9
114.4
110.3
105.6

Fig. 15

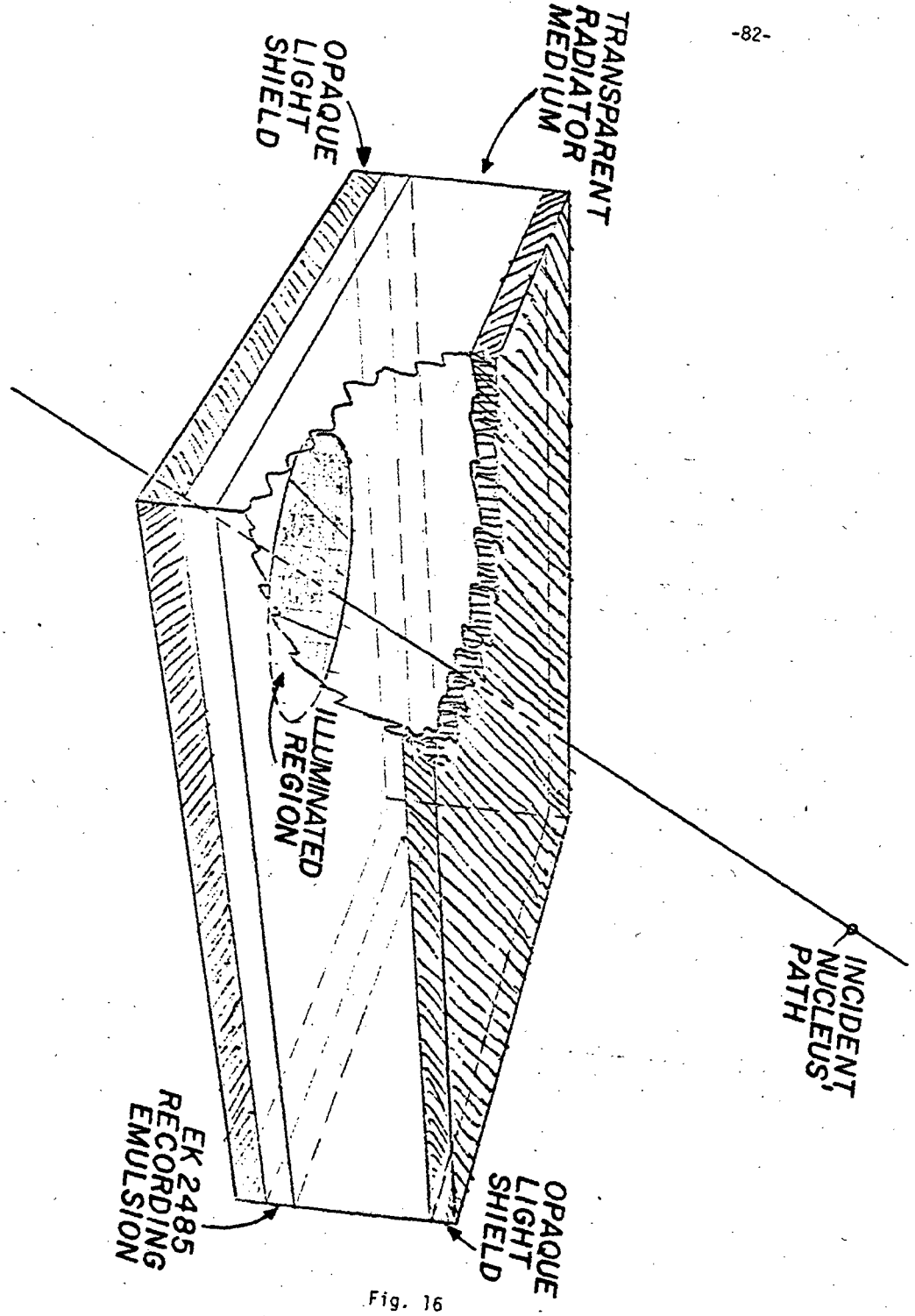
TRANSPARENT RADIATOR MEDIUM
OPAQUE LIGHT SHIELD
ILLUMINATED REGION
INCIDENT NUCLEUS' PATH
EK 2485 RECORDING EMULSION
OPAQUE LIGHT SHIELD

Fig. 16

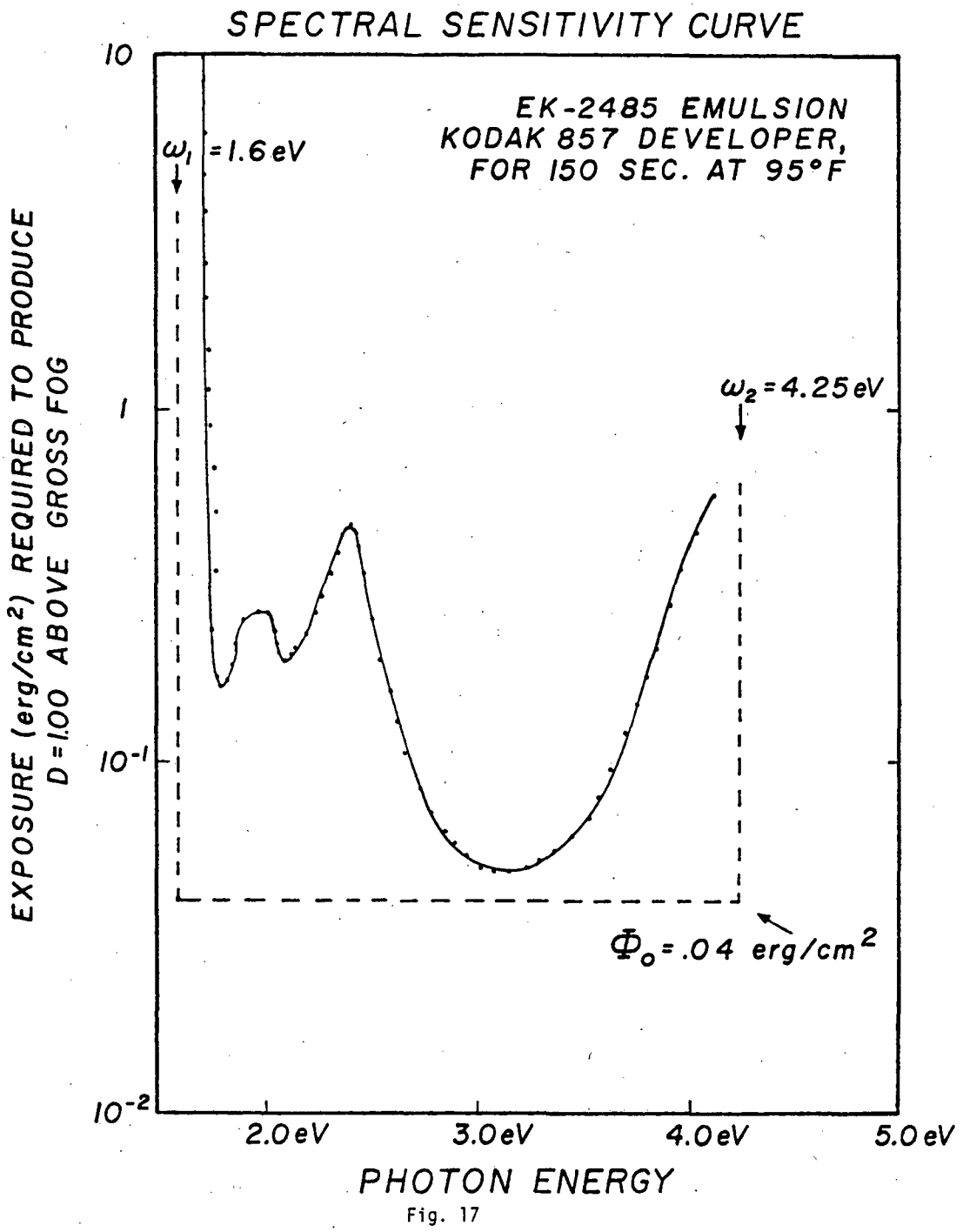
SPECTRAL SENSITIVITY CURVE
EK-2485 EMULSION
KODAK 857 DEVELOPER,
FOR 150 SEC. AT 95°F
ω_1 = 1.6 eV
ω_2 = 4.25 eV
Φ_o = .04 erg/cm^2
EXPOSURE (erg/cm^2) REQUIRED TO PRODUCE D = 1.00 ABOVE GROSS FOG
10
1
10^{-1}
10^{-2}
2.0 eV
3.0 eV
4.0 eV
5.0 eV
PHOTON ENERGY

Fig. 17

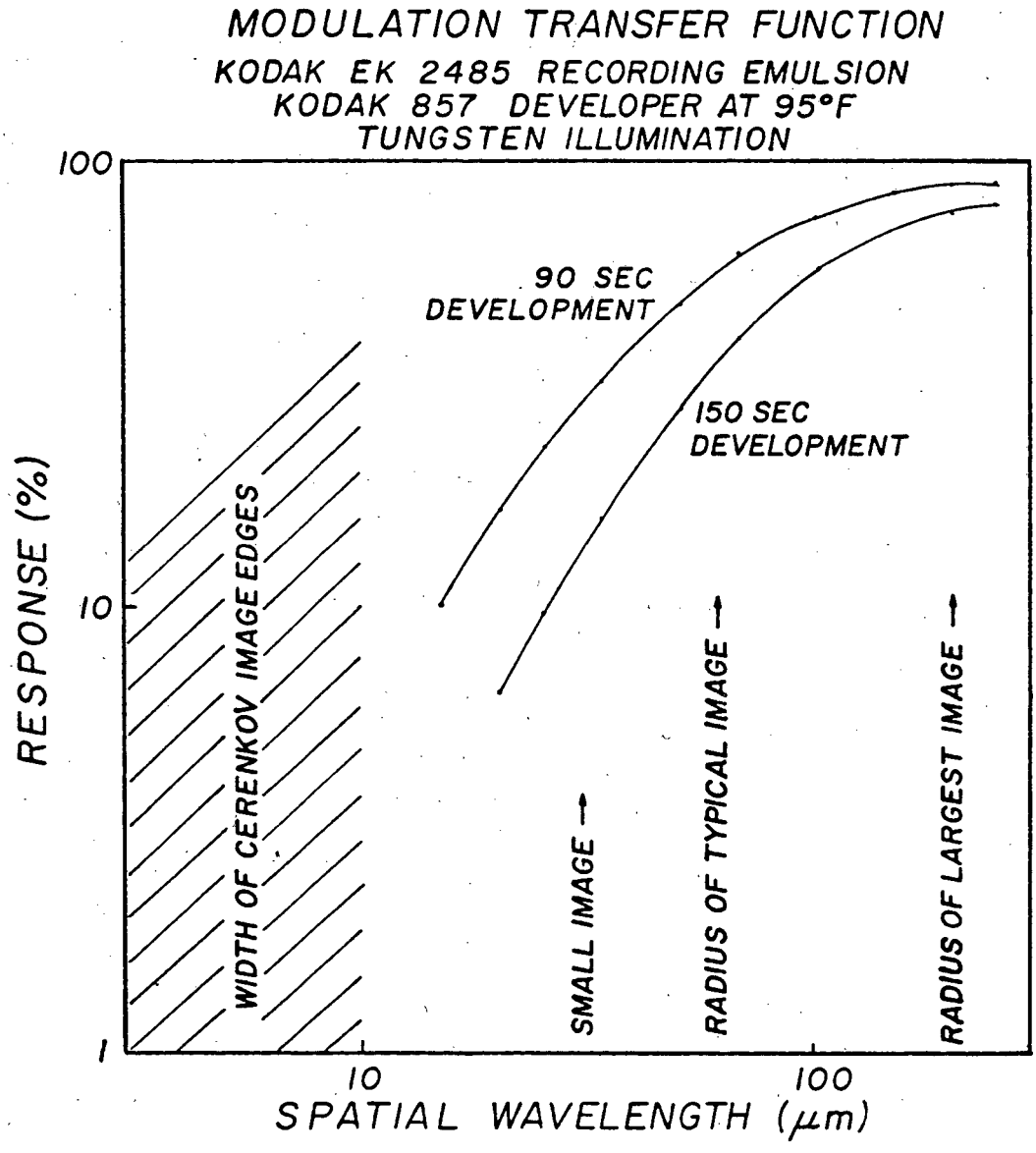
MODULATION TRANSFER FUNCTION
KODAK EK 2485 RECORDING EMULSION
KODAK 857 DEVELOPER AT 95°F
TUNGSTEN ILLUMINATION
100
10
1
RESPONSE (%)
90 SEC
DEVELOPMENT
150 SEC
DEVELOPMENT
WIDTH OF CERENKOV IMAGE EDGES
SMALL IMAGE →
RADIUS OF TYPICAL IMAGE →
RADIUS OF LARGEST IMAGE →
10
100
SPATIAL WAVELENGTH (μm)

Fig. 18

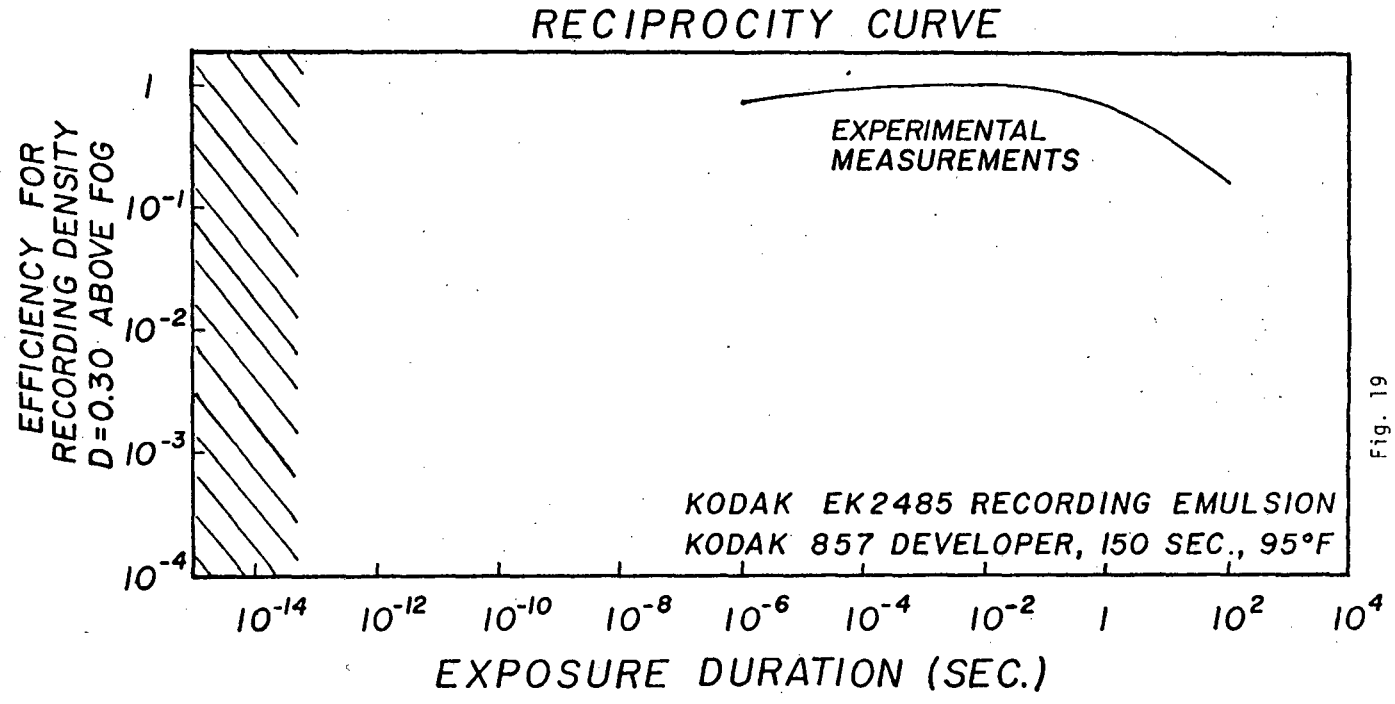
RECIPROCITY CURVE
EFFICIENCY FOR RECORDING DENSITY D=0.30 ABOVE FOG
1
10-1
10-2
10-3
10-4
EXPERIMENTAL MEASUREMENTS
KODAK EK2485 RECORDING EMULSION
KODAK 857 DEVELOPER, 150 SEC., 95°F
10-14
10-12
10-10
10-8
10-6
10-4
10-2
1
102
104
EXPOSURE DURATION (SEC.)

Fig. 19

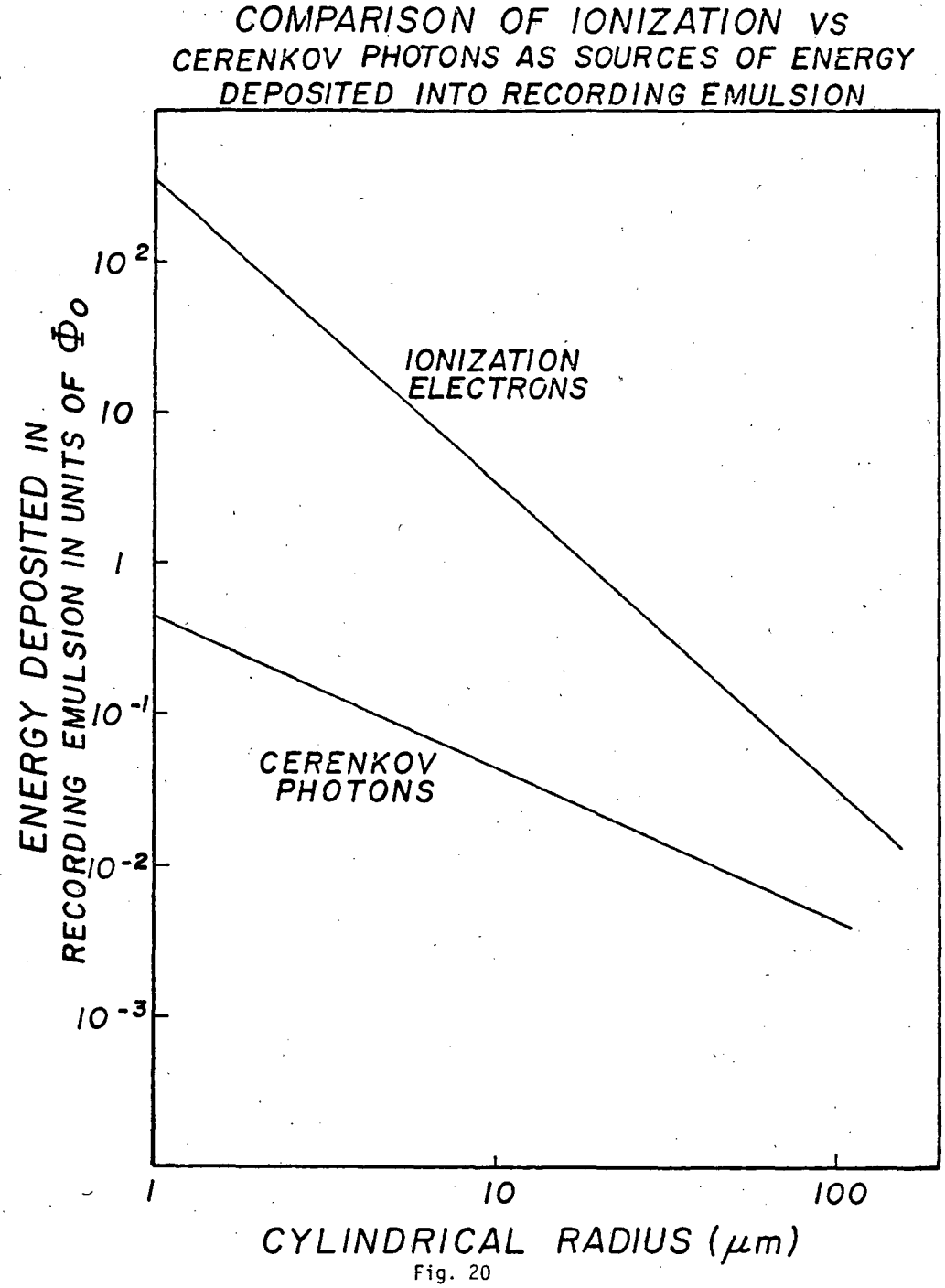
COMPARISON OF IONIZATION VS
CERENKOV PHOTONS AS SOURCES OF ENERGY
DEPOSITED INTO RECORDING EMULSION
ENERGY DEPOSITED IN
RECORDING EMULSION IN UNITS OF Φ_0
10^2
10
1
10^{-1}
10^{-2}
10^{-3}
IONIZATION
ELECTRONS
CERENKOV
PHOTONS
1
10
100
CYLINDRICAL RADIUS (μm)

Fig. 20

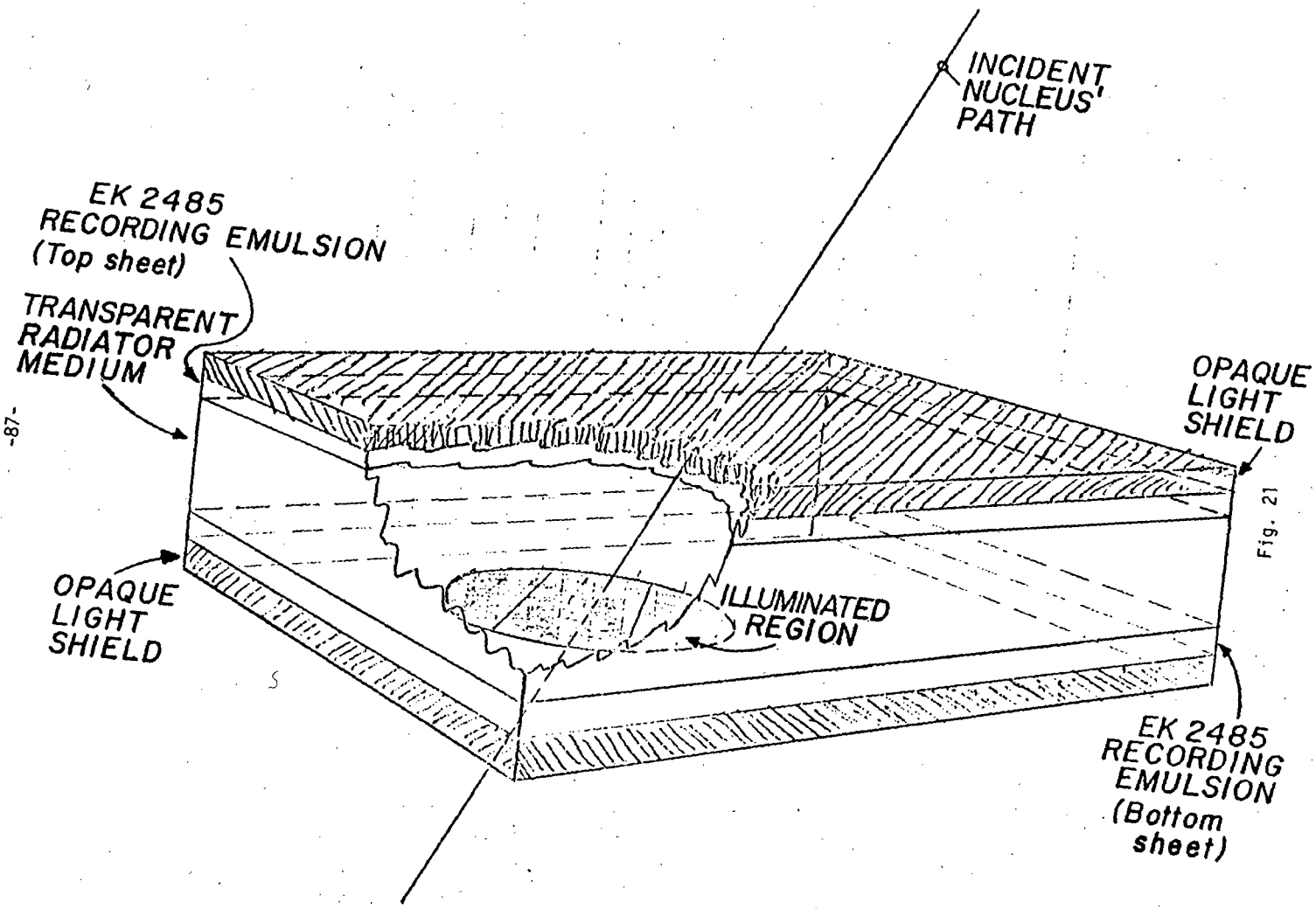
INCIDENT NUCLEUS' PATH
EK 2485 RECORDING EMULSION (Top sheet)
TRANSPARENT RADIATOR MEDIUM
OPAQUE LIGHT SHIELD
OPAQUE LIGHT SHIELD
ILLUMINATED REGION
EK 2485 RECORDING EMULSION (Bottom sheet)

Fig. 21

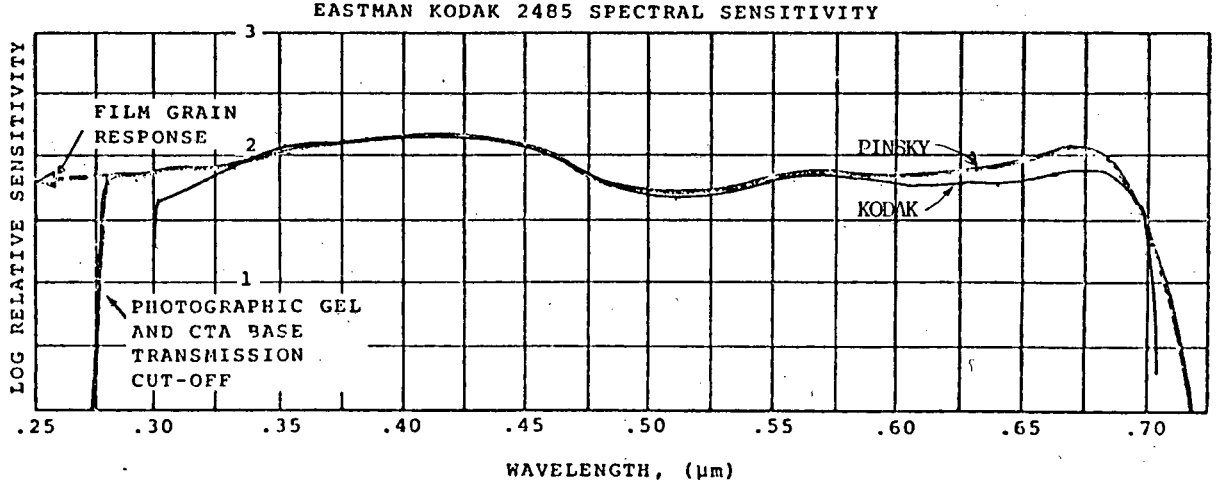
EASTMAN KODAK 2485 SPECTRAL SENSITIVITY
LOG RELATIVE SENSITIVITY
3
2
1
FILM GRAIN RESPONSE
PINSKY
KODAK
PHOTOGRAPHIC GEL AND CTA BASE TRANSMISSION CUT-OFF
.25
.30
.35
.40
.45
.50
.55
.60
.65
.70
WAVELENGTH, (μm)

Fig. 22

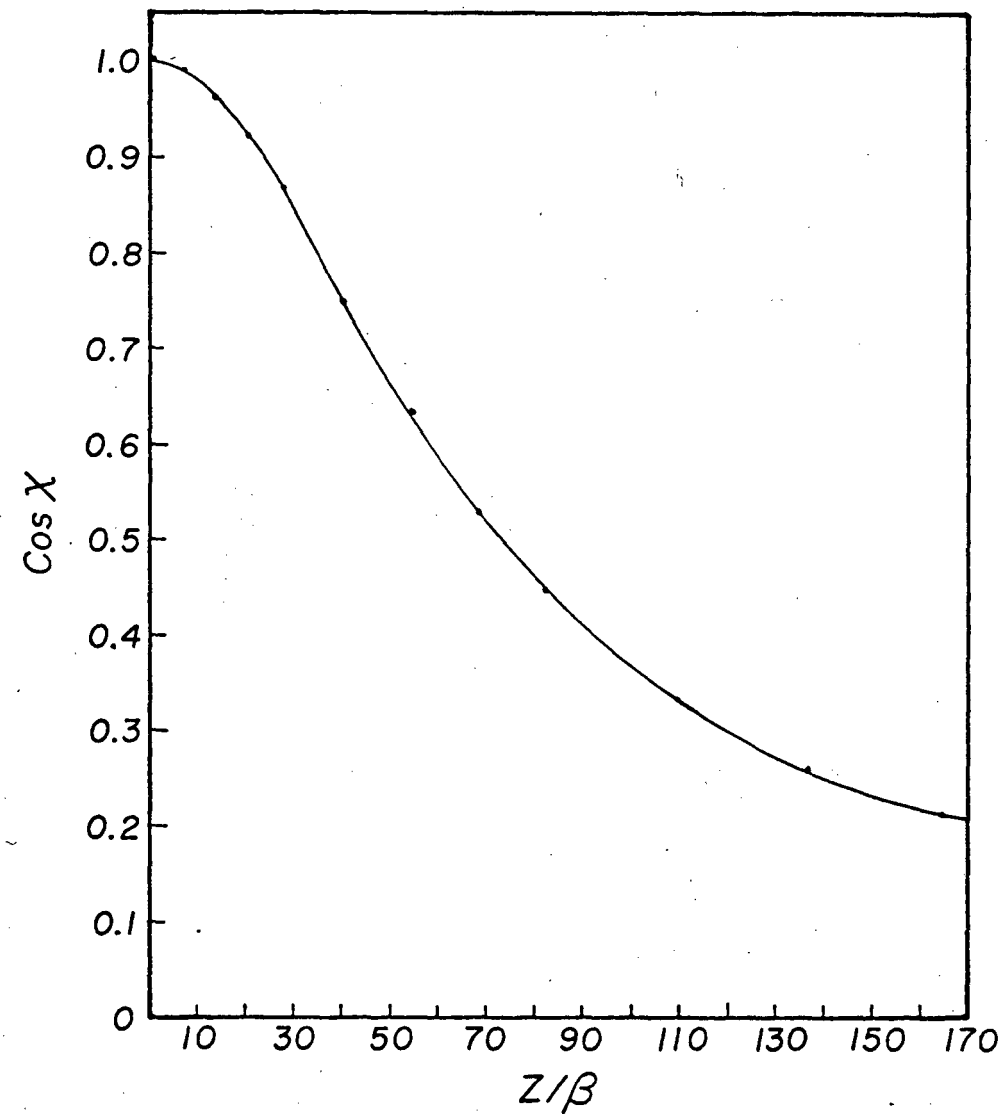

Fig. 23

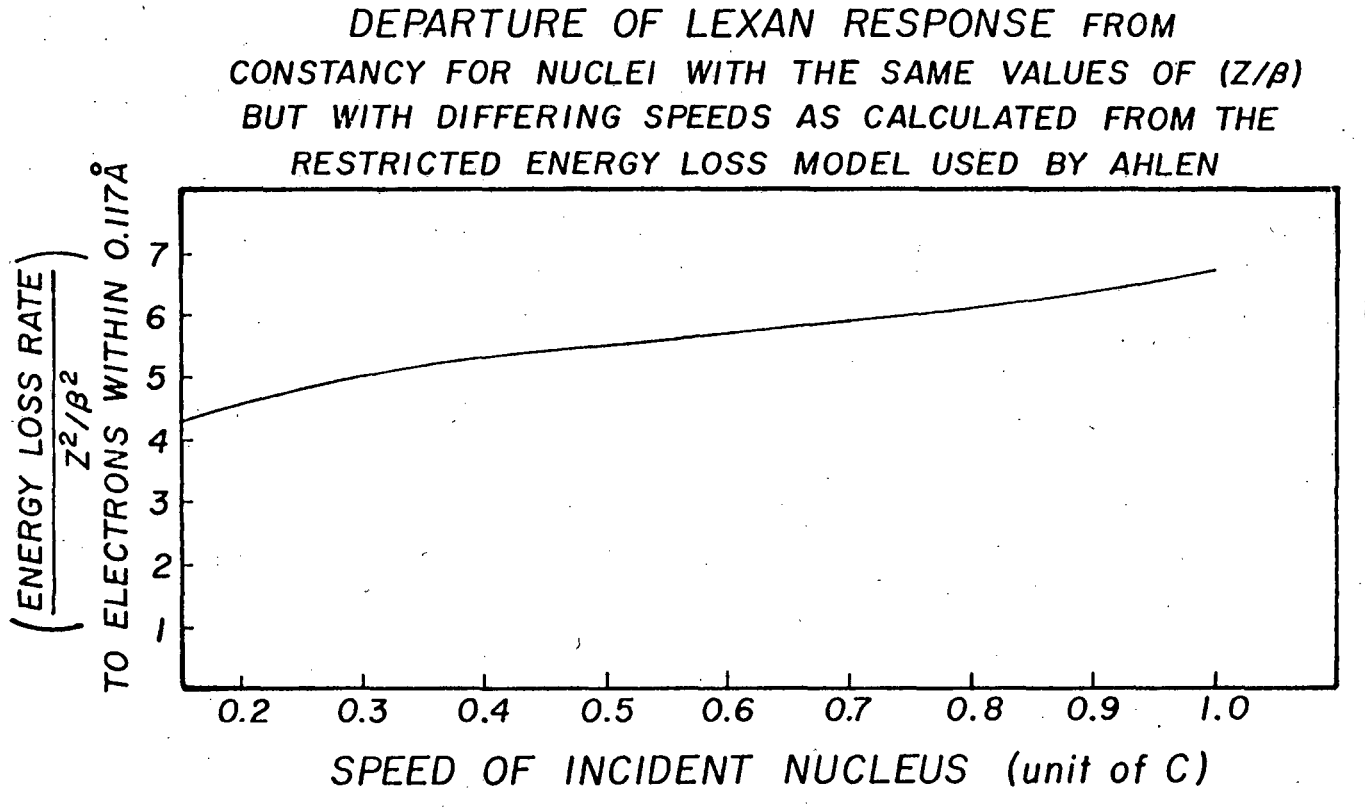
DEPARTURE OF LEXAN RESPONSE FROM
CONSTANCY FOR NUCLEI WITH THE SAME VALUES OF (Z/β)
BUT WITH DIFFERING SPEEDS AS CALCULATED FROM THE
RESTRICTED ENERGY LOSS MODEL USED BY AHLEN
(ENERGY LOSS RATE / Z²/β²) TO ELECTRONS WITHIN 0.117Å
1
2
3
4
5
6
7
0.2
0.3
0.4
0.5
0.6
0.7
0.8
0.9
1.0
SPEED OF INCIDENT NUCLEUS (unit of C)

Fig. 24

VALUE OF $|Z/\beta|$ NEEDED TO PRODUCE THE MEASURED MEAN ETCH RATE OF $|Q/\beta| = 114$ AS A FUNCTION OF SPEED AS CALCULATED FROM THE RESTRICTED ENERGY LOSS MODEL OF AHLEN

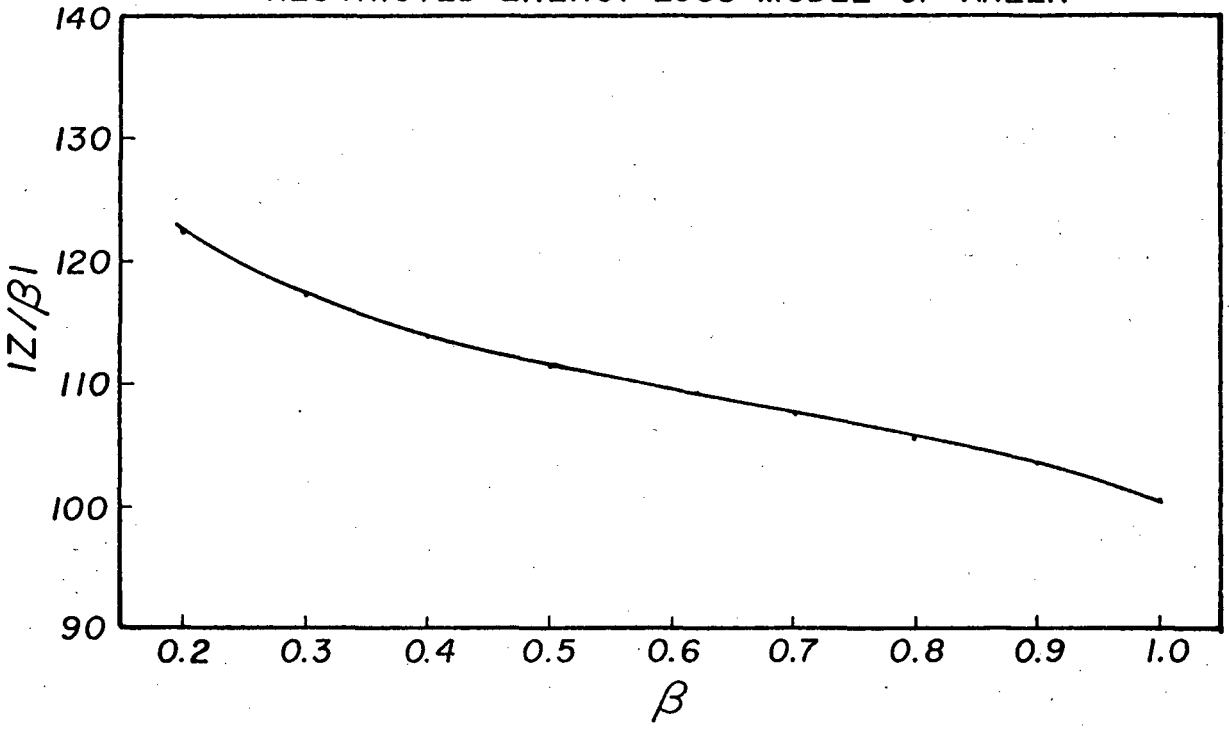

Fig. 25

TECHNICAL INFORMATION DEPARTMENT
LAWRENCE BERKELEY LABORATORY
UNIVERSITY OF CALIFORNIA
BERKELEY, CALIFORNIA 94720